

NASA CR-144962

TECHNICAL AND ECONOMIC ASSESSMENT

OF

SPAN-LOADED CARGO AIRCRAFT CONCEPTS

(NASA-CR-144962) TECHNICAL AND ECONOMIC
ASSESSMENT OF SPAN-LOADED CARGO AIRCRAFT
CONCEPTS (McDonnell-Douglas Corp.) 142 p HC
\$6.00 CSCL 01C

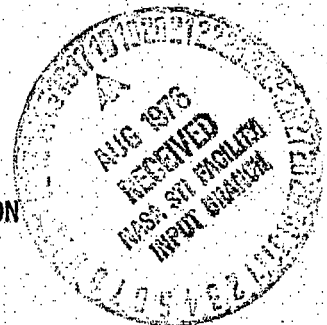
N76-28225

G3/05 Unclass
47656

Prepared under Contract No. NAS1-13964 by
MC DONNELL DOUGLAS CORPORATION
Douglas Aircraft Company
Long Beach, Ca., 90846
for



NATIONAL AERONAUTICS AND SPACE ADMINISTRATION



TECHNICAL AND ECONOMIC ASSESSMENT
OF
SPAN-LOADED CARGO AIRCRAFT CONCEPTS

January 1976

Distribution of this report is provided in the interest of
information exchange. Responsibility for the contents
resides in the organization that prepared it.

Prepared under Contract No. NAS1-13964 by
McDonnell Douglas Corporation
Douglas Aircraft Company
Long Beach, Ca., 90846

for

Langley Research Center
NATIONAL AERONAUTICS AND SPACE ADMINISTRATION

Page intentionally left blank

TABLE OF CONTENTS

<u>Section</u>	<u>Page</u>
TABLE OF CONTENTS	
LIST OF ILLUSTRATIONS	
LIST OF TABLES	
1.0 SUMMARY	1
2.0 INTRODUCTION	2
3.0 PARAMETRIC STUDIES	4
3.1 Study Scope and Depth	6
3.2 Configuration Conceptualization	15
Landbased spanloader	15
Seaplane	21
3.3 Parametric Results	25
Landplane spanloader parametric results	25
Hybrid seaplane parametric results	41
3.4 Concept Selection	43
4.0 DETAILED CONFIGURATION ANALYSIS	52
4.1 Point Design Spanloader Description	51
Configuration selection	51
Mass properties analysis	57
Aerodynamic characteristics	60
Performance summary	63
Economic analysis	73
Stability and control	74
Structure and loads analysis	81
4.2 Conventional Aircraft Description	102
Configuration arrangement	102
Structures and mass properties	105
Performance summary	105
Economic analysis	105
5.0 VEHICLE COMPETITIVE ANALYSIS	111
5.1 Dimensional Data Comparison	111
5.2 Structures and Weight Comparison	113
5.3 Structural Arrangement Comparison	115

<u>Section</u>	<u>Page</u>
5.4 Aerodynamic Characteristics Comparison	117
5.5 Performance Comparison	119
5.6 Economic Comparison	121
6.0 CONCLUSIONS	125
7.0 RECOMMENDATIONS FOR FUTURE WORK	127
7.1 Airfoil Design	127
7.2 Winglet Design	128
7.3 Composite Structures	128
7.4 Wing Internal Arrangement Studies	129
7.5 Structural Design Refinements	130
7.6 Payload Characteristics	131
7.7 Engine Technology Requirements	132
7.8 Dynamic Stability	132
7.9 Operational Considerations	133
7.10 Military Logistics Evaluation	133
APPENDIX A - NOMENCLATURE	135

LIST OF ILLUSTRATIONS

<u>Figure</u>		<u>Page</u>
3-1	Parametric Baseline Spanloader	11
3-2	Comparison of Drag Divergence Mach Numbers for Various Types of Airfoils	17
3-3	Internal Wing Arrangement Trends	18
3-4	Efficiency of Wing Cargo Packaging	20
3-5	Hybrid Seaplane	22
3-6	Hybrid Seaplane Wing Sizing Limitations	24
3-7	Effect of Aspect Ratio on Landbased Spanloader	27
3-8	Effect of Wing Thickness on Landbased Spanloader	28
3-9	Swept Wing Spanloader	30
3-10	The Effects of Range on Landbased Spanloader	33
3-11	Effect of Range on Landbased Spanloader Performance	34
3-12	The Effects of Payload on Landbased Spanloader	35
3-13	Effect of Payload Density on Landbased Spanloader	37
3-14	Cargo Compartment Pressurization	38
3-15	Container Pressurization	40
3-16	Economic Trends of Landbased Spanloader	42
3-17	Effect of Payload Density Fuselage Loaded Seaplane	44
3-18	Effect of Range on Fuselage Loaded Seaplane	45
3-19	Aspect Ratio Effects as Function of Aircraft Concept	47
3-20	Payload Density Effects as Function of Aircraft Concept	48
3-21	Range Effects as a Function of Aircraft Concept	49
4-1	Point Design Spanloader	53
4-2	Point Design Performance and Economic Characteristics	56
4-3	Total Skin Friction for Smooth Surface	61
4-4	Point Design Spanwise Lift Distribution	64
4-5	Winglet Effect on Induced Drag of Point Design	65
4-6	Point Design Compressibility Drag	66
4-7	High Speed Point Design Trim Drag	67
4-8	Point Design Trimmed Lift to Drag Ratio	68
4-9	Point Design Lift Curves	69
4-10	Low Speed Point Design Trim Drag	70
4-11	Low Speed Point Design Aerodynamic Characteristics	71

<u>Figure</u>		<u>Page</u>
4-12	Airframe Cost Price Versus Quantity	76
4-13	Point Design Horizontal Tail Sizing	79
4-14	Point Design Tail Lift Coefficient Required for Trim	80
4-15	Wing Structural Arrangement	83
4-16	Typical Wing Rib	84
4-17	Wing Landing Gear Structure	85
4-18	Critical Wing Ultimate Shear Force	90
4-19	Critical Wing Ultimate Bending Moment	91
4-20	Critical Wing Ultimate Torque	92
4-21	Wing Skin Panel Thickness	94
4-22	Typical Wing Rib Loading	96
4-23	Typical Rib Shear	97
4-24	Typical Rib Bending Moment	98
4-25	Typical Wing Rib Thickness	99
4-26	Wing Rib Commonality	100
4-27	Wing Spar Shear Material Thickness	101
4-28	Conventional Aircraft	103
4-29	Airplane Price Versus Quantity	110
5-1	Winglet Aerodynamic Payoff	118
5-2	Aircraft Price Versus Quantity	124

LIST OF TABLES

<u>Table</u>		<u>Page</u>
3-1	Parametric Study Direct Operating Cost Assumptions	5
3-2	Parametric Study Variables	6
3-3A	Study Matrix (English)	7
3-3B	Study Matrix (Metric)	8
3-4A	Wing Loading Conditions Investigated (English)	12
3-4B	Wing Loading Conditions Investigated (Metric)	13
3-5	Wing Sweep Study - Spanloader	33
3-6	Landbased Spanloader Pressurization Study Summary	40
4-1	Point Design Spanloader - Design Data and Geometry	55
4-2	Point Design Spanloader - Weight Summary	59
4-3	Parasite Drag Summary	62
4-4	Point Design Performance Summary	72
4-5	Airplane Pricing	75
4-6	Direct Operating Cost Breakdown	77
4-7A	Design Load Conditions (Limit) (English)	87
4-7B	Design Load Conditions (Limit) (Metric)	88
4-8	Conventional Aircraft - Design Data and Geometry	104
4-9	Conventional Aircraft - Weight Summary	106
4-10	Conventional Aircraft Performance Summary	107
4-11	Airplane Pricing (Conventional Design)	109
4-12	Direct Operating Cost Breakdown	108
5-1	Dimension Data - Spanloader vs Conventional Aircraft	112
5-2	Weight Data	114
5-3	Aerodynamic Parameters Comparison	117
5-4	Performance Comparison	120
5-5	Economic Data Comparison	122
5-6	Spanloader Economic Potential	123

TECHNICAL AND ECONOMIC ASSESSMENT OF SPAN-LOADED CARGO AIRCRAFT CONCEPTS

1.0 SUMMARY

The objective of the study documented in this report is to enumerate and quantify the benefits of span distributed loading concepts as applied to future commercial air cargo operations. A two phased program is used to perform this assessment. The first phase consists of selected parametric studies to define significant configuration, performance and economic trends. The second phase consists of more detailed engineering design, analysis and economic evaluations to define the technical and economic feasibility of a selected spanloader design. A conventional all-cargo aircraft of comparable technology and size is used as a comparator system.

The investigations of this report generally substantiate the technical feasibility of the spanloader concept with no new major technology efforts required to implement the system. However, certain high pay-off technologies such as winglets, airfoil design, and advanced structural materials and manufacturing techniques need refinement and definition prior to application. In addition, further structural design analysis could establish the techniques and criteria necessary to fully capitalize upon the high degree of structural commonality and simplicity inherent in the spanloader concept.

The most economical spanloader configuration indicated by the studies is a 40 degree swept wing design with twin outboard mounted empennages. This configuration showed approximately 13 percent lower direct operating cost than the conventional aircraft. Additional configuration optimization items could increase this value to about 15 percent.

The lift-to-drag ratios (L/D) of the typical moderate aspect ratio (4 to 5) spanloader configurations using large effective winglets can be as high as 21. This is considerably greater than today's jet aircraft but slightly less than an advanced high aspect ratio conventional aircraft. These high L/D values result from the substantial increase in effective aspect ratio resulting from the use of winglets, the high flight Reynolds number with the attendant reduction in skin friction coefficient, and the use of negative static stability margins with the resulting reductions in tail size and trim drag.

The weight empty-to-gross weight ratio of the spanloader can be as low as .26 compared to .32 for the advanced conventional aircraft. This improvement is anticipated from the distributed span loading feature of the concept. The unit weight of the spanloader wing, in fact, is approximately half that of the conventional wing. The impact of these considerations on aircraft procurement cost is a potential price reduction of 15 to 20 percent compared to the conventional aircraft.

The spanloader offers a rapid load and off load capability because of its multi-channel arrangement and the loadability from both wing tips. A potential operational problem exists, however, relative to the compatibility of the spanloader with existing facilities because of the large wing span (approximately 300 feet) and the large gear tread (approximately 200 feet).

The payoffs and incentives using the spanloader concept as a basis for a 1990 all-cargo dedicated air freight system are sufficient to warrant further study and detailed analysis in specific areas. These areas of additional study are identified in the report.

2.0 INTRODUCTION

The current air cargo market represents only a small percentage of the total cargo traffic of the world (.1 percent in 1973). In this year, this actually consisted of approximately 16 billion ton miles of air freight, mail and express. Of this amount approximately 50 percent was carried in airliner bellypits and the remainder in all-freight configurations (DC-8F, 747F, 707F). Considerable uncertainty exists in the projection of future air cargo growth and a wide dispersion of estimates is reported in the literature. The maturing market of air cargo is assumed in this study to be 100 billion ton miles per year by the year 1990.. This projected volume is sufficient to seriously consider the development of a dedicated all-cargo air freight system.

New design options and configuration alternatives are being considered for evaluation for this potential dedicated cargo system. It is noteworthy that a number of foreign programs are in existence which address dedicated air cargo and which are targeted for operation near the end of this century. These systems include a proliferation of lighter-than-air projects, hybrid systems which cruise in-ground-effect over the ocean, seaplane programs, and conventional all-freighter aircraft.

Two advanced configuration possibilities are evaluated in this report and are compared to a large conventional high speed jet all-freighter configuration. These are;

- (1) Span distributed loading cargo aircraft (spanloader) which feature containerized cargo loaded spanwise in a nontapered wing, and
- (2) a hybrid seaplane concept which would carry containerized cargo in the fuselage (hull), and would operate primarily from and over ocean routes.

The emphasis of the study, however, was placed on the landbased spanloader.

Significant parametric studies are conducted to identify payoff trends in configuration geometry, performance requirements, cargo related characteristics and economics. Future technology requirements required for program implementation and major technology payoffs are identified. A near optimum spanloader configuration is selected for detailed analysis and a comparison to the conventional aircraft mode.

3.0 PARAMETRIC STUDIES

In order to derive valid comparisons between the unorthodox large aircraft concepts under study (landbased spanloader and hybrid seaplane) and advanced conventionally configured large cargo aircraft, it is necessary to conduct select parametric studies of the major design parameters of the unorthodox configurations. This is necessary because the impact of the major design parameters on the technical and economic performance of these new concepts is not as well understood as for the conventional configurations which have the advantage of extensive historical development.

This section discusses the results of the parametric or "trend" studies performed. The selection of an optimum Point Design landbased spanloader configuration from the parametric results for more detailed evaluation is contained in Section 4.0. Final comparison to the conventional concept is presented in Section 5.0.

Direct operating cost (DOC) was the primary selection criteria although other criteria, such as fuel efficiency and operational considerations, are also weighed. The DOC formulation utilized is a 1975 update of the 1967 ATA equation, the major assumptions of which are summarized in Table 3-1. Three levels of fuel costs were used for each variation as noted. While the above assumptions are sufficient to determine consistent trends and valid optimum values in the parametric analyses they are inadequate for the critical comparisons between generic types of vehicles in the later report sections. For the latter comparisons the assumed values were re-examined in the light of the specific characteristics of the respective vehicle types. As an example, while the parametric studies used \$90 per pound (\$198/kg) of structure for airframe cost, the detail design assessments of Sections 4.0 and 5.0 employ detailed cost evaluations that reflect the major differences in structural complexities existing between general types. DOC values for the parametric studies have been given the subscript "p" to preclude confusion with the more refined DOC values of the later sections. It is important to note that the parametrically derived operating costs (DOC_p) cannot be compared directly to the direct operating cost (DOC) of Section 4.0 derived through the

TABLE 3-1
PARAMETRIC STUDY DIRECT OPERATING COST ASSUMPTIONS

Crew Excalation Factor		1.59
Weight Pay Factor		0.05
Speed Pay Factor		0.00
Insurance Rate		0.015
Depreciation Period	years	16
A/C Residual Value Ratio		0.10
Spare Ratio		0.15
Fuel Price	cents/gal	10, 25, 40
Cost Weight Pricing	\$/lb (\$/kg)	90 (198)
Engine Price Factor		1.00
Maintenance Labor Rate	\$/hr	6.70
Labor Burden Ratio		1.8
Airframe Labor Factor		0.057
Airframe Materials Factor		1.71
Engine Labor Factor		1.68
Engine Materials Factor		23.6
Operation		Domestic
Op Pay Factor		135
Utilization	hr/hr	ATA

detailed cost analysis. To compare these values requires consideration for the value differences existing between the underlying assumptions and weighting factors utilized in deriving the respective direct operating costs.

Parametric studies conducted include critical geometric, performance, payload related characteristics, and economic parameters. While the resulting fundamental trends are not likely to be invalidated by more detailed analysis, additional extensive optimization studies will be necessary to mature the study configurations to the same level of design finesse as the conventional configurations.

3.1 Parametric Study Scope And Depth

The primary variables treated in the parametric analysis are shown in Table 3-2.

TABLE 3-2
PARAMETRIC STUDY VARIABLES

PARAMETER	SPANLOADER	HYBRID SEAPLANE
Geometric variables	Aspect Ratio	Aspect Ratio
	Wing Thickness Ratio	
	Wing Sweep	
Performance variables	Range	Range
Payload variables	Payload Quantity	Payload Density
	Payload Density	
	Payload Pressurization	
Economic variables	Fuel Price	Fuel Price

The specific combinations of these variables is shown in the matrix of Table 3.3. This matrix was planned so as to cover expected critical regions of the parametric variations, without generating undue information in anticipated non-optimum regions.

Less parametric coverage is shown for the hybrid seaplane than for the landbased spanloader because the study ground rules identified the latter to be the primary generic type of configuration for investigation. In addition, the available in-ground-effect aerodynamic data base upon which the evaluation of the hybrid aircraft is based is less well developed and therefore less reliable than that for the spanloader. Only the spanloader is carried into the analyses and comparisons of Sections 4.0 and 5.0.

TABLE 3-3A

PARAMETRIC STUDY MATRIX

English Units

Landplane (t/c = .20)	Aspect Ratio			
	4	5	6	7
Gross Payload 10 Density (ρ_{PLG}) (lb/ft ³)	$\Lambda = 40^\circ$ (AR = 4.45)	PL = 400,000 lb 600,000 lb 800,000 lb R = 3000 n.mi.		
15	PL = 600,000 lb R = 3000 n. mi. t/c = .17, .23 (AR = 5.4)	PL = 600,000 lb R = 2000 n.mi. 3000 n.mi. 4500 n.mi. 6000 n.mi.	PL = 600,000 lb R = 3000 n.mi.	PL = 600,000 lb R = 3000 n.mi.
20		PL = 500,000 lb R = 3000 n.mi.		
Seaplane (t/c = .20)	Aspect Ratio			NOTE: All Configurations evaluated at 10, 25 and 40 cents/gal
	2	4		
Gross Payload 10 Density (ρ_{PLG}) (lb/ft ³)	PL = 600,000 lb R = 3000 n.mi. 4500 n.mi. 6000 n.mi.	PL = 600,000 lb R = 4500 n.mi.		
15	PL = 600,000 lb R = 2000, 3000, 4500, 6000, 8000 n.mi.	PL = 600,000 lb R = 4500 n.mi.		
20	PL = 600,000 lb R = 4500 n.mi.	PL = 600,000 lb R = 4500 n.mi.		

TABLE 3-3B
PARAMETRIC STUDY MATRIX
Metric Units

Landplane (t/c = .20)	Aspect Ratio			
	4	5	6	7
Gross Payload 160 Density (ρ_{PLG}) (kg/m ³)	$\Lambda = 40^\circ$ (AR = 4.45)	PL = 181,437 kg 272,155 kg 362,874 kg R = 5,550 km		
240	PL = 272,155 kg R = 5,550 km t/c = .17, .23 (AR = 5.4)	PL = 272,155 kg R = 3,700 km 5,550 km 8,326 km 11,101 km	PL = 272,155 kg R = 5,550 km	PL = 272,155 kg R = 5,550 km
320		PL = 272,155 kg R = 5,550 km		
Seaplane (t/c = .20)	Aspect Ratio			
	2	4		
Gross Payload 160 Density (ρ_{PLG}) (kg/m ³)	PL = 272,155 kg R = 5,550 km 8,326 km 11,101 km	PL = 272,155 kg R = 8,326 km		NOTE: All Configurations evaluated at 10, 25 and 40 cents/gal
240	PL = 272,155 kg R = 3,700, 5,550, 8,326, 11,101, 14,801 km	PL = 272,155 kg R = 8,326 km		
320	PL = 272,155 kg R = 8,326 km	PL = 272,155 kg R = 8,326 km		

A number of ground rules were established to maintain study consistency and to appropriately represent technology anticipated for the 1990 time period. These ground rules are listed as follows:

- o Cargo is to be carried in 8 x 8 x 20 foot (2.44 x 2.44 x 6.10 m) containers. Since there is some current pressure to increase container height to 8.5 to 9 feet (2.59 to 2.74m), this ground rule may become restrictive by 1990. The penalty to the vehicle for increased height, however, is significant since the wing chord and associated drag and weight are largely determined by physical wing thickness.
- o All containers are uniformly loaded (constant density). No anomalies in cargo characteristics are considered. As discussed for the later Point Design analyses, such non-uniformities are not expected to create conditions more critical than those evaluated.
- o No pressurization for the cargo is assumed for the basic parametric aircraft. This has been assumed for two reasons; (1) pressurization will not effect the parametric trend results, and (2) statistics show that only three percent of current air cargo carried requires pressurization. Pressurization, of course, is not required for the sea level cruise hybrid seaplane. Alternative pressurization schemes, however, are evaluated for the spanloader in this section and pressurization has been included in the later Point Design analysis.
- o In accordance with the study guidelines, the spanloader and conventional aircraft design field lengths should be less than 12,000 feet (3,658 m) on a standard day at sea level. This requirement impacts only a few of the parametric aircraft. The hybrid seaplane design takeoff distance (clear the water) has been chosen to be 8,000 feet (2,438 m) to minimize excessive pounding of the structure during takeoff.
- o Complete use of graphite epoxy composites was assumed for all airframes including all primary and secondary structure. This represents the single largest advanced technology payoff. Others were assumed and are identified in the detail discussions.

- o Reasonable negative static margins were permitted for all configurations evaluated.
- o All performance was based upon a high bypass ratio (9) fanjet engine, typified by the TF-39 engine, with the SFC reduced by five percent from current levels. A high usage of composites as currently being exploited in the QCSEE engine is also assumed for weight reduction purposes. No attempt was made to optimize the cycle for any of the configurations studied.

The basic structural, weight and aerodynamic characteristics of the vehicles were investigated in sufficient depth to guarantee identification of valid trends and selection of optimum vehicle parameters. Primary attention was given to assumptions or trends that might "tilt" the parametric curves and less attention paid to those items which would "shift" the curves. For instance, insufficient attention to the variation of structural weight with aspect ratio might result in the choice of a non-optimum aspect ratio for subsequent analyses and comparisons. On the other hand, the use of \$90 per pound of structure weight for airframe costing is likely to shift the parametric curves but not invalidate the choice of critical geometries.

In order to guarantee a sufficient depth of analysis, a nominal spanloader configuration was designated as the baseline from which the characteristics for the entire parametric matrix could be generated. This Parametric Baseline configuration was defined to have an aspect ratio 5 non-tapered wing and a gross payload of 600,000 pounds (272,155 kg) at a gross cargo density of 15 pounds per cubic foot (240 kg per cubic m) (Figure 3-1). The analysis of this Parametric Baseline was of only slightly less depth than that conducted for the Point Design aircraft discussed later in the report. The analysis consisted of the following basic elements:

- o Loads determination - The seven critical loading conditions identified in Table 3-4 were investigated. Uniform cargo loading distributions were considered in conjunction with aerodynamic loads

FIGURE 2-1
PARAMETRIC BASELINE SPANLOADER

CHARACTERISTICS DATA			
	WING	H. TAIL	V. TAIL
AREA	18,000 ft ² (1672m ²)	3600 ft ² (335m ²)	1435 ft ² (133m ²)
AR	5.0	3.0	1.9
T.R.	1.0	1.0	.30
$\Lambda, c/4$	0°	0°	23°
t/c	.20	.12	.12
Vol. Ratio		.40	.033

Fuel Shown: 120,000 lb (54,432 kg) x 2 FWD
94,000 lb (42,638 kg) x 2 AFT

Gross Payload = 600,000 lbs (272,155 kg)

32 Containers $\rho_{PLG} = 15 \text{ lb/ft}^3$ (240 kg/m³)

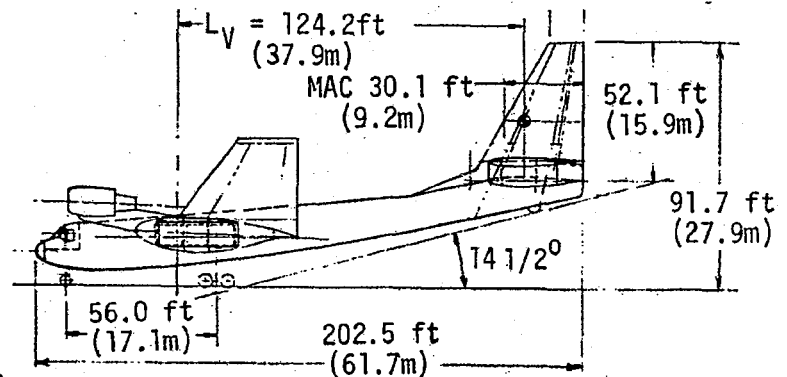
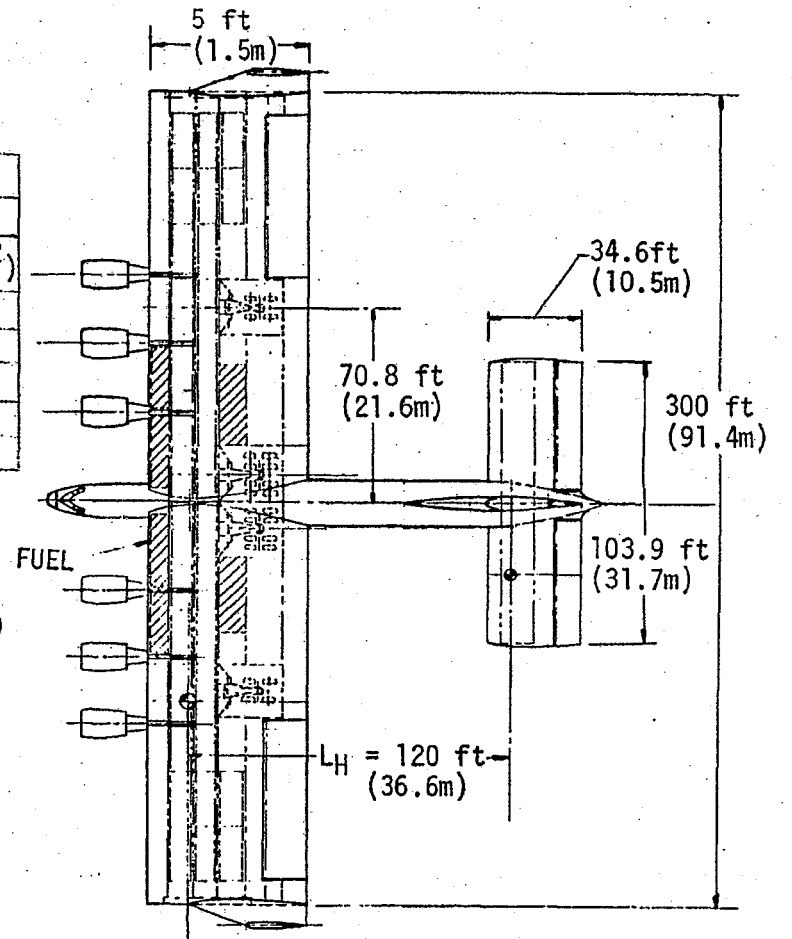
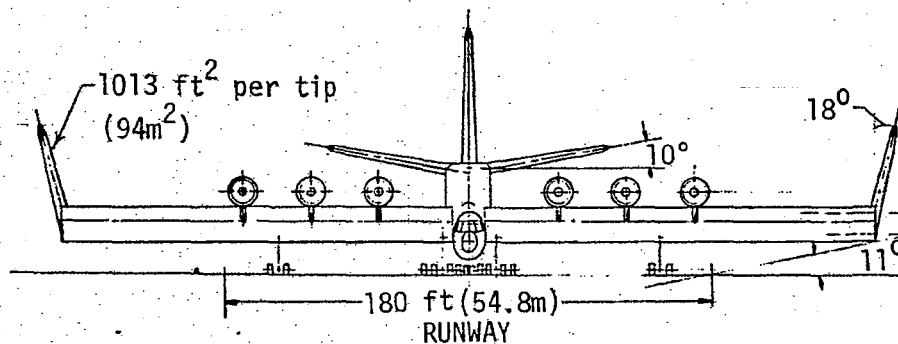
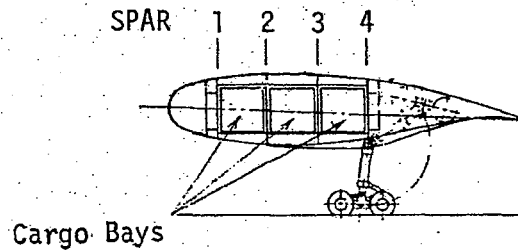


TABLE 3-4A
WING LOADING CONDITIONS INVESTIGATED
English Units

- *A. 50 fps up gust at 20,000 ft at maximum gross weight
($n = 2.91$)
- B. 50 fps up gust at 20,000 ft at minimum gross weight
($n = 4.12$)
- C. 10 fps landing at maximum landing gross weight
($n = 1.83$)
- D. 10 fps landing at maximum landing gross weight
($n = 1.83$) - Outer Gear Load - 2 x Cond 3.
- *E. Taxi at maximum gross weight
($n = 2.0$)
- F. Turn and swing at maximum gross weight - to left
($n = 1.0, n_y = 0.5$)
- G. Turn and swing at maximum gross weight - to right
($n = 1.0, n_y = 0.5$)

*Critical conditions

TABLE 3-4B
WING LOADING CONDITIONS INVESTIGATED
Metric Units

- *A. 15.2 mps up gust at 6,096 m at maximum gross weight
($n = 2.91$)
- B. 15.2 mps up gust at 6,096 m at minimum gross weight
($n = 4.12$)
- C. 3.1 mps landing at maximum landing gross weight
($n = 1.83$)
- D. 3.1 mps landing at maximum landing gross weight
($n = 1.83$) - Outer Gear Load - 2 x Cond 3
- *E. Taxi at maximum gross weight
($n = 2.0$)
- F. Turn and swing at maximum gross weight - to left
($n = 1.0, n_y = 0.5$)
- G. Turn and swing at maximum gross weight - to right
($n = 1.0, n_y = 0.5$)

*Critical Conditions

and the weight distributions due to major configuration elements such as propulsion, landing gear, fuel, and fuselage. Wing shear, moment and torque distributions were determined using computer analysis from which items A and E of Table 3-4 were found to be critical. Analytical checks of the other parametric matrix configurations were sufficient to establish the load levels necessary to determine the respective weight allocations.

- o Structural Analysis - Structural layouts and member sizing of the wing structure was performed where conventional weight estimating methodologies would not be valid. This analysis sized the skin/stringer, rib, spar and cargo floor members for the Parametric Baseline aircraft to the same depth as that for the spanloader Point Design of Section 4.0.

The hybrid seaplane structure was analyzed to a comparable depth in a previous contract and is not documented in this report.

- o Weight Analysis - Weights were developed for the various spanloader configurations utilizing configuration drawings, design criteria assumptions, and structural analyses where appropriate. Empirical analyses were used wherever practical with the structural analyses being employed for those components where little or no previous weight estimating data existed. Weights for the Parametric Baseline (Figure 3-1) were derived by the same methods applied to the Point Design. The general ground rules applied to the former were identical to those for the Point Design with two major exceptions; namely, the cargo bays in the Parametric Baseline wing were assumed to be unpressurized, and the nacelle and propulsion weights used were based on a scaled up General Electric QCSEE installed weight allocation.
- o Aerodynamic Characteristics - The estimation of the aerodynamic characteristics for the Parametric Baseline used conventional methodology except for those areas related to the use of the large end plates (winglets). The induced drag effect associated with the latter were estimated using a vortex lattice computer program.

The aerodynamic methodology applied to the parametric aircraft was identical to that utilized for estimating the characteristics of the Point Design aircraft. Empennage surface area requirements were determined based on 10 percent negative stability margins.

The depth of analysis performed for both the spanloader and hybrid seaplane configurations is comparable and trends for each generic type of vehicle emanating from the study are judged to be reliable. Considerable discussion is offered later concerning the relative standing of the individual generic types and additional desirable optimizations relative to engine cycle selection.

3.2 Configuration Conceptualization

Utilizing the baseline spanloader configuration of Figure 3-1 analysis were conducted on the basic design considerations such as payload containment, aerodynamic geometry, and the inboard profile. A major portion of these efforts were devoted toward the landbased concept, and comparable information on the seaplane leaned heavily upon the results of a previously conducted study.

Landbased spanloader. - The typical spanloader configuration used as a base throughout this study (Figure 3-1) is dominated by the very large wing, the size of which is determined by the payload characteristics. The use of the standard 8 x 8 x 20 foot (2.44 x 2.44 x 6.10 m) containers dictates a two-dimensional wing ($\lambda = 1.0$) in order to minimize the wing area and produce minimum drag and weight characteristics. The straight wing has been assumed as a prime configuration throughout the study since the centerline break of a swept wing necessitates loading from both sides of the configuration with associated major complications in the ground facilities requirements. Structural simplicity is also maximized since use of the straight wing facilitates the application of simple wrap skins with innumerable right and left hand common parts. The impact of this structural simplicity upon the cost of the spanloader configurations is summarized in Section 4.0. However, as previously noted the swept wing concept was explored to a limited extent with the resulting data included as a point design in the parametric matrix.

A majority of the parametric configurations employed spanwise loading of the cargo containers into three horizontal channels with the appropriate fore and aft spacing to accommodate a multiple spar structure (four spars) as illustrated in Figure 3-1. The remaining parametric configurations utilized three spars with two container channels. The wing chord is determined by the eight foot container height dimension, appropriate clearances for wing structure at the critical corner points, and the selected airfoil thickness ratio. These considerations combined with the thickness and weight interrelation dictated the selection of the supercritical wing airfoil section assumed throughout this study. Attention is called to the characteristic bulge in the lower aft section of the airfoil (Figure 3-1) which is particularly favorable in accommodating the cargo compartment of the spanloader concept.

Open literature wind tunnel data for supercritical wings is somewhat limited and is currently restricted to thickness ratios of 17 percent and less. The use of thicker sections, however, is possible without incurring trailing edge separation at the relatively low cruise lift coefficients appropriate to the study airplanes. The variation of drag divergence Mach number (M_{DD}) with wing thickness is shown in Figure 3-2 for a cruise lift coefficient of 0.6. Based on Douglas in-house theoretical analyses, a thickness ratio of 20 percent has been determined as a nominal thickness ratio that could feasibly be employed and has been used as a base throughout this study. The data of Figure 3-2 shows the drag divergence Mach number for this selection to be approximately .69 to .70.

The primary determining factor of the wing geometry is the payload characteristics including payload size, density and the packaging of the cargo containers. Wing general arrangement drawings were derived for many of the aspect ratios, payload values, and payload density values of the parametric matrix. Typical wing geometries are shown in Figure 3-3 for aspect ratios of 4, 5 and 7 with a payload density of 15 lb/ft³ (240 kg/cm) and aspect ratio 5 for a gross payload density (ρ_{PLG}) of 10 lb/ft³ (160 kg/cm).

FIGURE 3-2
COMPARISON OF DRAG DIVERGENCE MACH
NO'S. FOR VARIOUS TYPES OF AIRFOILS

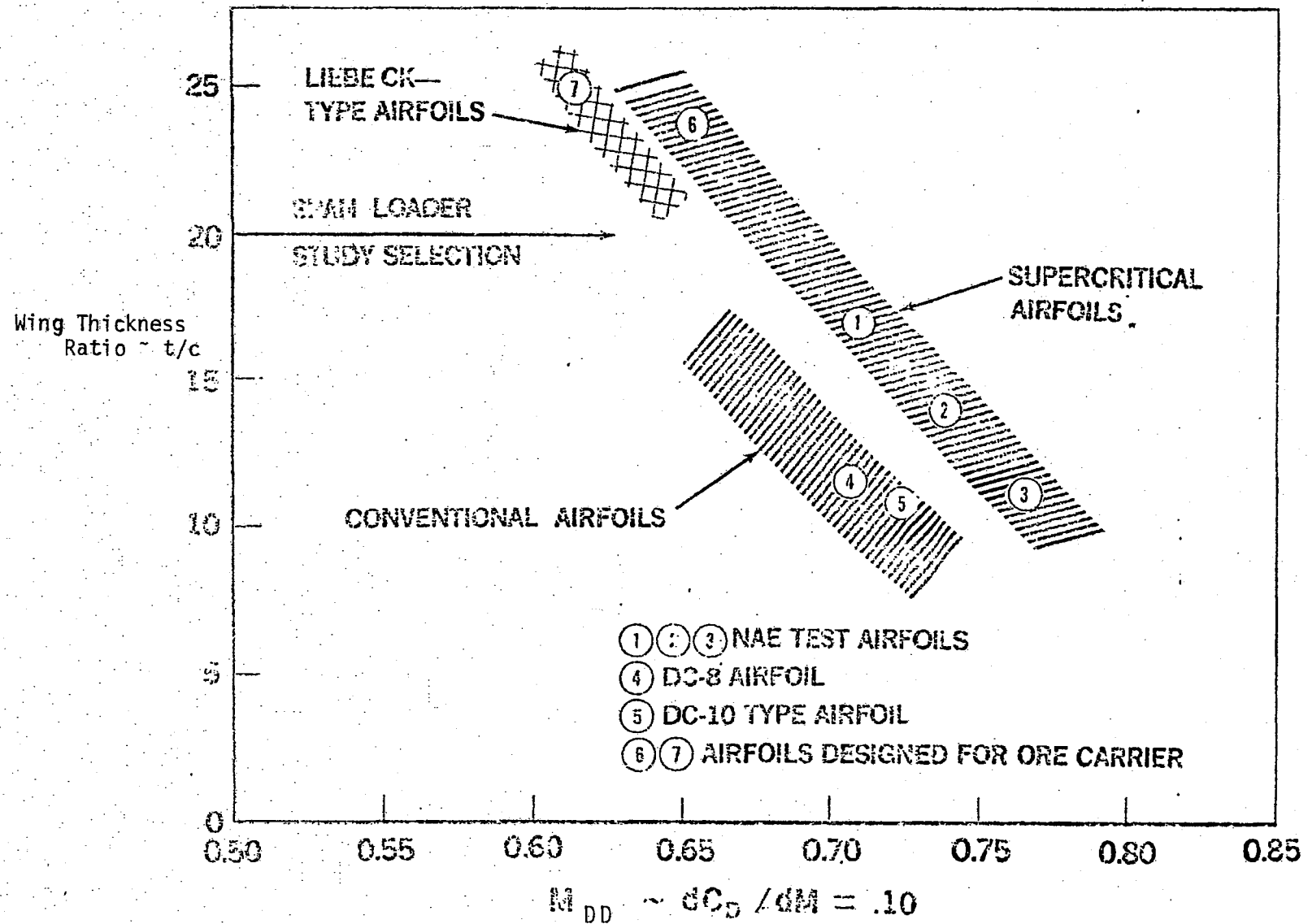
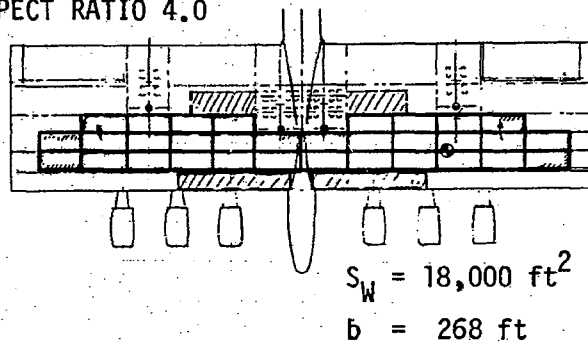


FIGURE 3-3
INTERNAL WING ARRANGEMENT TRENDS

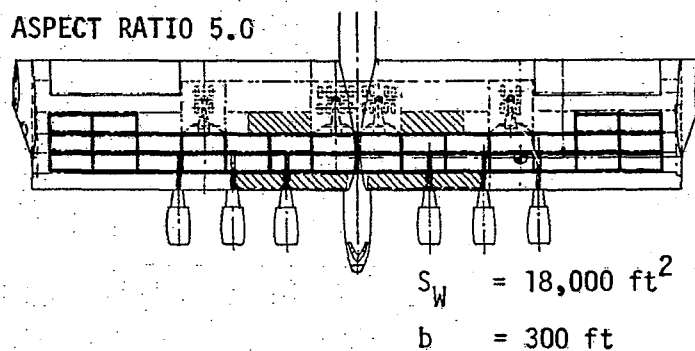
$$\rho_{PLG} = 15 \text{ lb/ft}^3 \text{ (240 kg/m}^3\text{)}$$

$$\rho_{PLG} = 10 \text{ lb/ft}^3 \text{ (160 kg/m}^3\text{)}$$

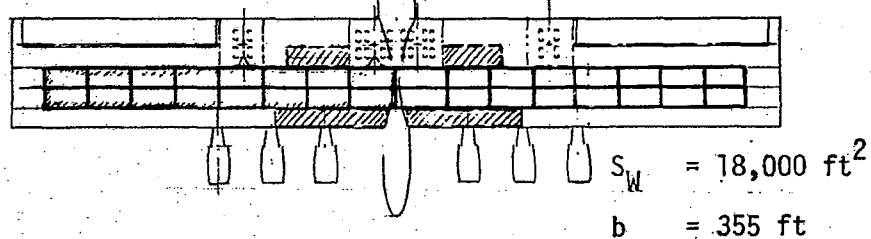
ASPECT RATIO 4.0



ASPECT RATIO 5.0

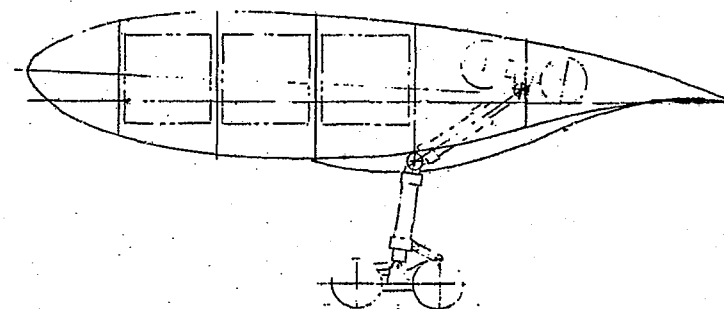
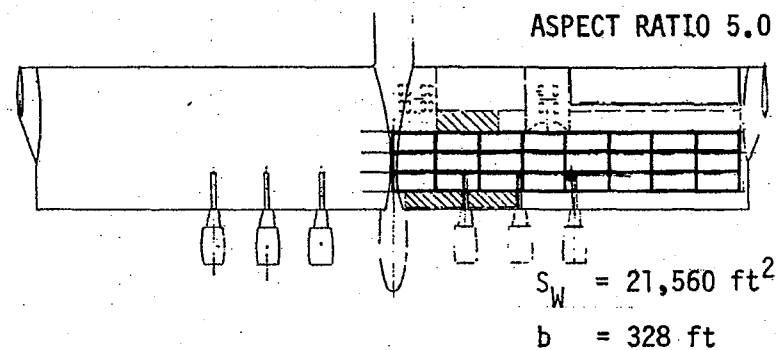


ASPECT RATIO 7.0



/// FUEL

ASPECT RATIO 5.0



TYPICAL WING CROSS SECTION

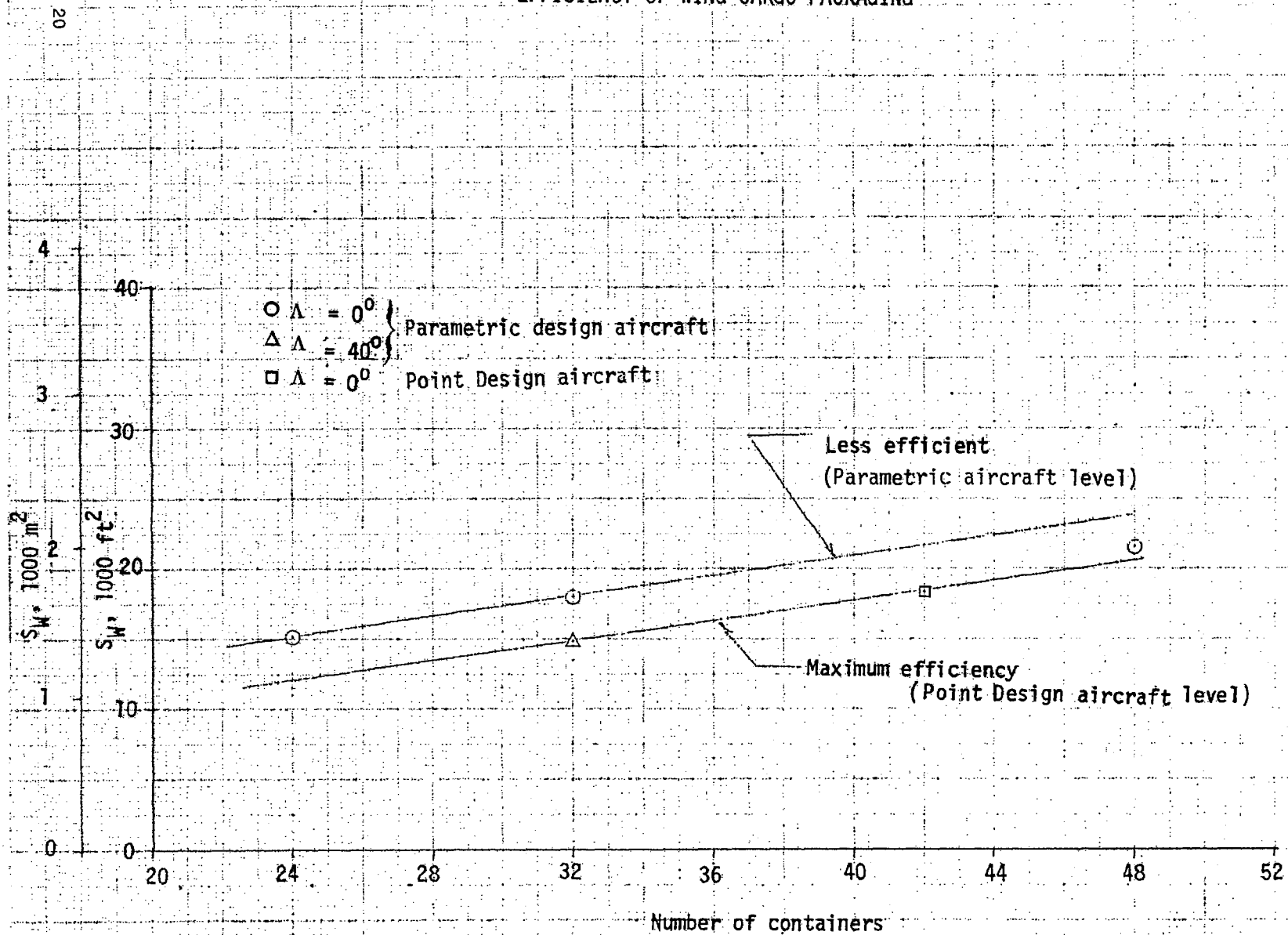
Detailed examination of the aspect ratio 4, $\rho_{PLG} = 15 \text{ lb/ft}^3$ (240 kg/cm), shows that the wing is not efficiently used from a cargo containment viewpoint. With the wing chord set by the requirement to contain the three, 8 foot (2.44 m) high rows of containers, the stipulation of an aspect ratio 4.0 dictates a wing span which is slightly larger than that required to contain the cargo. It is evident therefore that a slight reduction of the aspect ratio to a value below that used for the matrix point would result in a more efficiently packaged wing. For this particular configuration, $AR = 4$, the incomplete usage of the aft channel for cargo containers exaggerates the inefficient utilization of available wing volume. These comments are generally applicable to most of the parametric configuration layouts which were performed for specific "even" values of geometries.

The selected Point Design aircraft analyzed in detail in Section 4.0 was carefully designed for efficient cargo packaging and therefore generally represents a more efficient aircraft than those used in the parametric study. A comparison of the various parametric and the Point Design aircraft relating the wing area to the number of containers is shown in Figure 3-4 and illustrates the relative efficiency of the wings. The use of consistent but non-optimum configurations in the parametric studies does not invalidate the parametric trends derived or the selection of optimum parameters.

As shown in Figure 3-3 the fuel tanks are located in the leading edge of the wing and aft of the cargo bay. Because of the large wing volume available in these areas of the wing, fuel could be distributed both along the span and fore and aft of the cargo bay in an optimum manner to help achieve optimum loading conditions and minimum structural weight. This refinement, however, would result in a more complex fuel system. The landing gear is distributed into four main gear bogies; two inboard near the centerline and two outboard. Each gear is supported primarily by the rear spar structure and pivots into the wing trailing edge and landing gear pod.

Winglets were found to have a high aerodynamic payoff due to the non-taper wing and the relatively small aspect ratio and were therefore assumed for all spanloader configurations. This payoff is shown later in the study

FIGURE 3-4
EFFICIENCY OF WING CARGO PACKAGING



to amount to 30-35 percent reduction in induced drag compared to a reduction of the order of five percent for a conventional high aspect ratio tapered wing.

The configuration shown in Figure 3-1 does not include high lift devices either on the wing leading or trailing edge. Due to the low wing loading typical of the spanloader concept only a few of the spanloader configurations were field length performance critical without the use of high lift devices. The overall desirability of these critical configurations was deemed insufficient to justify the weight, cost, and complexity of high lift systems for the configurations analyzed.

A conventional empennage is shown in Figure 3-1 consisting of a vertical tail and a straight taper horizontal tail. The choice of horizontal tail geometry is in keeping with the prime motive to use simple low cost structure. These empennage surfaces have been sized to accommodate negative static stability margins and the attendant use of augmentation devices. Conventional rudder and elevator surfaces were assumed.

The fuselage has been minimized and serves the sole purpose of structural support for the empennage and an enclosure for the flight crew. The upsweep of the fuselage is necessitated by rotation requirements for takeoff and landing. The use of a simple flap would reduce the rotation requirement.

Six pod mounted engines are shown in an over-the-wing arrangement. This position has been shown to have some potential induced drag payoffs in cruise although these benefits have not been estimated nor used in the current study.

Seaplane - A novel hybrid seaplane configuration is shown in Figure 3-5. The wing consists of a low aspect ratio end plated arrangement designed to take advantage of the well known reduction in induced drag attendant with in-ground-effect flight. The configuration shown is an augmented ram wing utilizing the deflected thrust of the forward mounted engines to pressurize the cavity created by the wing lower surface, water surface, wing end plates, and simple trailing edge flaps. The resulting positive pressure differential generated on the wing lower surface is

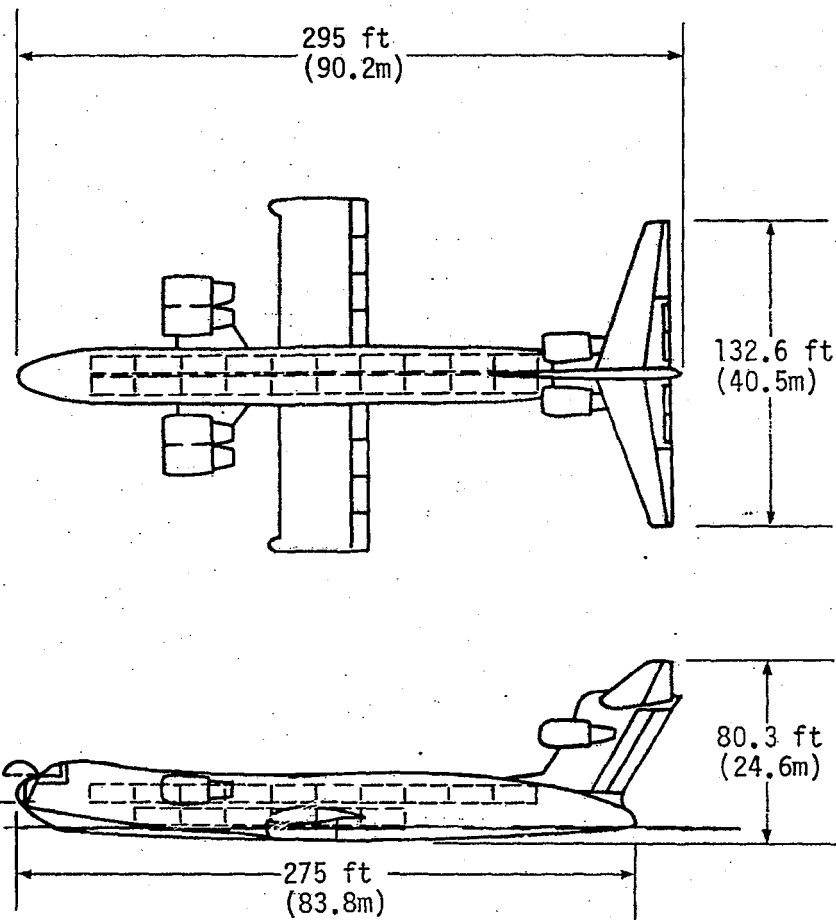
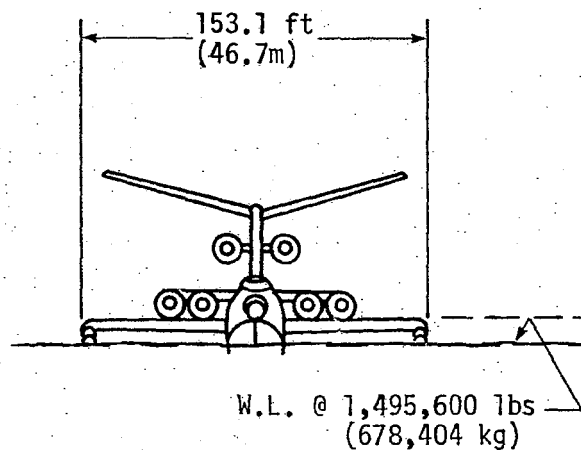
FIGURE 3-5
HYBRID SEAPLANE

CHARACTERISTICS DATA			
	WING	H. TAIL	V. TAIL
AREA	5865 ft ² (545.m ²)	2933 ft ² (272m ²)	1642 ft ² (152m ²)
AR	4.0.	6.0	1.0
T.R.	1.0	.30	1.0
$\Lambda, c/4$	0°	15°	30°
t/c	.20	.12	.13
Vol. Ratio		.60	.12

Gross Payload = 600,000 lbs (272,155 kg)

32 Containers

$\rho_{PLG} = 15 \text{ lb/ft}^3 \text{ (240 kg/m}^3\text{)}$



sufficient to lift the configuration at least partially out of the water thus reducing hydrodynamic drag, particularly near the conventional critical hump drag speeds. A very low thrust-to-weight ratio compared to normal seaplane requirements (about 1/2) is therefore adequate for water takeoff. The center of lift at low speeds and in-ground-effect tends to be aft of the 50 percent wing chord creating the requirement for an extreme aft center of gravity. During cruise this aft c.g. requires a lifting tail that minimizes trim drag and results in a reasonably high lift-to-drag ratio, particularly when flown in the ground effect mode.

Preliminary investigations of the use of this configuration as a span-loaded concept generated the key results shown in Figure 3-6. This figure shows the variation of vehicle efficiency parameters (payload/fuel and payload/OWE) as a function of design wing area for a selected set of design requirements; gross PL = 600,000 pounds (272,155 kg), $\rho_{PLG} = 15 \text{ lb/ft}^3$, and R = 3,000 nautical miles (5,550 km). These data substantiate the conclusion that in order for the hybrid seaplane concept to be efficient, a small wing with a high wing loading is required. However, there is a practical limit to which the design wing loading can be increased. Previous investigations considered the pertinent interrelated parameters involved and established this upper limit at 255 lb/ft^3 ($1,245 \text{ kg/m}^3$). Applying this limit in conjunction with the selected 8,000 foot (2,438 m) takeoff distance dictated a wing area of approximately 5,865 square feet (545 square meters) for the configuration shown in Figure 3-5. Limiting wing areas required from the standpoint of cargo containment volumes for gross payload densities of 10, 15 and 20 lb/ft^3 (160, 240 and 320 kg/m^3) are identified in Figure 3-6. It is seen that the wing areas required to meet the cargo volumetric requirements greatly exceed the preceeding area required for operational effectiveness. On this basis it was concluded that the hybrid seaplane should not be designed as a spanloaded configuration but should be designed with the cargo compartment in the hull. This conclusion is further amplified by the buoyancy requirement which necessitates a large volume hull that can be effectively used for cargo storage.

Because the hybrid seaplane and the spanloader concepts strive to capitalize upon the same configuration advantages (low aspect ratio simple

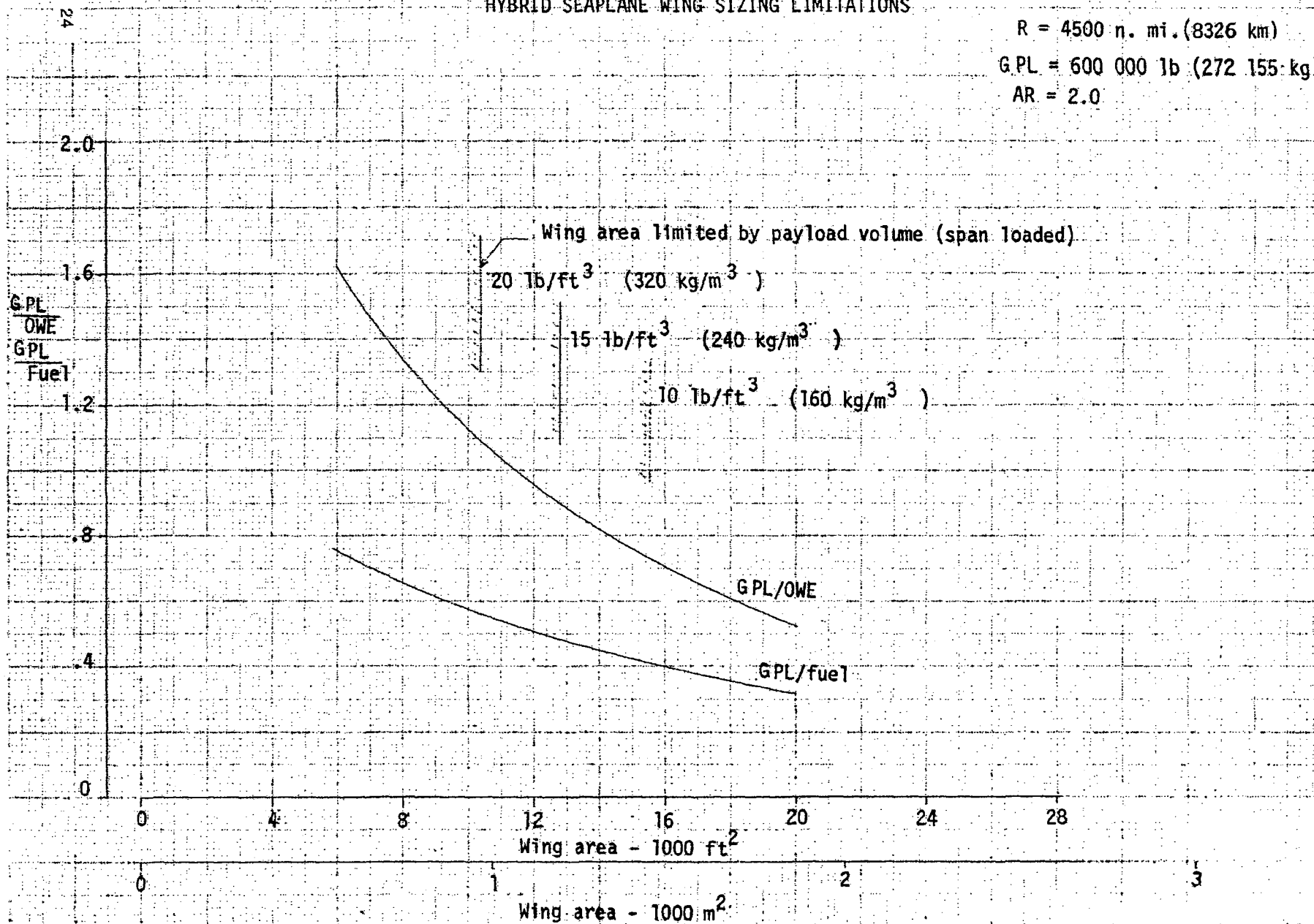
FIGURE 3-6

HYBRID SEAPLANE WING SIZING LIMITATIONS

$R = 4500 \text{ n. mi. (8326 km)}$

$G.P.L. = 600\,000 \text{ lb (272\,155 kg)}$

$AR = 2.0$



structure wings), both configurations have been retained in the current study for comparative purposes. The key configuration concept which is cogent to each of these generic types of configurations is the lift-to-drag ratio characteristics of the low aspect ratio wings, traded against the high structural and cost efficiencies accruing from the use of simple light weight structures.

3.3 PARAMETRIC RESULTS

The results of the parametric trend studies are discussed in this section. Only the "optimum" designs (minimum DOC_p) for each set of performance and vehicle geometry parameters as tabulated in the parametric matrix (Table 3-3) are shown.

Landplane spanloader parametric results. - Parametric studies considered the basic and interrelated effects arising from variations in configuration geometry, performance requirements, cargo characteristics and economics. Results of these analyses provided the basis for selection of the near optimum spanloader configuration that was subsequently studied to greater depth.

Geometric variables: For the landbased spanloader, the performance design optimization technique is not typical of that followed in the design of conventional aircraft. In the case of the landbased spanloader the wing area is essentially determined by the desired thickness ratio, payload, payload density, and cargo container arrangement which in turn, sets the entire vehicle geometry before its performance is generated. For a given set of design conditions, then, the only major independent variables are related to the engine size and cycle. The variation of engine size determines the proper airframe/engine match which occurs when the vehicle cruise ceiling and optimum cruise altitude are essentially identical. If the cruise ceiling is higher, the engine is oversized and if it is lower the engine is undersized. After the engine size is selected, it must be determined if that engine can then meet the additional requirements of takeoff field length and second segment climb gradients. For the parametric study vehicles, the proper airframe/engine match usually provided for minimum direct operating cost at a fuel price of twenty-five cents per gallon, hence, this fuel cost was identified as an independent variable for engine

size selection. It should be noted that for all the landplane spanloader configurations considered the airframe engine match occurred below the Mach divergence of the respective airframe indicating the need for additional engine cycle studies. It should be emphasized that the same engine cycle was used (except for scaling effects) for all the parametric design airplanes.

Aspect ratio. - The aspect ratio (AR) trend was developed for a gross payload (including container tare weight) of 600,000 pounds (272,155 kg), a gross payload density of 15 pounds per cubic foot (240 kg/cm³) and a design range of 3,000 nautical miles (5,550 km). The variation of DOC_p with aspect ratio, as shown in Figure 3-7, is mild with a nominal optimum of about 5.0. The weight fraction PL/Fuel favors a higher aspect ratio whereas the fraction PL/OWE favors a lower aspect ratio. Both of these latter trends are to be expected because of the documented effects of aspect ratio on induced drag and structural weight, respectively. A minimum gross weight criteria would favor an aspect ratio of about 4.5, while other performance parameters seem to be relatively insensitive as seen.

Wing thickness ratio. - Three wing thickness ratios were evaluated; 17 percent, 20 percent and 23 percent, at a gross payload of 600,000 pounds (272,155 kg) and a payload density of 15 lb/ft³ (240 kg/cm³). Aspect ratios of 5.4, 5.0, and 5.4 were established for the respective thicknesses by laying out corresponding wing designs to a consistent level of cargo loading efficiency while maintaining a relatively constant AR. The apparent irregularity in the variation of AR with thickness is due to the dimensional requirements of the cargo containers. The resulting aircraft and economic characteristics of primary interest are summarized in Figure 3-8. The minimum DOC_p favors (by only four percent) the thinner, larger wing because of the increase in cruise Mach number capability for the thinner wing (.65 compared to .61 for $t/c = .23$) and the better lift-to-drag ratio resulting from the lower profile drag. The four percent gain is thus the result of a balance between opposing effects of vehicle weight empty (cost), wing profile drag (fuel) and cruise Mach number.

According to the drag divergence capability of these wings shown in Figure 3-2, the assumed engine cycle was not able to cruise the vehicles into the initial drag rise as is customary with jet aircraft. The trends

FIGURE 3-7

EFFECT OF ASPECT RATIO ON LANDBASED SPANLOADER

$GPL = 600\ 000\ lb\ (272\ 155\ kg)$
 $S_W = 18\ 000\ ft^2\ (1672\ m^2)$
 $\rho_{PLG} = 15\ lb/ft^3\ (240\ kg/m^3)$
 $R = 3000\ n.\ mi.\ (5550\ km)$
 $\Lambda = 0$

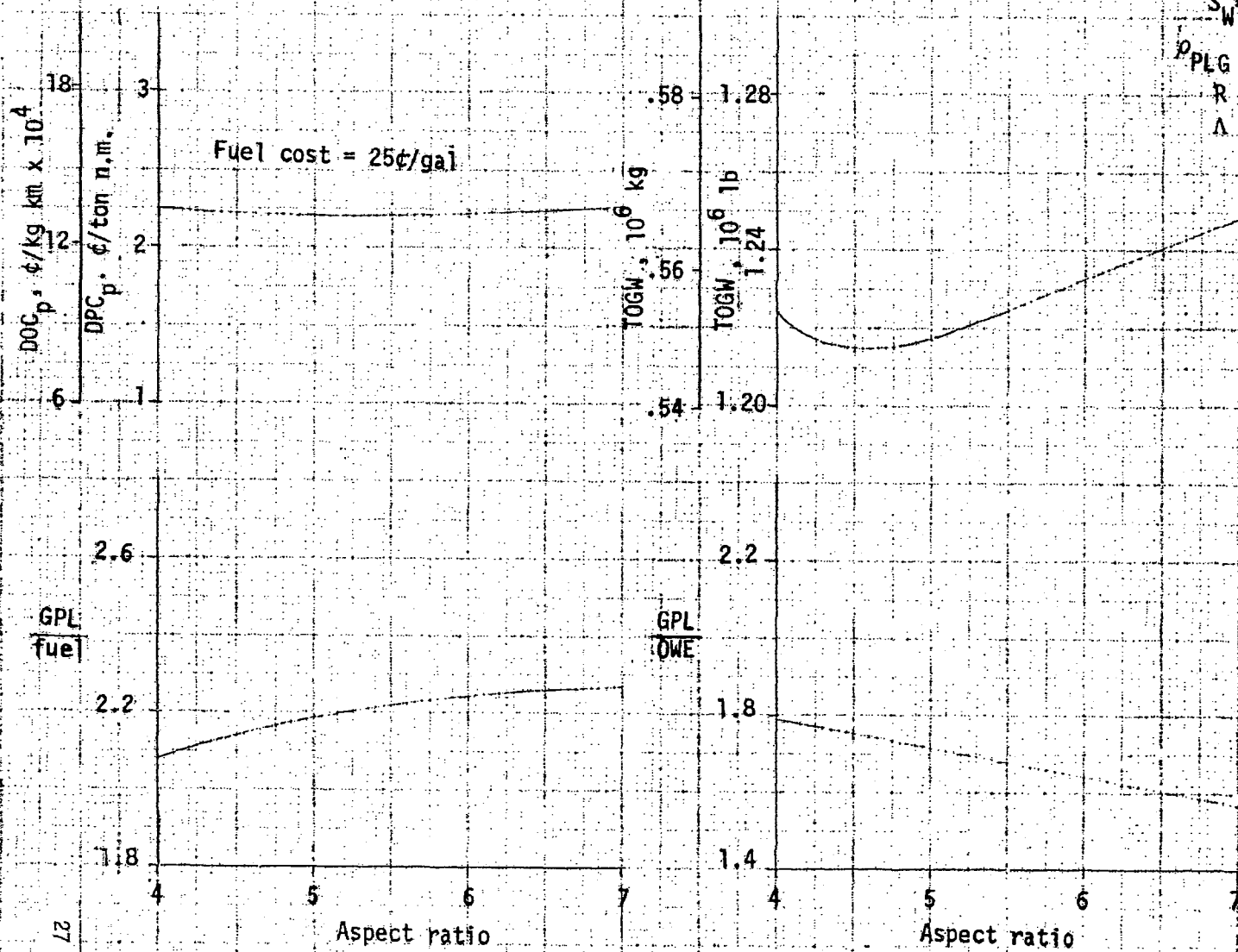
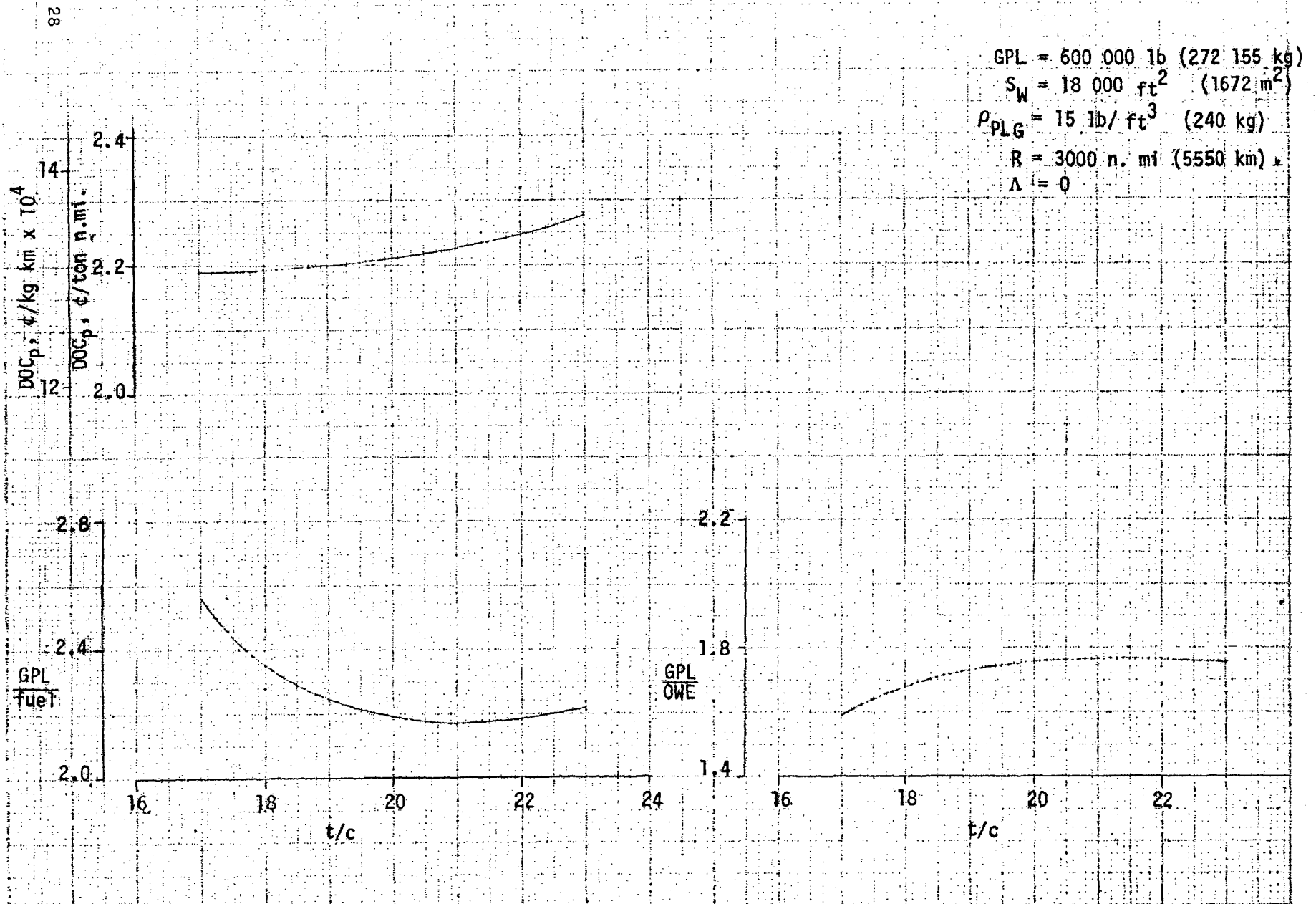


FIGURE 3-8
EFFECT OF WING THICKNESS ON LANDBASED SPANLOADER



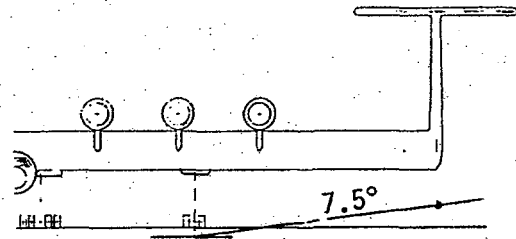
resulting from the many interacting effects shown in Figure 3-8, are valid; however, the use of optimum engine cycles could somewhat alter the level of the variations noted. The overall conclusion is that the effects of airfoil thickness on vehicle operating economics is probably small but favorable to the thinner wing.

Wing sweep. - A swept wing configuration was conceived with a 40 degree sweep and zero taper as shown in Figure 3-9. This configuration is designed for a gross payload of 600,000 pounds (272,155 kg) and a gross payload density of 15 lb/ft³ (240 kg/cm). It accordingly contains 32 containers arranged in two complete rows. With sufficient sweep (such as 40 degrees) the center aft fuselage, which normally functions only to support the empennage on the straight wing configurations, can be eliminated in favor of twin empennage assemblies mounted on the wing tips. However with intermediate degrees of sweep the tail arm is reduced sufficiently to preclude the use of wing mounted empennage assemblies and only a nominal gain in Mach number capability is obtained. Characteristics of the considered configuration are presented in Table 3-5.

The placement of the empennage at the wing tips has several advantages:

- o the vertical tails double as winglets thus saving structural weight and drag;
- o the aft fuselage can be eliminated with additional weight and drag savings as already stated;
- o the dead weight of the center fuselage and empennage of the straight wing partially destroy the benefits of the distributed span load concept. The mounting of the empennage at or near the wing tips in conjunction with other properly distributed dead weight components (engines, landing gears, cockpit, fuel, etc.) can provide more favorable moments of inertia within the wing with attendant structural weight savings.
- o a favorable downwash field exists in the vicinity of the wing tip mounted horizontal tails. A vortex lattice computer program was used to calculate this flow field. The downwash gradient $d\epsilon/d\alpha$ is only - .1 across the span of horizontal tail as located in Figure

FIGURE 3-9
SWEEP WING SPANLOADER



Gross Payload = 600,000 lbs (272,155 kg)

32 Containers

$\rho_{PLG} = 15 \text{ lb/ft}^3 \text{ (240 kg/m}^3\text{)}$

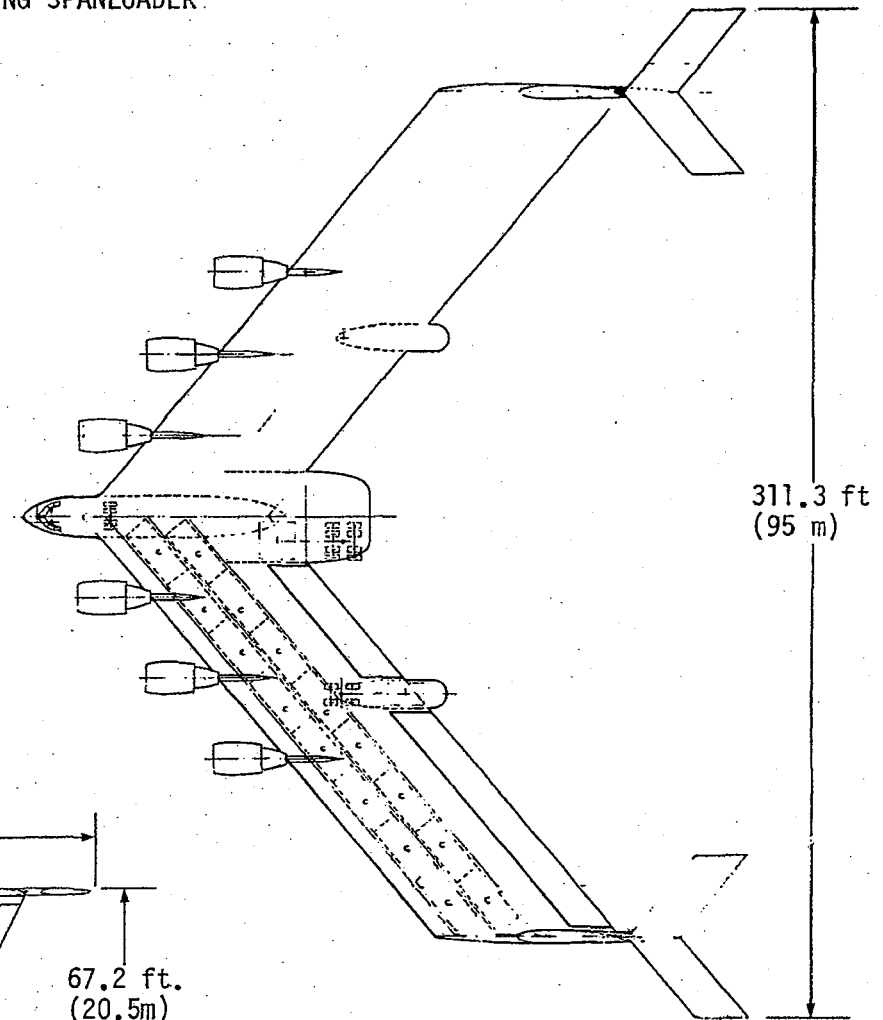
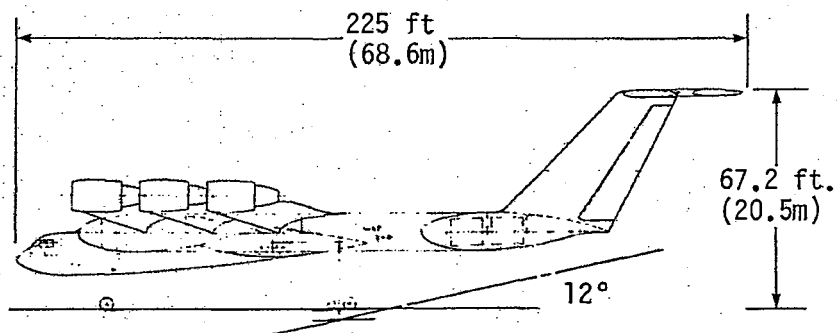


TABLE 3-5
WING SWEEP STUDY - SPANLOADER
GROSS P.L. = 600,000 lb (272,155 kg)
R = 3,000 n mi (5,550 km)
 $\Lambda = 40$

	<u>English</u>	<u>Metric</u>
Aspect Ratio	4.54	4.54
Wing Area $\text{ft}^2 (\text{m}^2)$	14,896	1,384
Wing Loading $\text{lb}/\text{ft}^2 (\text{kg}/\text{m}^2)$	74.9	367
Thrust/Engine lb (N)	40,000	177,920
Thrust to Weight Ratio	.2151	2.109
Takeoff Weight lb (kg)	1,115,746	506,102
Operating Weight Empty lb (kg)	296,978	134,709
Fuel Weight lb (kg)	218,768	100,585
Ratio Gross Payload Weight to Fuel Weight	2.743	2.743
Ratio Gross Payload Weight to Operating Weight Empty	2.020	2.020
Ratio Operating Weight Empty to Takeoff Weight	.266	.266
Cruise Mach Number	.701	.701
Initial Cruise Altitude ft (m)	31,090	9,476
Final Cruise Altitude ft (m)	35,406	10,792
DOC _p at 25¢/gal $\text{¢/ton n.mi. (¢/kg km)}$	1.850	1.102×10^{-3}
Field Length ft (m)	12,025	3,655

3.9, whereas it is approximately -.5 for the straight wing location. The horizontal tail areas for the swept wing can therefore be surprisingly small for a given stability level.

With lower $C_{L_{max}}$ available from the swept wing ($C_{L_{max}} = 1.03$ for $\Lambda = 40$ vs. $C_{L_{max}} = 1.34$ for $\Lambda = 0$, and the higher wing loading (74.9 vs. 67.6 lb/ft² (365.7 vs. 330.1 kg/m²)) the swept wing configuration requires a simple flap as shown in Figure 3-9 to achieve the 12,000 foot (3.658 m) field length. While performance with the wing-tip empennage appears favorable there are many stability and control questions that require investigation. As an example, there is the question of mutual interference between the wing and tail that may cause premature separation on the tail in the region of the wing-tail juncture. This problem is similar to but more complex than the weight problem and hence could be analyzed by modifying existing methods utilizing the vortex-lattice technique.

Range performance: The variation of key design parameters with design ranges from 2,000 (3,700 km) to 6,000 nautical miles (11,101 km) is shown in Figure 3-10. The decay in PL/Fuel and PL/OWE as well as the required increase in gross weight with increasing design range is as expected. The sensitivity of DOC_p to design range is mild with a flat optimum around 3,500 nautical miles (6,475 km).

Other performance data has been parametrized and is presented in Figure 3-11. A review of these data shows the 12,000 foot (3,658 m) takeoff field length becoming critical for a range of about 3,500 nautical miles (6,476 km) and second segment climb becomes FAR critical for 5,500 nautical miles (10,176 km). At these or greater ranges flaps would be required to maintain the specified field length. Although the cruise Mach number varies only slightly with range the initial cruise altitude decreases markedly as the range is increased.

Payload variables: The size and density of the payload were parametrically considered along with environmental requirements for their impact on the landplane spanloader design characteristics and performance.

Design payload. - Design payload variations at a given design range are shown in Figure 3-12. The improvement in vehicle efficiency with increasing payload size is evident (PL/Fuel, PL/OWE). Takeoff field length increases

FIGURE 3-10
THE EFFECTS OF RANGE ON LANDBASED SPANLOADER

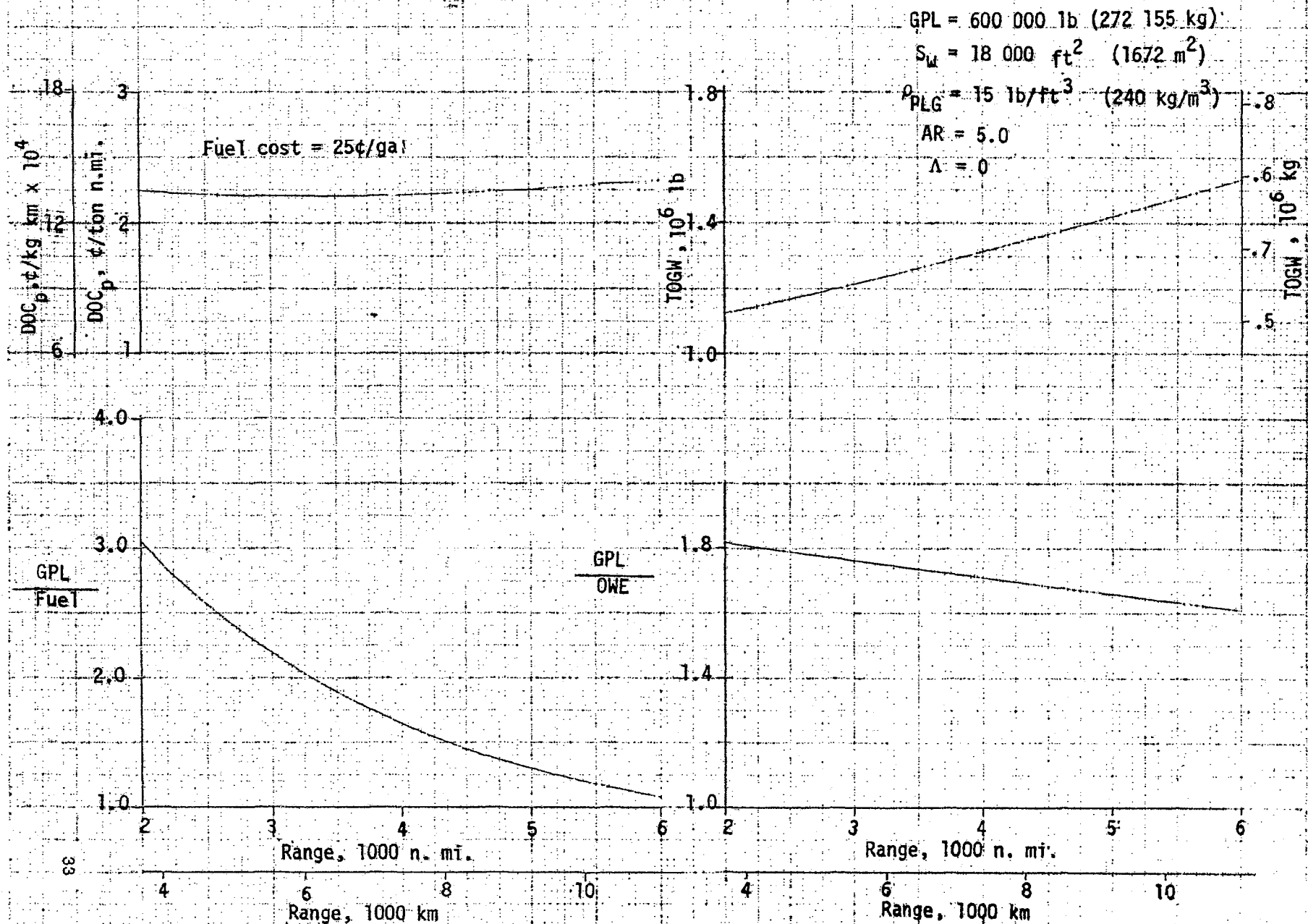


FIGURE 3-11

EFFECT OF RANGE ON LANDBASED SPANLOADER PERFORMANCE

$GPL = 600,000 \text{ lb}$
 $S_w = 18,000 \text{ ft}^2$
 $\rho_{PLG} = 15 \text{ lb/ft}^3$
 $AR = 5.0$
 $\Lambda = 0$

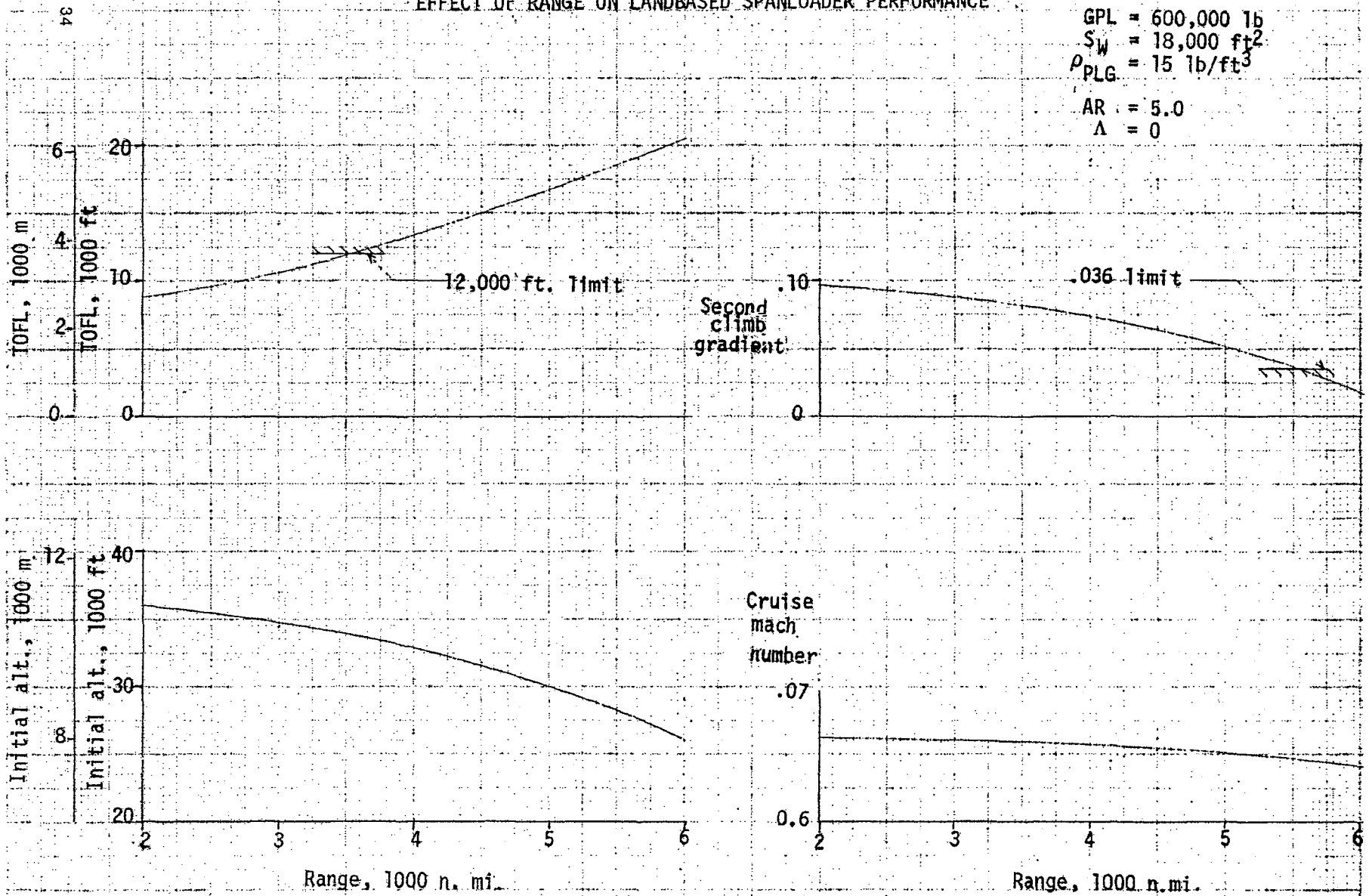
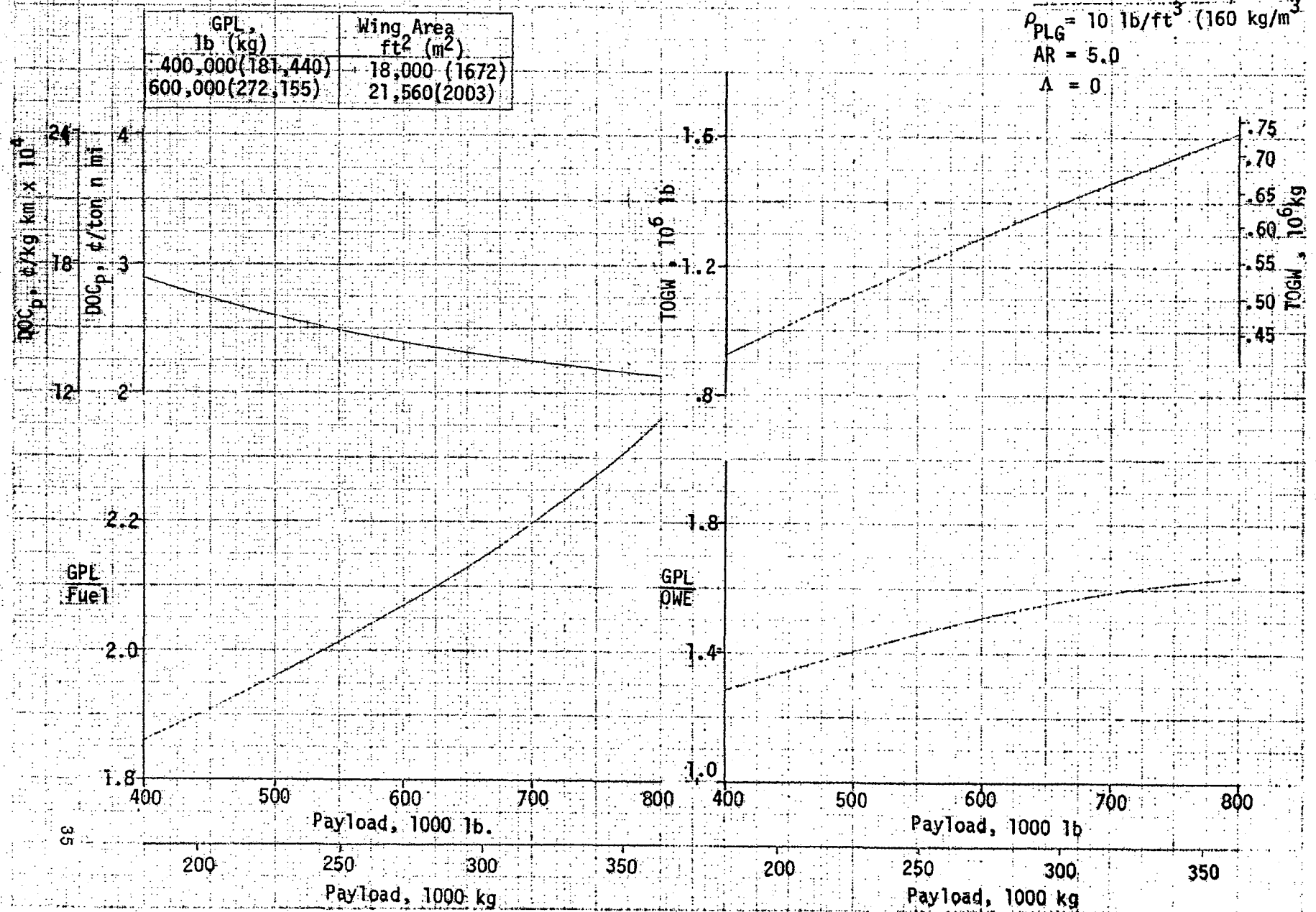


FIGURE 3-12

THE EFFECTS OF PAYLOAD ON LANDBASED SPANLOADER



and second segment climb gradient decreases as payload increases, although neither one is critical and flaps are not required. Cruise Mach number and initial cruise altitude both decrease as payload increases.

Payload density. - Payload density also has a pronounced effect upon the vehicle operating efficiency since in conjunction with the selected container size it is the determining factor in sizing the wing area. The data of Figure 3-13 shows the lower DOC_p and more efficient vehicle to result at the higher density.

The takeoff field length increases with increasing payload density (ρ_{PLG}) to the point of becoming critical at a payload density of 18 lb/ft^3 (288 kg/m^3). Density exceeding this value would necessitate the application of flaps to maintain the 12,000 foot (3,658 m) takeoff limit. The second segment climb gradient decreases with increasing density as does cruise altitude but the variation of cruise Mach number is small.

Cargo pressurization. - Two methods of providing pressurization for the cargo were evaluated. The two approaches consist of (1) pressurizing the entire cargo compartment to 5 psia (34,475 Pa) (18,000 foot (5,486 m) pressure altitude at 42,000 feet (12,802 m)) and (2) pressurizing special containers for use only when commodities carried require pressurization.

The pressurized boundaries of the vehicle for the first approach are shown in Figure 3-14. Structural weight penalties in the skin panels, ribs and spars required to support pressurization loads were determined and are summarized in Table 3-6. Also shown is the pneumatic pressurization system weight required to supply the conditioned air. These values represent dead weight penalties and do not account for the normal weight growth factors necessary to maintain constant performance.

The container design used in the second approach is shown in Figure 3-15 and used a rounded upper contour to minimize the weight penalties. The container, however, has 21.9 percent less volume than the standard $8 \times 8 \times 20$ foot ($2.44 \times 2.44 \times 6.10 \text{ m}$) container used in the study. The container density is increased from 1.50 lb/ft^3 to 2.42 lb/ft^3 (24.0 to 38.8 kg/m^3) or a penalty of 500 pounds (227 kg) per container. Again a pressurization system must be added which would require less capacity than that for the completely pressurized compartment, but would require more equipment.

FIGURE 3-13

EFFECT OF PAYLOAD DENSITY ON LANDBASED SPANLOADER

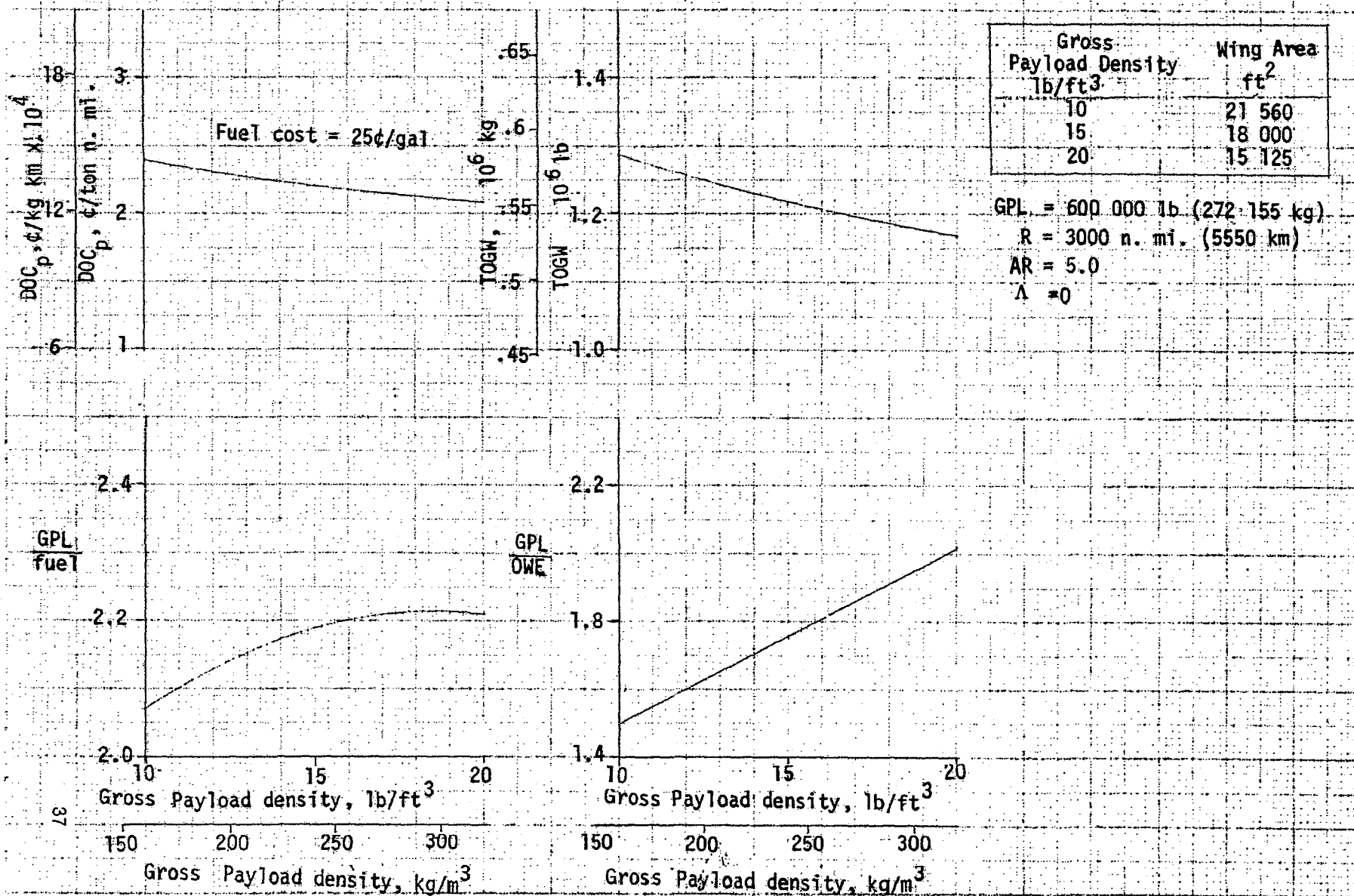


FIGURE 3-14

CARGO COMPARTMENT PRESSURIZATION

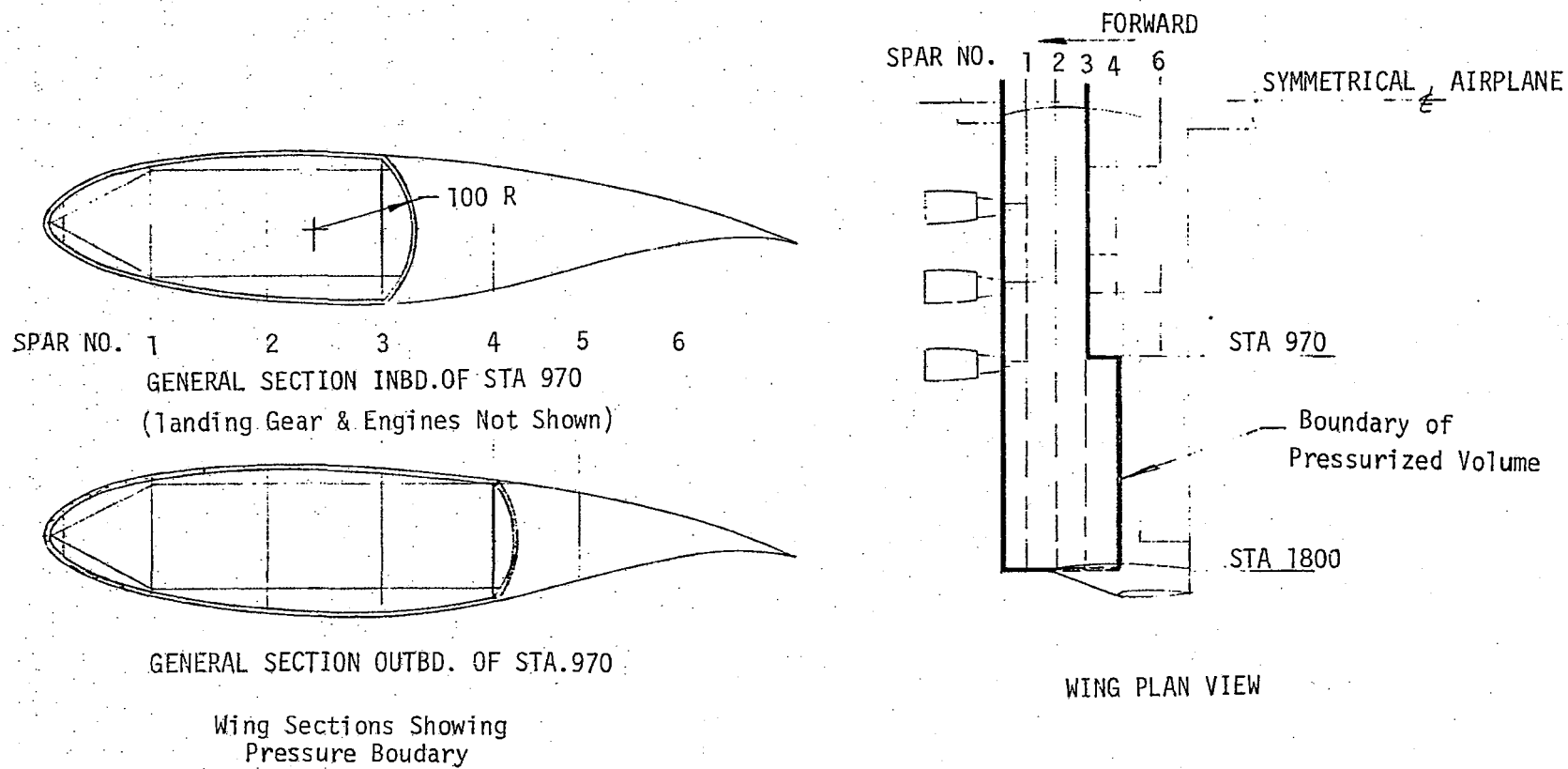


TABLE 3-6
 LANDBASED SPANLOADER PRESSURIZATION STUDY SUMMARY

Structural Section	$\Delta \bar{t}$		Δ Weight	
	inches	mm	lb	kg
Upper Skin Panel	0	0	0	0
Lower Skin Panel	.010	(.254)	963	(446)
Leading Edge Skin	.010	(.254)	403	(183)
Ribs	see curve		3,404	(1,544)
Spar No. 3 or 4	.086	(2.184)	3,930	(1,783)
End Rib & Door	.086	(2.184)	965	(438)
Structural Total			9,685	(4,394)
Pressure Subsystem Weight			8,799	(3,991)
Total Penalty			18,484	(8,385)

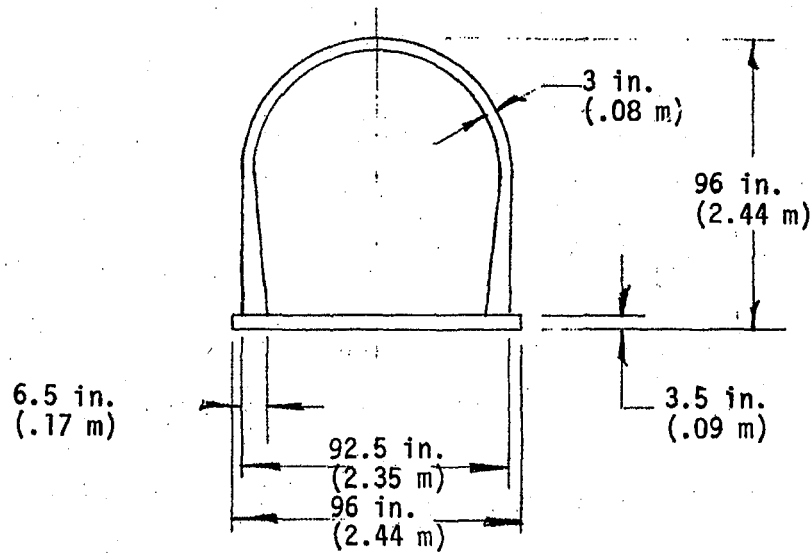
1. For spar weight penalty, \bar{t} of spar must be increased by $\Delta \bar{t}$ then the total increased by the difference in height between the curved and flat webs.

2. $\Delta \bar{t}$ represents additional thickness of distributed material required in pressurized areas.

3. No penalty in fuel tank bays.

4. Leading edge rib penalty same as ribs between spars 1 and 2.

FIGURE 3-15
CONTAINER PRESSURIZATION



Container Section

Weight Penalties For Container Pressurization
5 psia (34,475 Pa)

Component	Δ Weight	
	lbs	kg
42 Containers	21,000	9,526
Pressure Subsystem	<u>6,091</u>	<u>2,763</u>
Total Penalty	27,091	12,289

because of the distribution system necessary to service each container. A summary of the weight penalties using this approach is also shown in Figure 3-15.

Economic variations: All parametric calculations were performed at three values of fuel cost; 10, 25 and 40¢ per gallon and sensitivities determined. Figure 3-16 shows that the choice of optimum aspect ratio increases with increasing fuel costs although not rapidly ($AR_{opt} = 4.5$ to 5.0 for 10¢/gallon to 40¢/gallon, respectively). Also, as shown previously the sensitivity of DOC_p to the selection of optimum aspect ratio is very small. There appears to be little incentive to select configuration aspect ratio based on operating economics for the spanloader concept.

The variation of optimum design range with fuel cost also is very small as shown in Figure 3-16. For design payload and payload density, no optimum values appear within the limits of the values analyzed.

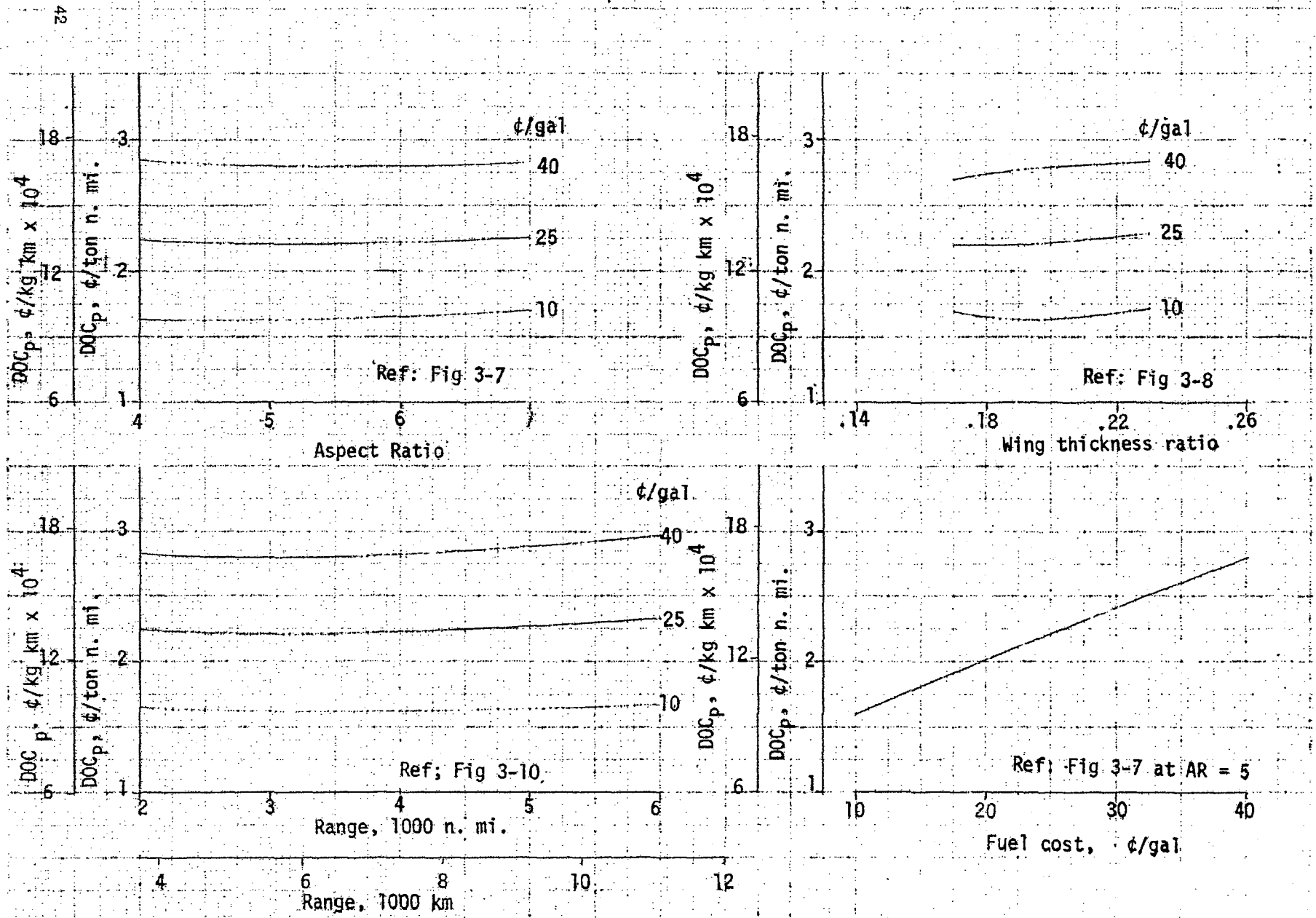
The wing thickness ratio analysis, Figure 3-16, shows the optimum thickness to be about 20 percent for low fuel costs (10¢/gallon) but to be less than 17 percent for the two higher fuel cost values used. This trend results from the lower C_{D_0} value of the thinner wing, particularly at the higher fuel costs.

Finally, Figure 3-16 shows the variation in DOC_p with fuel costs for the parametric baseline aircraft $AR = 5.0$, $R = 3.000$ nautical miles (5,550 km), Gross PL = 600,000 pounds (272,155 kg), and $\rho_{PLG} = 15 \text{ lb/ft}^3$. A four-fold increase in fuel costs results in a 70 percent increase in DOC_p .

Hybrid seaplane parametric results. - The parametric results for the hybrid seaplane study are summarized in this section. For the seaplane spanloader, the performance design optimization technique is different than that used for the landbased spanloader. A primary design requirement is that of overcoming the traditional hydrodynamic hump drag which occurs long before the lift off speed is reached. Existing seaplanes require a thrust-to-weight ratio of about .35 for reasonable takeoff accelerations. The hybrid seaplane used for this study is unique in that it employs the augmented ram wing concept which permits a lower design thrust-to-weight ratio of about .17 for takeoff. Another unique feature of this hybrid seaplane concept is that it can use and has optimum performance at a high

FIGURE 3-16

ECONOMIC TRANDS OF LANDBASED SPANLOADER



wing loading due to the augmented propulsive lift derived from the canard mounted engines. The limitation to the cruise in-ground-effect mode also permits a higher wing loading than usual due to the limited rate of climb or excess thrust required. The thrust-to-weight ratio of .17 and a wing loading of 255 lb/ft^2 ($1,245 \text{ kg/m}^2$) was therefore used as limiting design criterion for the purposes of this study.

The parametric results are summarized in Figures 3-17 and 3-18 for the aspect ratio, payload density and range trends, respectively. The impact of using a higher aspect ratio wing is substantial, providing a 11 percent improvement in DOC_p for an aspect ratio increase from two to four. Although these data indicate the potential for further gain with aspect ratio any such findings would be premature since test data on the augmented lift concepts is presently limited to an aspect ratio of two. Any extension of these data to higher aspect ratios must be qualified by an ever decreasing level of confidence. An extension to aspect ratio six would exceed the considered range of reasonable doubt. The improvement due to increased cargo density is as expected because of the smaller hull size possible for the higher densities.

The degradation in performance with increasing range (Figure 3-18) is also expected but is more accentuated than for the spanloader because of the higher fuel flow of the seaplane due to its sea level mission. This point is discussed in more detail in the following section.

3.4 Concept Selection

Based on the parametric trends presented above a comparison of the characteristics of the straight wing spanloader, swept wing spanloader and hybrid seaplane is made. The prime parameters compared are DOC_p , PL/Fuel and PL/OWE. In order to make consistent comparisons, one adjustment was made to the selected straight wing spanloader. This adjustment consisted of decreasing the wing area of the previously discussed Parametric Baseline, aspect ratio 5, straight wing spanloader to increase the cargo packing efficiency to a level of that of the swept wing configuration and hybrid seaplane. The latter two concepts represent the minimum wing area and fuselage volumes, respectively, possible for the study payloads and payload densities. This decrease in the area of the straight wing was about

FIGURE 3-17

EFFECT OF PAYLOAD DENSITY FUSELAGE LOADED SEAPLANE

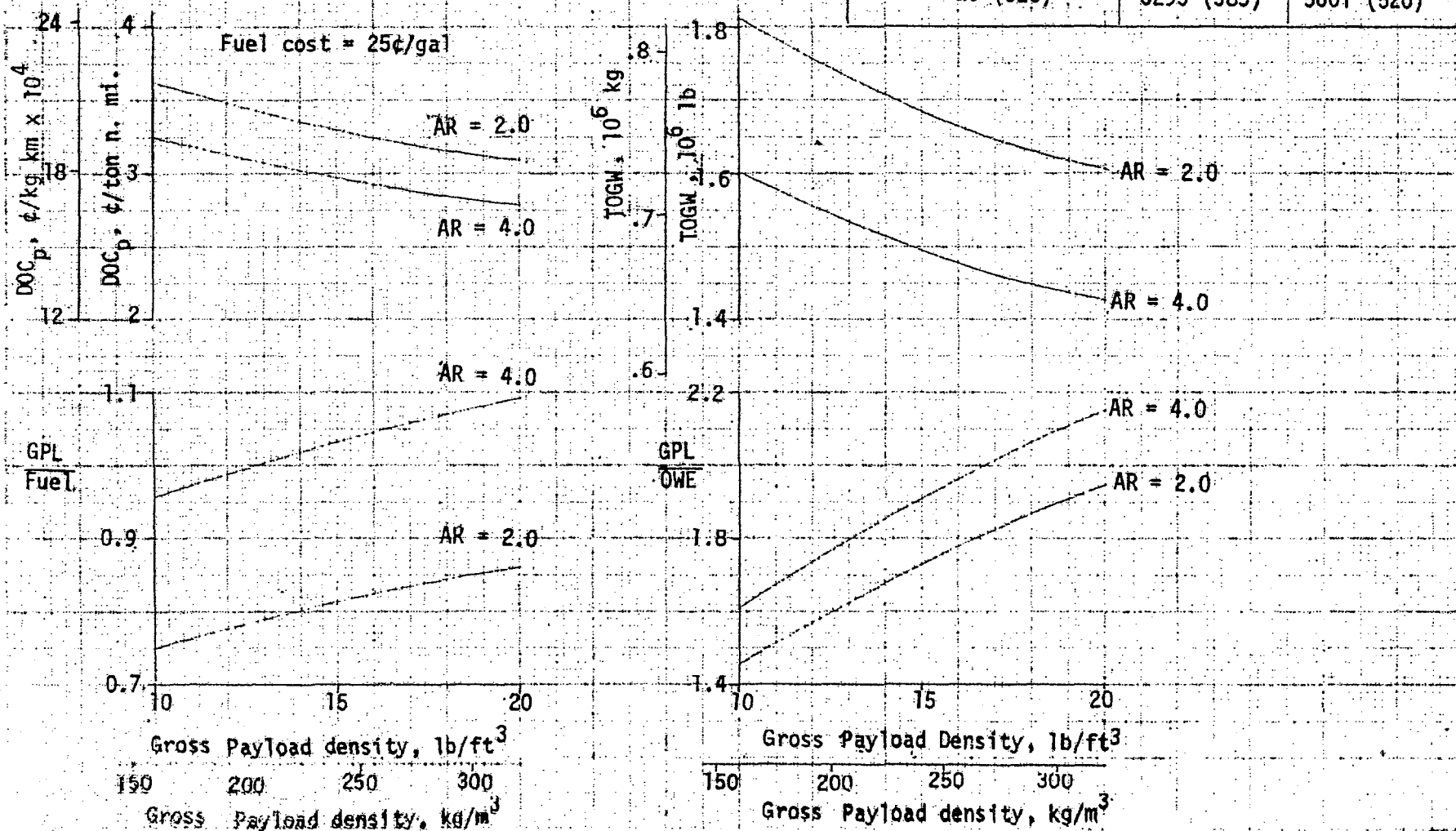
$R = 4500 \text{ n. mi. (8326 km)}$

$GPL = 600\,000 \text{ lb (272\,155 kg)}$

$WS = 255 \text{ lb/ft}^2 (1245 \text{ kg/m}^2)$

$I/W = 0.17$

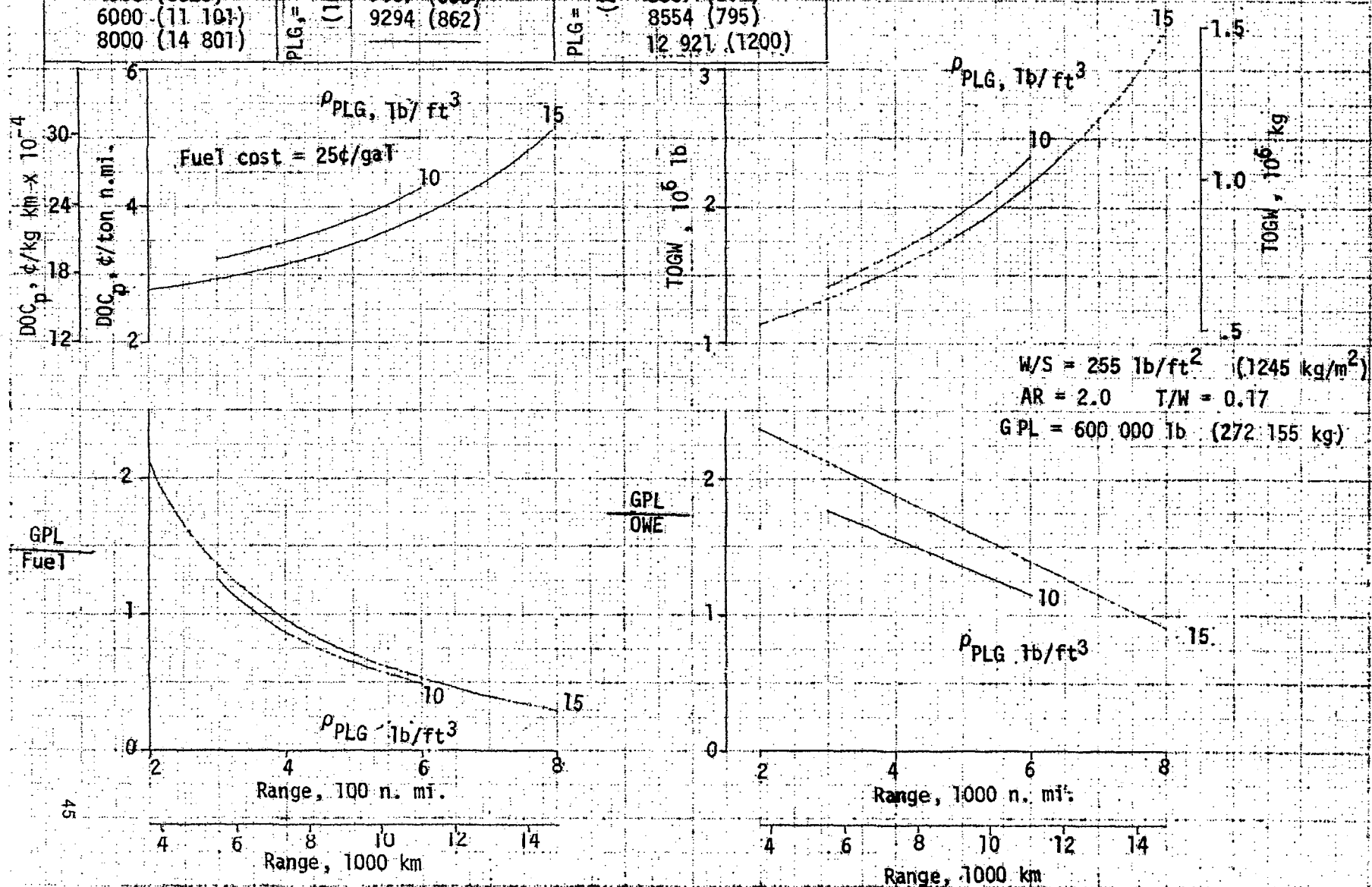
$p_{PLG}, \text{lb/ft}^3 \text{ (kg/m}^3\text{)}$	$AR = 2$	$AR = 4$
	$S_W, \text{ft}^2 \text{ (m}^2\text{)}$	$S_W, \text{ft}^2 \text{ (m}^2\text{)}$
10 (160)	7107 (660)	6277 (583)
15 (240)	6607 (614)	5865 (545)
20 (320)	6295 (585)	5601 (520)



R, n. mi. (km)	$\rho_{PLG}, \text{lb/ft}^3$ (160 kg/m ³)	$S_W, \text{ft}^2 (\text{m}^2)$	$\rho_{PLG}, \text{lb/ft}^3$ (240 kg/m ³)	$S_W, \text{ft}^2 (\text{m}^2)$
2000 (3700)				4456 (414)
3000 (5550)		5562 (517)		5203 (483)
4500 (8326)		7107 (660)		6607 (614)
6000 (11 101)		9294 (862)		8554 (795)
8000 (14 801)				12 921 (1200)

FIGURE 3-18

EFFECT OF RANGE ON FUSELAGE LOADED SEAPLANE



3,000 ft² (278.7 m²) which places all three generic type of configurations on the same cargo containment efficiency level as the Point Design aircraft discussed in Section 4.0

Figures 3-19 through 3-21 show a comparison of these vehicles. The swept wing spanloader has the highest potential for payoff in DOC_p and PL/Fuel factors followed by the straight wing spanloader and the hybrid seaplane. The superiority of the swept wing version results from its superior lift-to-drag ratio and weight empty-to-gross weight ratio. The general inferior standing of the seaplane results primarily from the high fuel flow of the fan jet engines due to its sea level cruise mode. Engines specifically optimized for the seaplane mission or the use of turboprop engines would greatly improve the relative standing of the seaplane. The seaplane, because of its extremely low OWE/TOGW ratio, has superior performance when compared on the basis of payload carried per pound of vehicle weight (PL/OWE).

The effect of aspect ratio is shown in Figure 3-19. The spanloader configuration is generally insensitive to aspect ratio, although the seaplane is highly sensitive. This is again the result of the high seaplane fuel flow and the extreme low aspect ratios of these configurations. Indications are that the hybrid seaplane could benefit significantly from the use of higher aspect ratios.

The payload density trends of Figure 3-20 also show the general trends and alignments between the generic classes. The range trends of Figure 3-21 show the unfavorable fuel trends (DOC_p) with increasing range of the seaplane and the high efficiency of the swept wing spanloader.

The straight wing type of spanloader has been selected for detailed analysis in the subsequent section and for comparison to a conventional all-freighter configuration. As stated above, this vehicle does not represent the most efficient spanloader configuration as evolved from the parametric studies, the swept wing having lower operating costs. However, the swept wing configuration evaluation was conducted late in the study and no variational trends were derived for it. The decision was therefore made to retain the straight wing for detailed analysis since considerable optimization data was accumulated for it as presented in this section.

FIGURE 3- 19

ASPECT RATIO EFFECTS AS FUNCTION OF AIRCRAFT CONCEPT

GPL = 600 000 lb (272 155 kg)

R = 3000 n. mi. (5550 km)

$\rho_{PLG} = 15 \text{ lb/ft}^3 \text{ (240 kg/m}^3\text{)}$

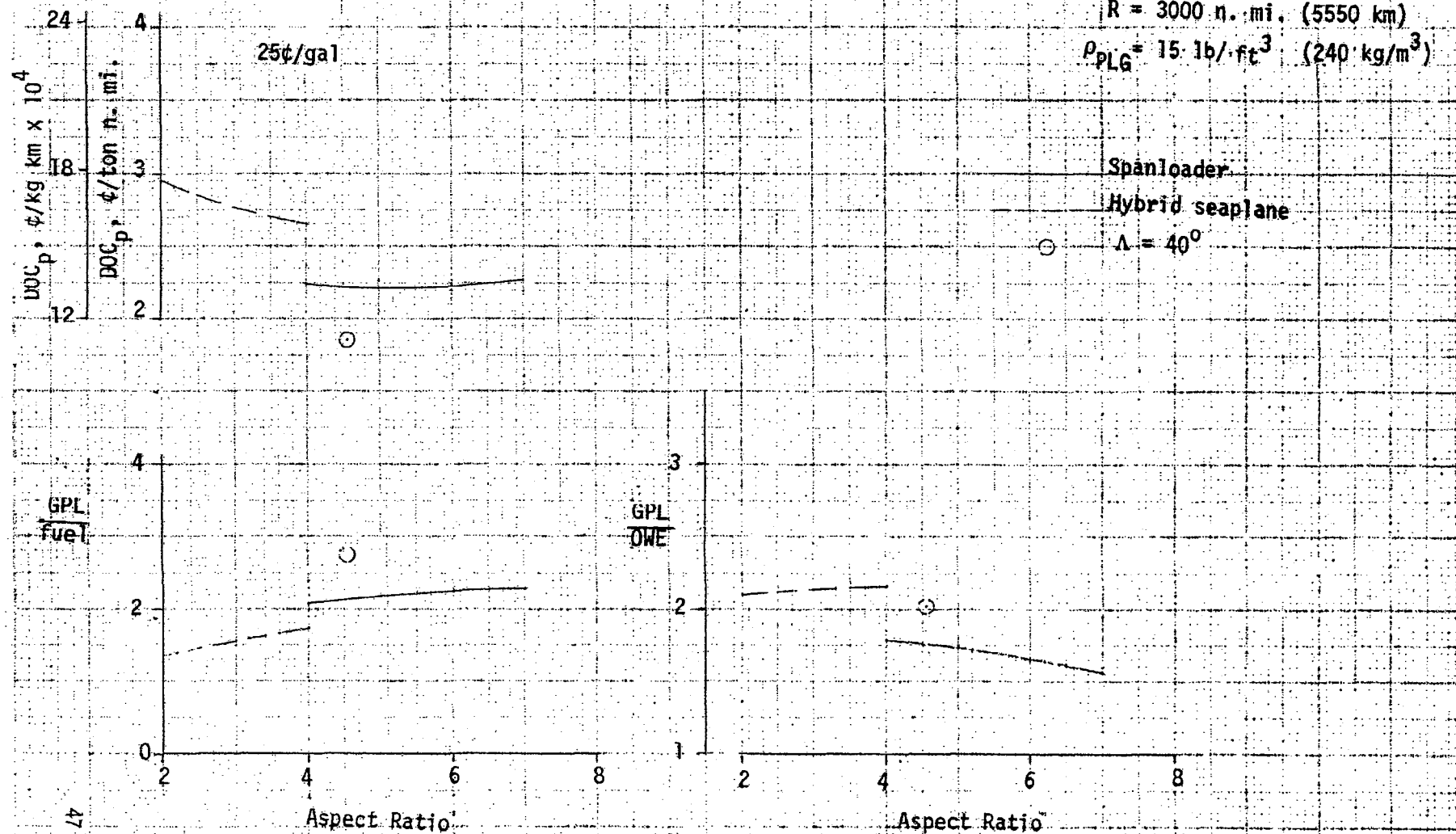


FIGURE 3-20

PAYLOAD DENSITY EFFECTS AS FUNCTIONS OF AIRCRAFT CONCEPT

GPL = 600 000 lb (272 155 kg)

R = 3000 n. mi. (3550 km)

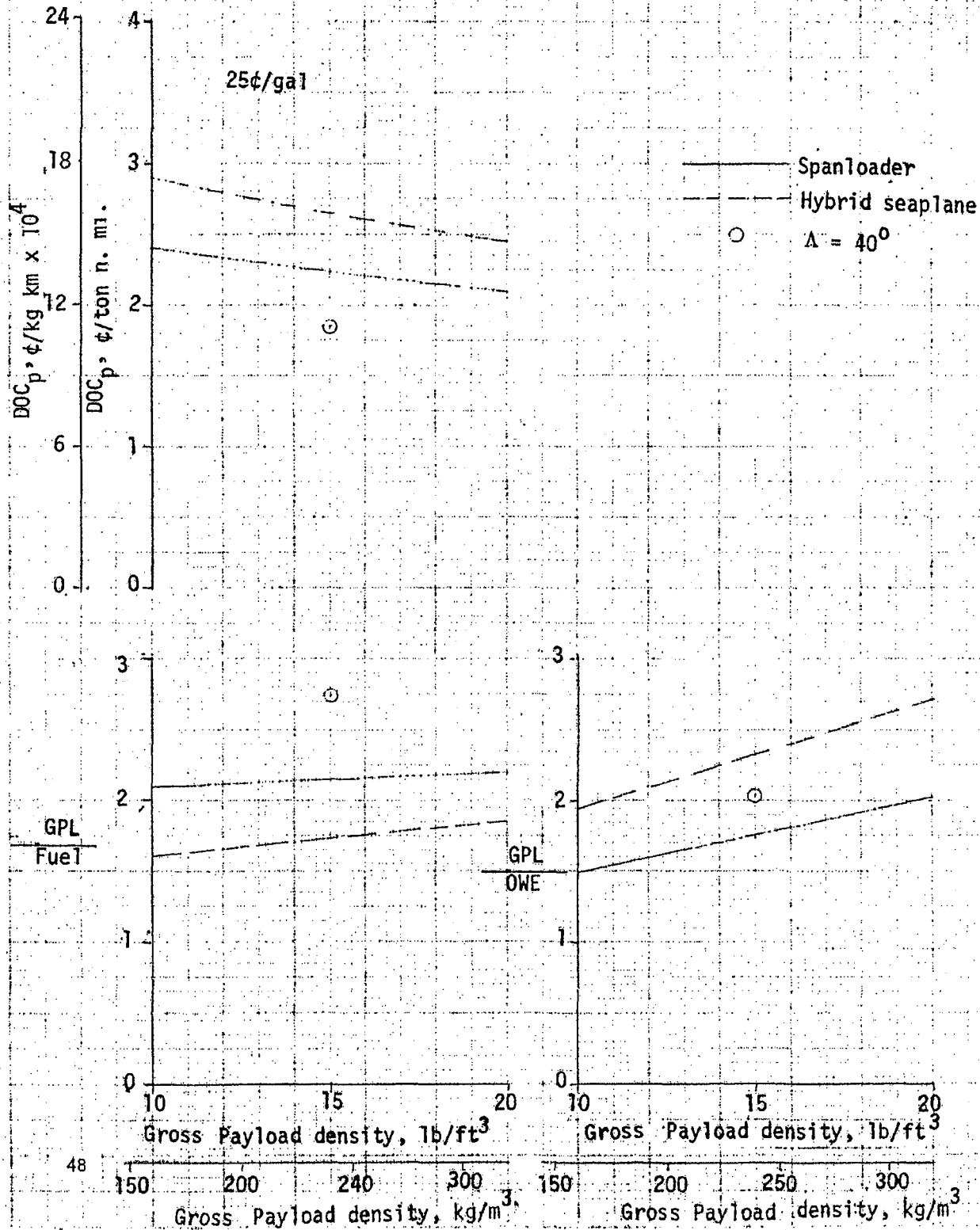
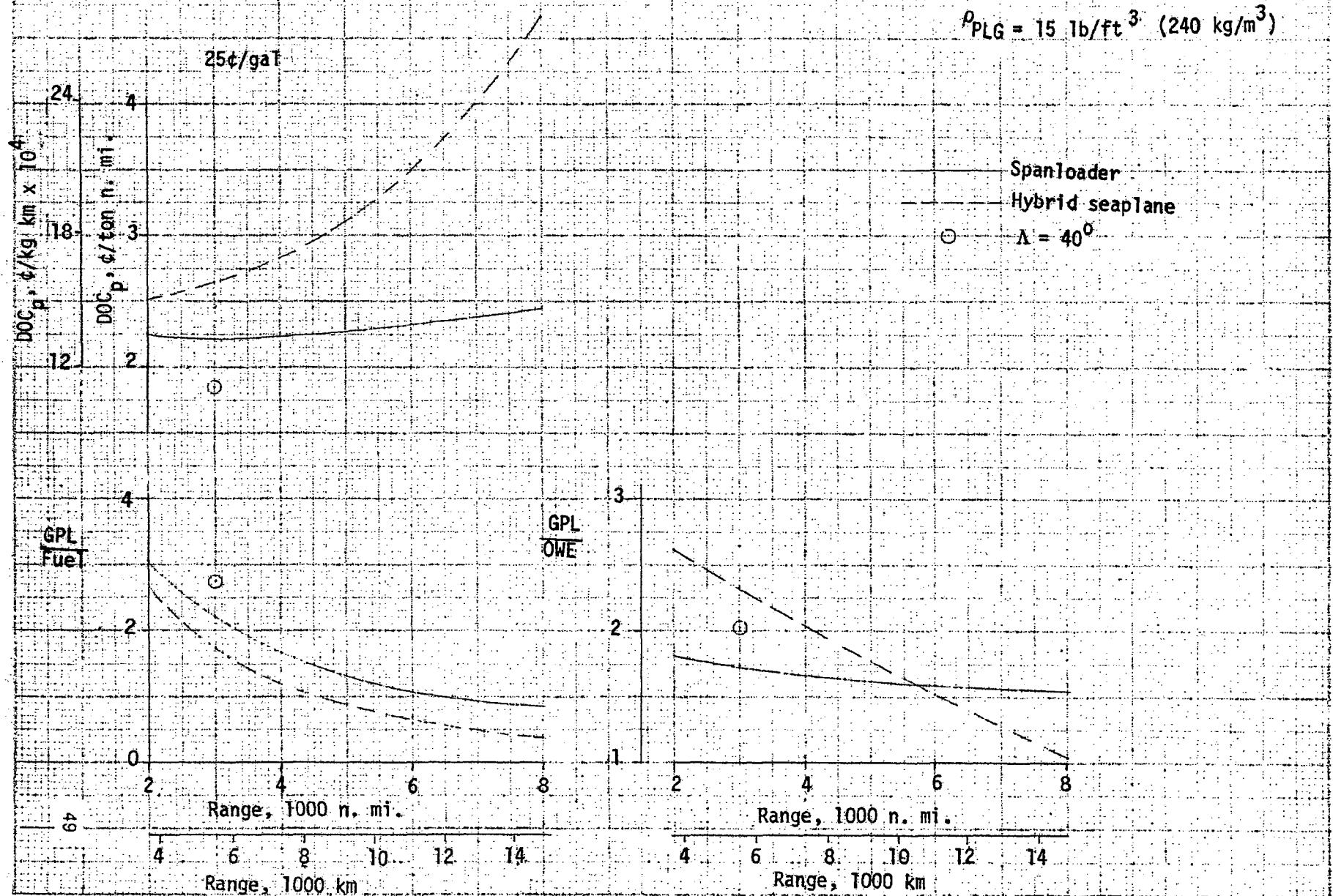


FIGURE 3-21

RANGE EFFECTS AS A FUNCTION OF AIRCRAFT CONCEPT

GPL = 600 000 lb (272 155 kg)

$\rho_{PLG} = 15 \text{ lb/ft}^3 \text{ (240 kg/m}^3\text{)}$



In addition, the straight wing configuration represents the simplest structural concept with lowest acquisition cost potential, simple loading through either or both wing tips with a minimum terminal complexity, and a lower required technology base for implementation.

Future studies should be conducted and should retain the three generic concepts with optimized engine cycles (including turboprop designs). The ultimate relationship between these concepts, however, largely hinges upon their relative advantages within a total cargo system context.

4.0 DETAILED CONFIGURATION ANALYSIS

Based on the parametric trend studies presented in Section 3.0, a straight wing spanloader configuration (Point Design) was selected for detailed analysis. This section discusses this selection and presents the detailed configuration, performance and economic characteristics of the resulting Point Design configuration along with a summary of the characteristics for a conventional all-freight aircraft designed to the same mission requirements and technology level. Because of the extensive understanding available for the conventional approach, however, this section places emphasis upon the analyses of the spanloader configuration only.

4.1 Point Design Spanloader Description

Prior to discussing the detailed analyses of the aerodynamic, structure and weight properties of the Spanloader Point Design aircraft, the governing design requirements and general characteristics of the configuration are presented.

Configuration selection. - The prime factor which sets configuration geometry is the cargo characteristics which determines the minimum wing area required. The wing area in turn determines empennage and winglet geometry. Standard 8 x 8 x 20 foot (2.44 x 2.44 x 6.10 m) containers are used throughout the study although taller containers of other lengths in multiples of 10 feet (3.05 m) are currently being considered. A total system oriented study based on the spanloader concept has not been conducted and system parameters such as optimum payload size or payload density have not been determined. The choice of payload size is contingent upon route characteristics such as anticipated payload availability, frequency of service, secondary distribution system requirements as a function of spanloader terminal site location, and a host of other considerations. Payload density depends upon the nature of world wide cargo anticipated for the operational time frame of the system. It also depends upon the capture of new markets by the spanloader system due to its potentially lower operating costs relative to conventional air freight systems.

Selections of payload size and density have therefore been made based upon the best available current information. The selected nominal gross payload size of 600,000 pounds (272,155 kg) offers a reasonable incremental

capability compared to the current system capacity of 190,000 pounds (86,184 kg) for the C-5A and 225,000 pounds (102,060 kg) for the 747F. The consensus of industry sources centers upon a net payload density (ρ_{PLN}) of approximately 10 pounds per cubic foot (160 kg/m^3), which differs little from today's values, as the more likely cargo density to be considered for the spanloader time frame. To this selected value of cargo density is added an average container density (ρ_{TARE}) of 1.50 pounds per cubic foot (24 kg/m^3) giving a gross payload density of 11.50 pounds per cubic foot (184 kg/m^3) to be applied to wing sizing and design.

With a gross density of 11.50 pounds per cubic foot (184 kg/m^3) the gross weight of each 8 x 8 x 20 foot ($2.44 \times 2.44 \times 6.10 \text{ m}$) container is therefore $8 \times 8 \times 20 \times 11.5 = 14,700$ pounds (6,668 kg) and the corresponding fractional number of containers for the 600,000 pound (722,155 kg) payload is $600,000 \div 14,700 = 40.8$. For aspect ratios in the neighborhood of 4.5 to 5.0 this number of containers dictates the 3-row cargo compartment configuration shown in the Point Design spanloader three-view drawing of Figure 4-1. However, in order to efficiently use the available wing volume each row of containers should be completely filled and thereby provides space for 42 containers, 14 in each row. On this basis the actual design gross payload was defined to be $42 \times 14,700 = 618,000$ pounds (280,325 kg) which has been used throughout the Point Design spanloader analysis. Compatible with the wing cargo compartment, the landing gears are arranged into two inboard and two outboard bogies mounted to the rear spar in a manner similar to that for the parametric aircraft. The fuel is contained within the inboard wing leading edge.

The wing geometry is further defined by the selection of a nominal wing thickness ratio of 20 percent. As shown in the parametric studies the impact of wing thickness ratio on DOC_p was small with a slight favor toward the thinner wing. The ratio $GPL/fuel$ also favors the thinner wing although the fraction GPL/OWE favors the thicker wing because of the better $OWE/TOGW$ ratio of the thicker configuration. A nominal value of 20 percent thickness was chosen because the majority of parametric analysis and understanding was accumulated at this value and the payoff for using a thinner wing was small. Future studies should perhaps use a thinner wing.

The preceding payload characteristics and airfoil geometry are

FIGURE 4-1
POINT DESIGN SPANLOADER

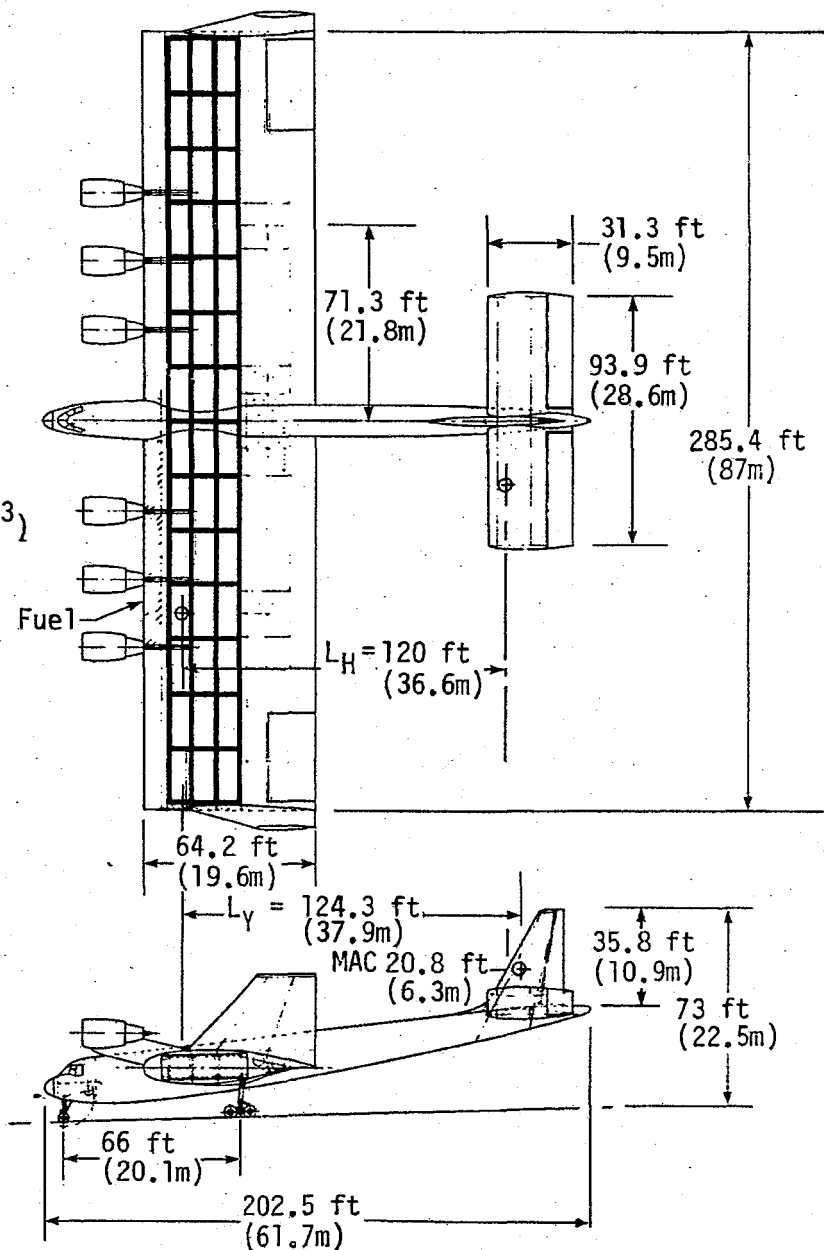
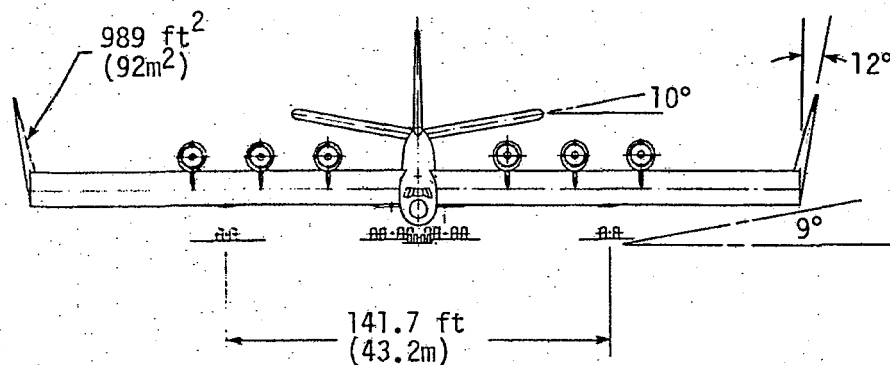
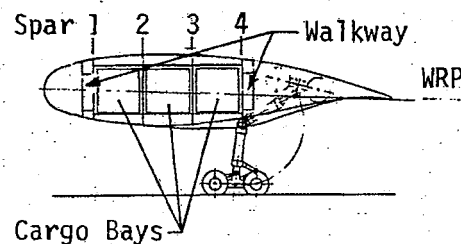
CHARACTERISTICS DATA			
	WING	H. TAIL	V. TAIL
AREA	18,314 ft ² (1701m ²)	2,938 ft ² (273m ²)	674 ft ² (62.6m ²)
AR	4.45	3.0	1.9
T.R.	1.0	1.0	0.3
Δ , C/4	0°	0°	23°
t/c	.20	.12	.12
Vol. Ratio		.30	.016

Gross Payload = 618,000 lbs (280,325 kg)

42 Containers $\rho_{PLN} = 10 \text{ lb/ft}^3 (160 \text{ kg/m}^3)$

$\rho_{TARE} = 1.50 \text{ lb/ft}^3 (7.38 \text{ kg/m}^3)$

TOGW = $1.35 \times 10^6 \text{ lbs (612,343 kg)}$



compatible with a minimum wing chord of 64.17 feet (19.56m), and a minimum span of 285.42 feet (87.00 m) resulting in an aspect ratio of $285.42 \div 64.17 = 4.45$.

Conventional ailerons are used and large fixed winglets with some outboard cant give the wing a much larger effective aspect ratio than the geometric value. The winglets are staggered (mounted aft) on the wing tip to avoid viscous separation problems in the wing/winglet intersection. The large wing area required to contain the payload results in a takeoff wing loading that is sufficiently low to negate the need for a high lift system to achieve the 12,000 foot (3,658 m) maximum field length requirement.

A conventional fuselage is used to support the empennage surfaces which are also conventional except for their size. The horizontal tail is sized for a negative longitudinal static margin of -10 percent MAC. This design philosophy is not only desirable from the standpoint of minimizing required tail area, it is also necessary because the spanloader configuration results in a center of gravity location as far aft as 43 percent MAC with partial payloads. In fact, it would be difficult to conceive of a straight wing spanloader design with a c.g. in the normal forward range. The straight, zero taper horizontal tail is in keeping with the general design philosophy of emphasizing structural simplicity and low cost.

A table of design data for the Basepoint Spanloader aircraft is summarized in Table 4-1.

Six high bypass ratio 9 engines are mounted in an over-the-wing arrangement permitting a relatively short landing gear and providing the potential for possible induced drag benefits due to favorable engine exhaust-wing flow effects. For the Point Design, DOC_p was calculated as a function of engine thrust (Figure 4-2), and was found to be minimized at a thrust of 52,500 pounds (233,520 N) per engine for the 25 cents per gallon fuel cost. However, the takeoff field length of 12,842 feet (3,914 m) exceeded the desired maximum. Increasing the thrust to 55,000 pounds (244,640 N) reduced the takeoff field length to 11,949 feet (3,642 m) with a sacrifice of .08 percent in DOC_p and an attendant increase in engine weight. In all cases the engine weight was varied with thrust. At a thrust level of 58,500 pounds (250,208 N) the corresponding takeoff weight was $1.35 \times$

TABLE 4-1
POINT DESIGN SPANLOADER
DESIGN DATA AND GEOMETRY

	English	Metric
Design Weights - lb (kg)		
Takeoff	1,350,000	612,350
Landing	1,077,800	488,882
Zero Fuel	1,033,525	469,799
Gross	618,000	280,325
Criteria		
Design Pressure Differential - Fuselage/Wing - psia (k Pa)	7.46/5	51.4/34.5
Design Limit Load Factor - Airplane @ TOGW	2.5	2.5
Design Cruise Speed - KTAS (m/sec)	379	195
Design Cruise Mach Number	.655	.655
Design Cruise Lift Coefficient	.444	.444
Engines		
Number Required	6	6
SLS Thrust/Engine - lb (N)	58,500	260,208
Specific Fuel Consumption-lb/hr/lb (kg/hr·(N)	.582	.059
Wing Geometry		
Area - ft ² (m ²)	18,314	1,701
Aspect Ratio	4.45	4.45
Taper Ratio	1	1
Sweep @ c/4 - degrees	0	0
Mean Thickness Ratio	.20	.20
Aileron Area - ft ² (m ²)	1,056	98
Tail Geometry		
Horizontal Tail Area - Theoretical - ft ² (m ²)	2,938	273
Horizontal Tail Length - in (m)	1,440	36.58
Horizontal Tail Volume	.30	.30
Vertical Tail Area - Exposed - ft ² (m ²)	674	63
Vertical Tail Length - in (m)	1,490	37.85
Vertical Tail Volume	.016	.016
Elevator Area - ft ² (m ²)	813	76
Rudder Area - ft ² (m ²)		
Fuselage Geometry		
Length - in (m)	2,430	61.72
Maximum Height - in (m)	220	5.59
Maximum Width - in (m)	160	4.06
Maximum Perimeter - in (m)	640	16.26
Wetted Area - Gross - ft ² (m ²)	8,085	751
Floor Area - ft ² (m ²)	469	44

FIGURE 4-2

POINT DESIGN PERFORMANCE AND ECONOMIC CHARACTERISTICS

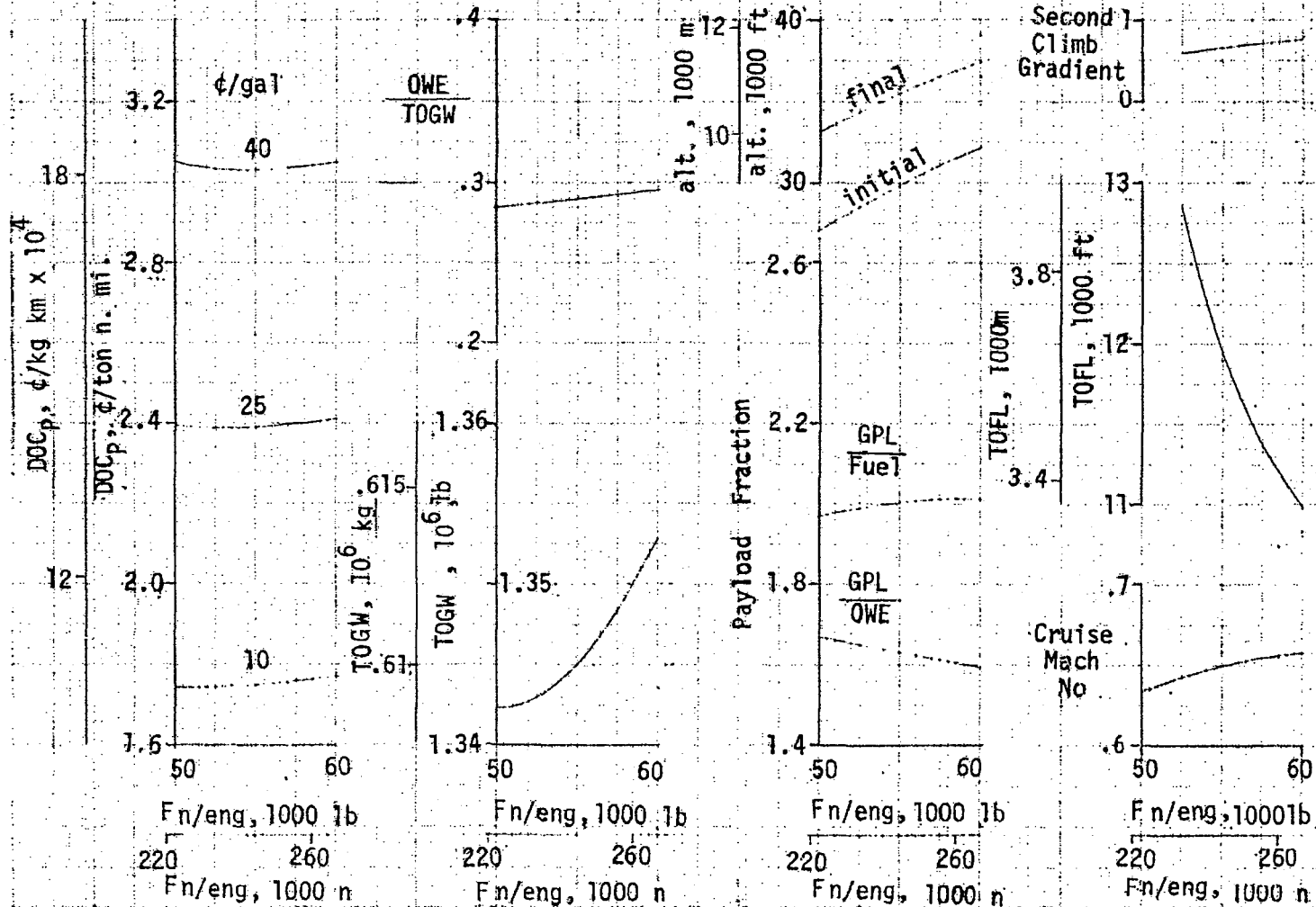
$G_{PL} = 618\,000\text{ lb}$ (280,325 kg)

$S_W = 18\,314\text{ ft}^2$ (1701 m²)

$\rho_{PLG} = 10\text{ lb/ft}^3$ (160 kg/m³)

$R = 3000\text{ n.mi.}$ (5550 km)

$AR = 4.45$ $\Delta = 0$



10^6 pounds (612,360 kg) a combination that represents the configuration for minimum fuel usage (maximum PL/fuel). While this minimization of energy useage is desirable the prime firgure of merit for this study remains the DOC. Considering the magnitude of the deviation from the configuration for minimum DOC_p , the latter values of thrust and design gross weight were chosen as the basis for the design performance of the vehicle. This selection entails a sacrifice of .5 percent from the minimum DOC_p and results in a takeoff field length of 11,200 feet (3.415 m).

Mass properties analysis. - Weights were derived for the Point Design aircraft utilizing applicable statistical methods supplemented by the wing structural analysis and summarized in Section 4.1

The structural weights of the Point Design aircraft reflect the incorporation of a pressurized cargo bay that was not considered for the parametric designs of Section 3.0. Necessary air conditioning, pneumatic and furnishings associated with the pressurization subsystem are included in the systems weight estimates. Propulsion weights for the Point Design also reflect the use of the bypass ratio 9 engines with appropriate use of advanced materials in the installation weights. This is contrasted to weight allocations based upon QCSEE technology used in the parametric studies.

Weights for the Point Design are based on the use of graphite epoxy composites for all primary and secondary structure, although the structural analysis of Section 4.1 was performed for aluminum structures. Weight values were therefore obtained by converting the aluminum alloy estimates to composite values for each major structural component. As an example, in the case of the wing this reduction amounted to 49,212 pounds (22,323 kg). This is a reduction in wing unit weight of from 12.0 pounds per square foot (58.7 kg/m^2) to 9.3 pounds per square foot (45.6 kg/m^2) or 22.4 percent. The spanloader concept is unique relative to the application of advanced materials in that reductions in vehicle physical size cannot be reflected because the wing area is set by cargo considerations. The application of advanced materials, therefore, becomes a material substitution only which limits the payoffs (approximately 15 percent of OWE) to considerably less than frequently quoted for conventional designs (approximately 30 percent).

Additional advanced technology used in the weight allocation include

- o minicomp wiring
- o multiplex wiring
- o fly-by-wire
- o integrated drive generators

The effects of these items on component weights were derived in the course of the detailed weight analysis utilizing factors integrated within the appropriate weight equations. It is difficult to identify the respective incremental weight savings; however, the cumulative saving resulting from the four items listed is estimated to be 3 percent.

The weight summary for the Point Design is presented in Table 4-2. The primary impact of the spanloader concept on vehicle weight is appreciated by considering the structural weight ratio, OWE/TOGW, which is .29 for the spanloader configuration analyzed compared to .32 for the conventional aircraft. The improvements and redistributions of weight for the spanloader is discussed later in Section 5.0 where additional comparisons are made with the conventional aircraft.

The permissible center of gravity range for a spanloader type aircraft is restricted by configuration considerations. For a conventional fuselage loaded aircraft, the c.g. range can be selected over relatively wide latitudes by the placement of the wing on the fuselage during the design stage. With the spanloader concept with the cargo in the wing, the c.g. range results from the configuration mass distribution with little option available to the designer for c.g. range selection. The c.g. values for various loading conditions for the Point Design is shown below;

- 21.8% max fuel no payload
- 26.7 % max fuel + payload to TOGW
- 29.5% max payload + fuel to TOGW
- 36.1% max payload, no fuel
- 37.8% OWE

These values are within the permissible aerodynamic c.g. range as shown in Figure 4-13 (15 to 43% mac). The 37.8% value corresponds roughly with neutral stability for which a stability and control augmentation system (SAS) would be required. The SAS system selected for the spanloader is capable of handling a 5% negative static margin (43% mac). These aft

TABLE 4-2
POINT DESIGN SPANLOADER
WEIGHT SUMMARY

	<u>lb</u>	<u>kg</u>
Wing	170,929	77,532
Winglets	7,392	3,353
Tail	14,667	6,653
Fuselage	38,236	12,808
Landing Gear	58,987	26,756
Nacelles	22,986	10,426
Propulsion	60,714	27,540
Fuel System	2,009	911
Flight Controls	5,322	2,414
Hydraulics	3,378	1,532
Instruments	1,199	544
Air Conditioning	3,766	1,708
Pneumatics	1,059	480
Electrical	2,925	1,327
Avionics	2,698	1,224
Furnishings	7,412	3,362
Ice Protection	386	175
Handling Gear	<u>104</u>	<u>45</u>
Manufacturer's Empty Weight	394,165	178,790
Operator's Items	<u>2,350</u>	<u>1,070</u>
Operator's Empty Weight	396,525	179,860
Manufacturer's Empty Weight	394,165	178,790
Less: Engines	58,500	26,535
Rolling Assembly	<u>18,280</u>	<u>8,292</u>
Basic Cost Weight	317,385	143,963
Basic Cost Weight	317,385	143,963
Less: Starters	150	68
Instrument Units	593	269
Electrical Units	511	232
Avionics Units	1,568	711
Air Conditioning Units	<u>757</u>	<u>343</u>
Defense Contractor Planning Report (DCPR) Weight	313,806	142,340

values can be approached for partial payload conditions if the aft wing loading channels are favored. Drag reductions and fuel savings can thus be realized if the aft loadings are used.

Aerodynamic characteristics. - This section deals with low and high speed drag, lift and the more general geometric considerations associated with the determination of performance. The accompanying stability and control analysis is discussed in a subsequent section.

High speed: The basic Point Design spanloader is unique in the sense that advanced technology items and large size combine to enable the thick wing, low aspect ratio aircraft to attain aerodynamic performance that is comparable to today's efficient thin wing higher aspect ratio transports. Low parasite drag due to the high Reynolds numbers of the spanloader combine with the supercritical wing performance, and high winglet effectiveness to produce favorable lift and drag characteristics at moderate cruise speeds.

The Point Design aerodynamics were based on empirical methods, DAC wind tunnel data and analytical methods. More specifically, the recently developed Douglas non-planar lifting systems computer program was used to assess the effect of winglets on vehicle performance both in free air and in ground effect.

Large aircraft benefit from high Reynolds numbers that result in skin friction drag coefficients that are significantly lower than those of conventional size aircraft. To illustrate, the Reynolds number, based on wing chord, for the conventional aircraft is 65×10^6 while that for the spanloader is 108×10^6 . The decrease in skin friction drag accompanying this increase in Reynolds number is illustrated by the data presented in Figure 4-3. The basic parasite drag build-up is presented in Table 4-3.

The spanloader type of vehicle with low aspect ratio and little or no wing taper can benefit significantly from winglets. Analytical exercises using the Douglas developed Non-Planar Lifting Systems program indicate that winglets are most effective on lower aspect ratio wings with little taper and little washout where the lift on the outboard portion of the wing is greater than that with an elliptical lift distribution. For this more uniform type of basic wing loading the effect of a large chord winglet is

FIGURE 4-3
TOTAL SKIN FRICTION FOR SMOOTH SURFACE

Transition at Leading Edge

$M = 0.5$

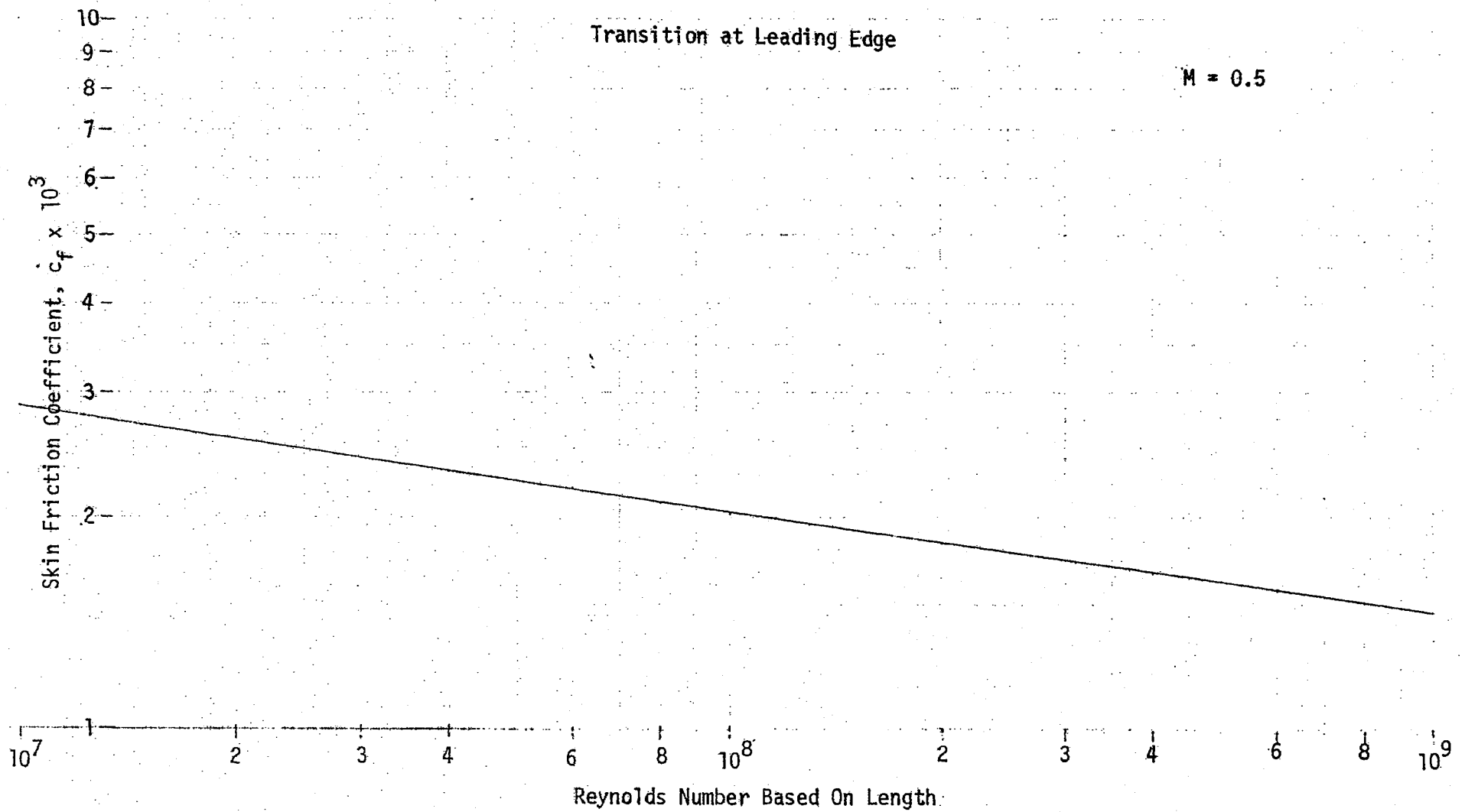


TABLE 4-3
PARASITE DRAG SUMMARY

$$R_N/ft = 1.68 \times 10^6$$

COMPONENT	S_{wet}		C_f	f	
	ft ²	m ²		ft ²	m ²
Wing	33,043	(3,070)	.00201	105.10	(9.76)
Horizontal	5,876	(546)	.00227	16.86	(1.57)
Vertical	1,348	(125)	.00241	4.06	(.38)
Fuselage	10,600	(985)	.00169	18.77	(1.74)
Canopy			$C_{D\pi} = .0025$.44	(.04)
Upsweep			$C_{D\pi} = .0186$	3.25	(.30)
Pylons	1,980	(184)	.00239	5.20	(.48)
Nacelles	2,930	(272)	.00250	11.72	(1.09)
Winglets	4.300	(400)	.00219	11.43	(1.06)
Control Gaps				.93	(.09)
Gear Bumps	2,300	(214)	.00220	5.06	(.47)
Subtotal				182.82	(16.98)
7.1% Dirt				12.98	(1.21)
				195.80	(18.19)
5% Pot. Interfer.				9.79	(.91)
High Speed Total				205.59	(19.10)
High Speed $C_{D_o} = \frac{205.59}{18,314} = .01123$					
Landing Gear				225.00	(20.90)
Low Speed Total				430.59	(40.00)
Low Speed $C_{D_o} = \frac{430.59}{18,314} = .02351$					

to further modify the lift distribution in the direction to achieve near two-dimensional span loading illustrated in Figure 4-4. The non-planar program separates out the induced drag forces acting on the wing and winglet components. These data indicate that the modification of the wing span loading by the winglet to a nearly two-dimensional distribution results in a drastic reduction of wing induced drag. In addition, the vector direction of the winglet lift is such as to produce a small net thrust force when added to the winglet induced drag. The overall induced drag reduction can be quite significant as indicated in Figure 4-5.

Estimated compressibility drag and trim drag are presented in Figures 4-6 and 4-7, respectively. Final resultant cruise lift-to-drag ratios are presented in Figure 4-8.

Low speed: Low wing loadings (less than 80 lb/ft^2 (390.6 kg/m^2)) combined with a non-critical design field length of 12,000 feet (3,658 m) made a low-speed high-lift system unnecessary. A pitch ground rotation limit of 15 degrees is more than adequate to attain maximum allowable lift coefficient (with speed margins), see Figure 4-9.

Cruise and low speed Reynolds numbers are the same, with resultant identical parasite drag except for gear drag.

Estimated trim drag and resultant low speed lift and drag summaries are presented in Figures 4-10 and 4-11, respectively.

Performance summary. - A performance summary for the Point Design Spanloader aircraft is shown in Table 4-4. The final configuration has a wing loading of 73.7 lb/ft^2 (359.8 kg/m^2) and a thrust-to-weight ratio of 0.259 (2.54 N/kg). The cruise C_L is 0.444 which yields a cruise L/D of 18.75 over the cruise Mach number and altitude range of 0.653 to 0.657 at 31,514 (9,606 m) to 36,830 feet (11,226 m), respectively.

The total fuel weight in the Point Design is 335,235 pounds (152,063 kg) which includes 63,048 pounds (28,599 kg) of reserve. Included in this reserve is 44,288 pounds (20,089 kg) of fuel to meet the FAR domestic landing reserve requirements plus an additional 18,760 pounds (8,510 kg) that will double the reserve cruise range at 30,000 feet (9,144 m) altitude to 400 nautical miles (370 km) total. This additional reserve range is provided as a safety factor in consideration for the spanloader operational

FIGURE 4-4.

POINT DESIGN SPANWISE LIFT DISTRIBUTION

$AR = 4.45$
 $M = 0.70$
 $C_L = 0.41$
 $\lambda = 1.0$

Note: Winglet Height = $.25 b/2$

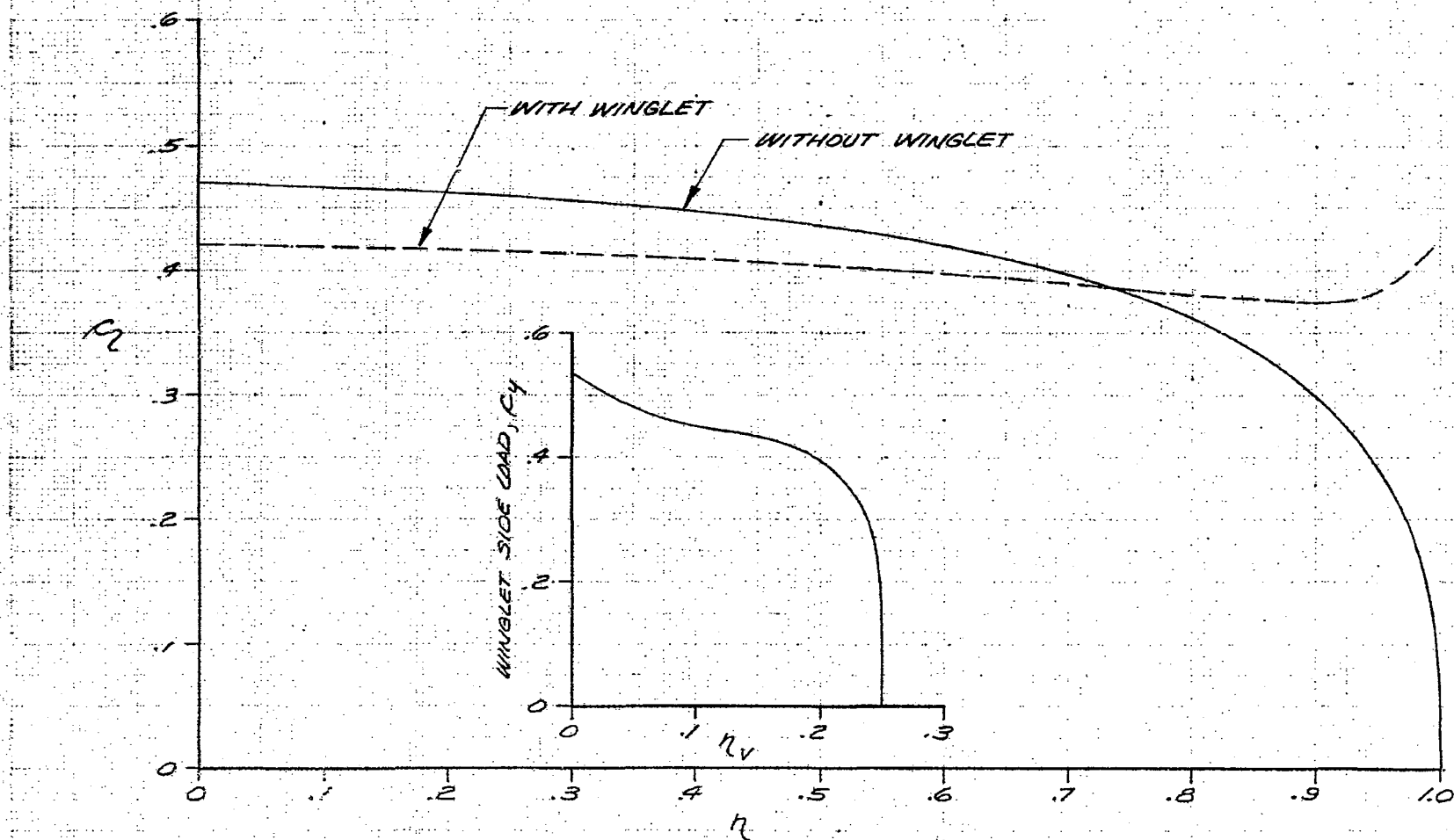


FIGURE 4-5
WINGLET EFFECT ON INDUCED DRAG OF POINT DESIGN

AR = 4.45

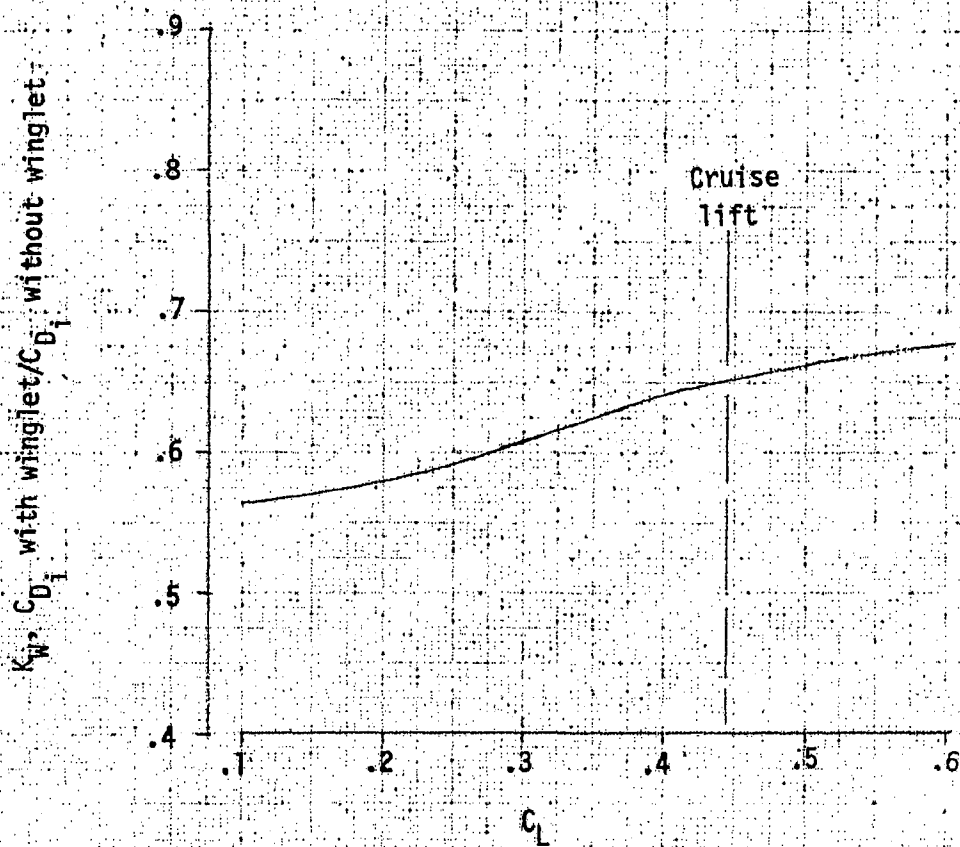


FIGURE 4-6
POINT DESIGN COMPRESSIBILITY DRAG

$t/c = .20$

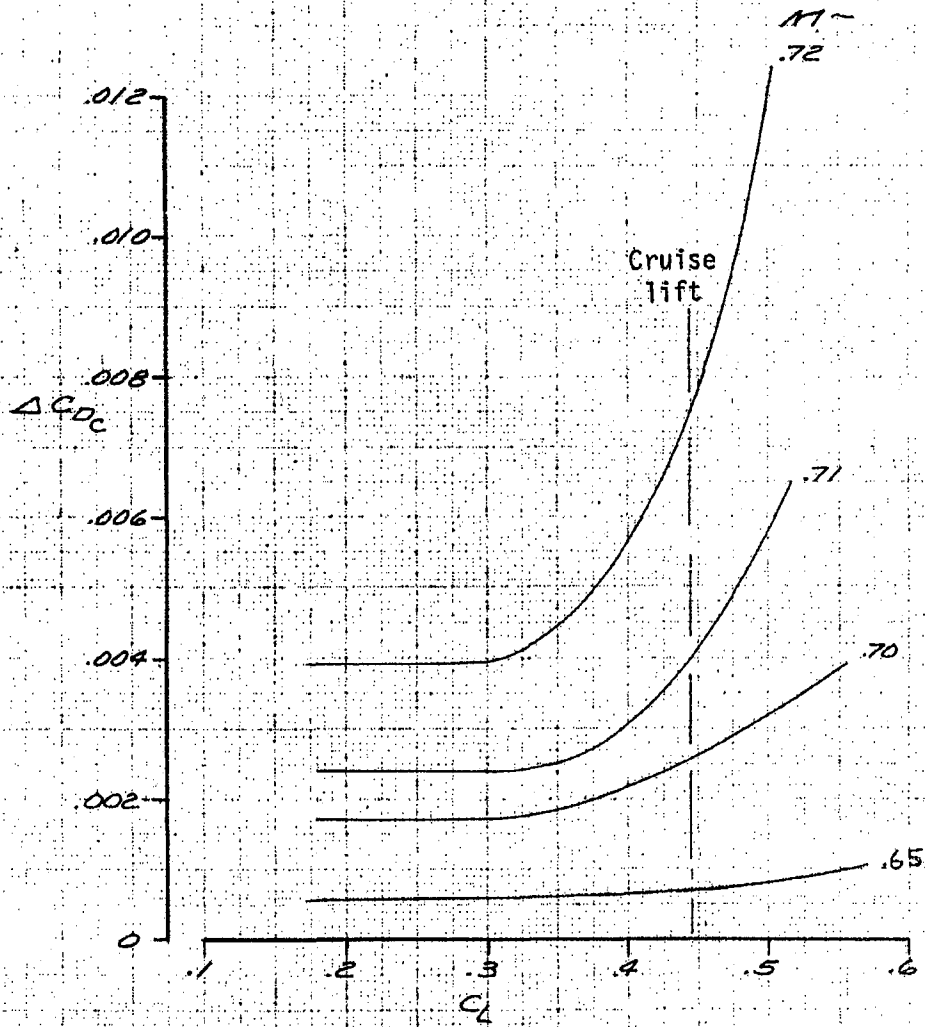


FIGURE 4-7

HIGH SPEED POINT DESIGN TRIM DRAG

AR = 4.45

Forward CG @ 36% MAC

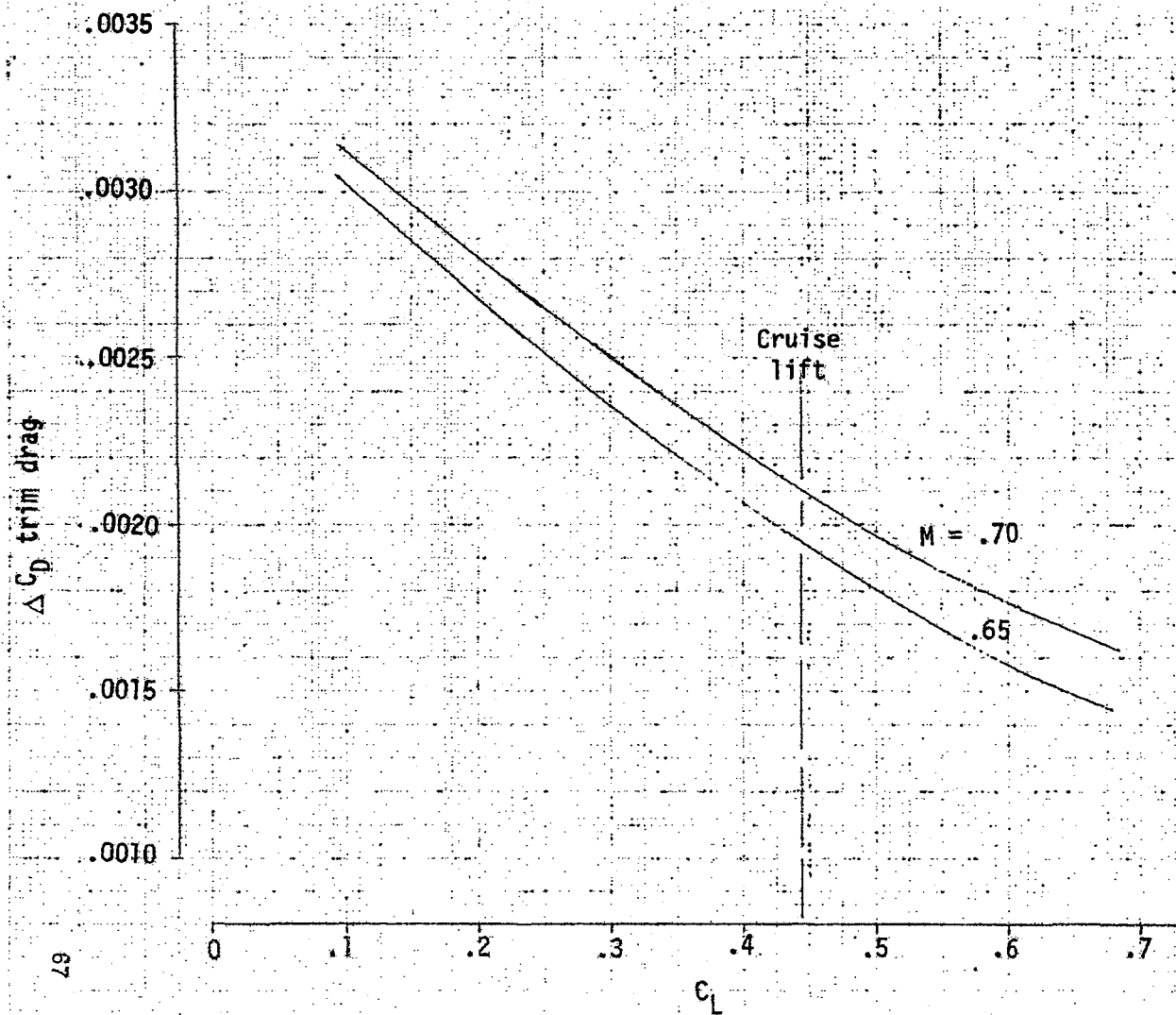


FIGURE 4-8
POINT DESIGN TRIMMED LIFT TO DRAG RATIO

AR = 4.45

Forward CG @ 36% MAC

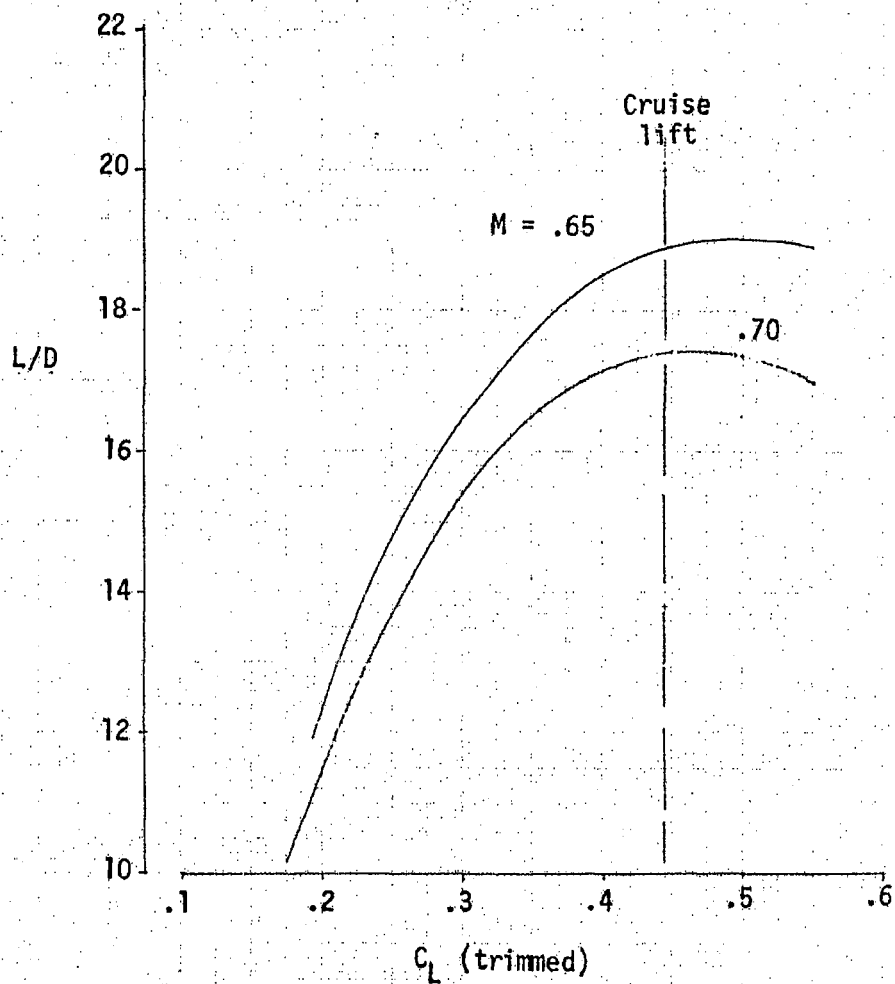


FIGURE 4-9
POINT DESIGN LIFT CURVES

$M = .70$

$AR = 4.45$

Forward CG @ 36% MAC

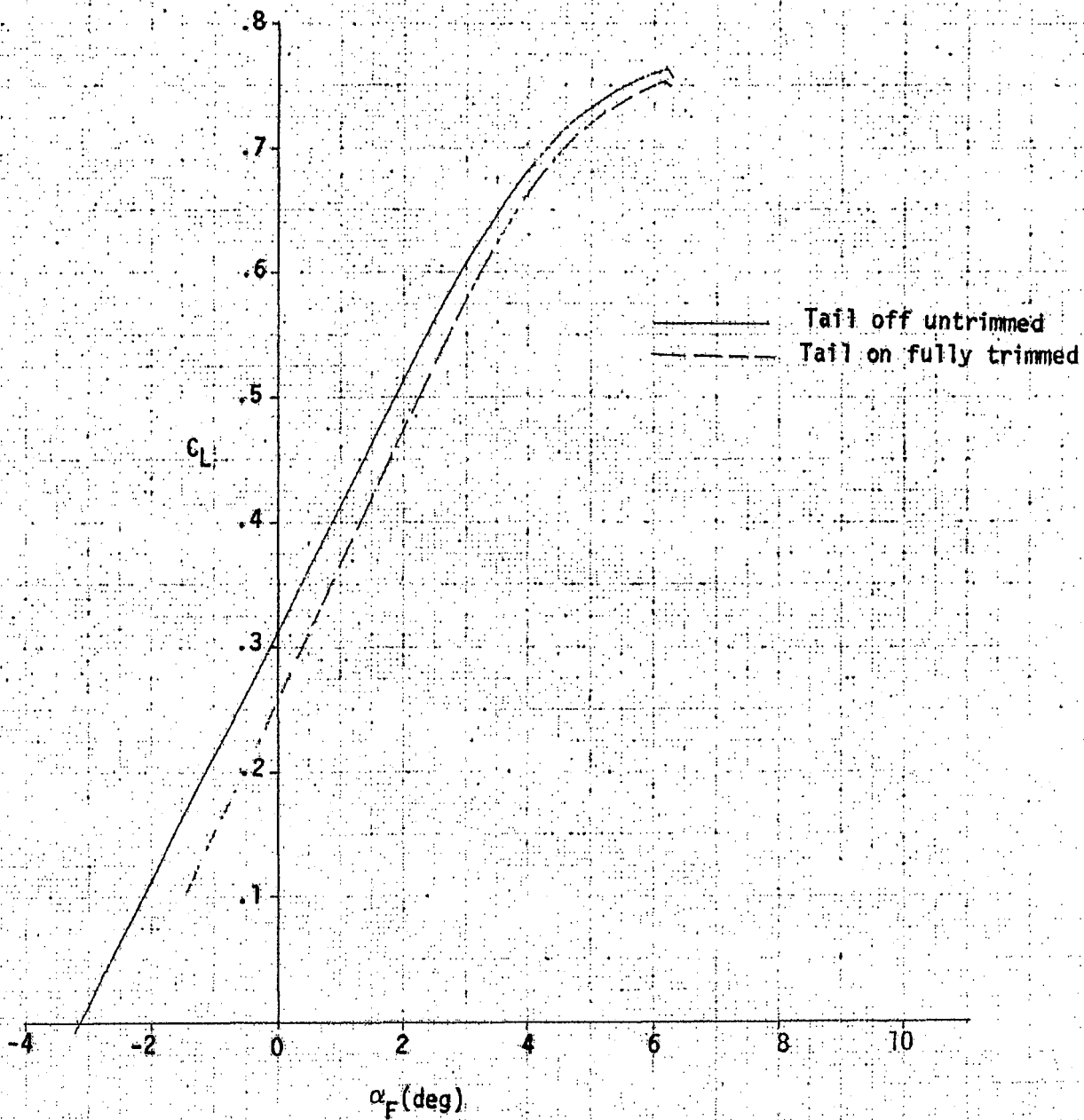


FIGURE 4-10
LOW SPEED POINT DESIGN TRIM DRAG

AR = 4.45
Forward CG @ 36% MAC

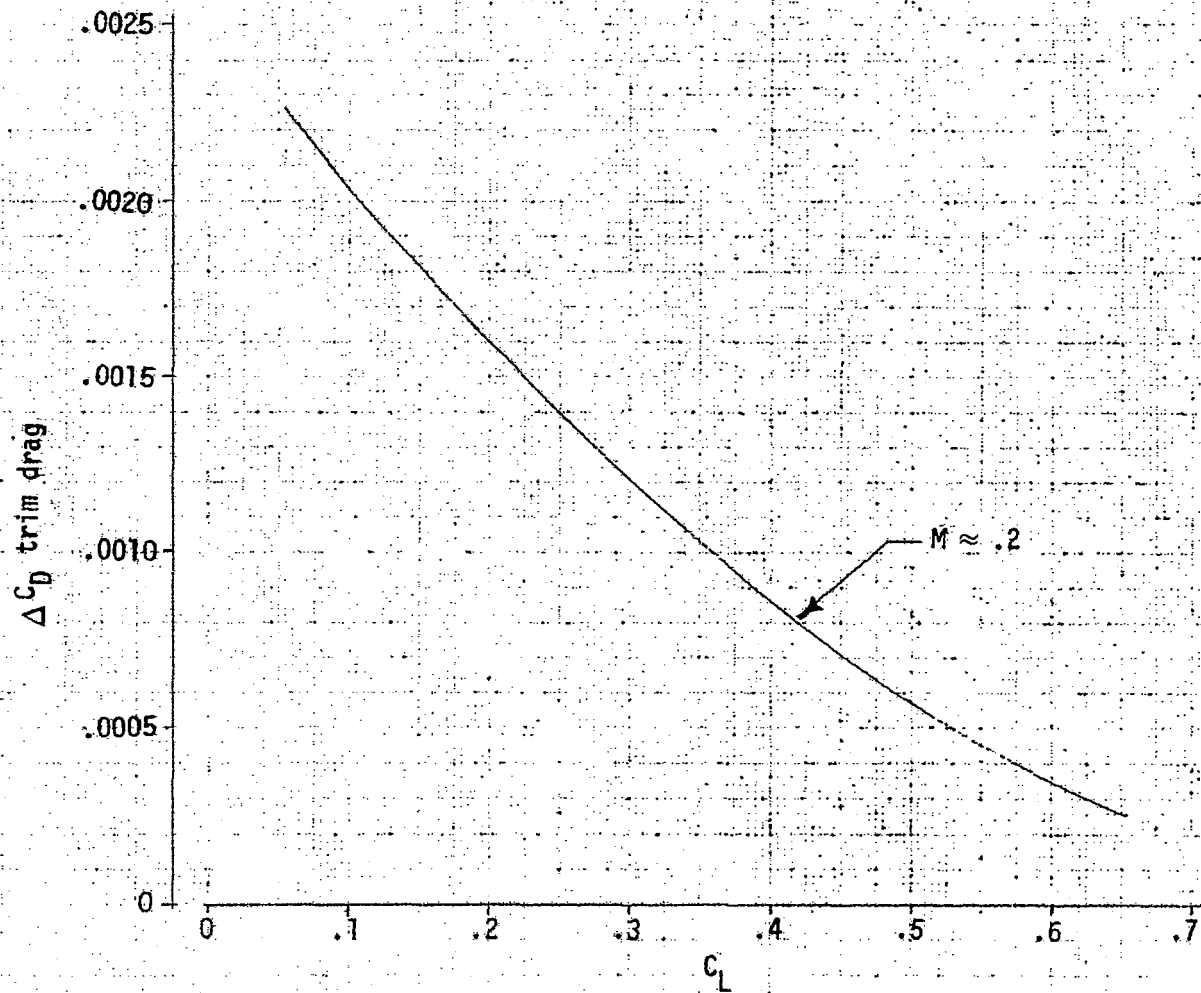


FIGURE 4-11

LOW SPEED POINT DESIGN AERODYNAMIC CHARACTERISTICS

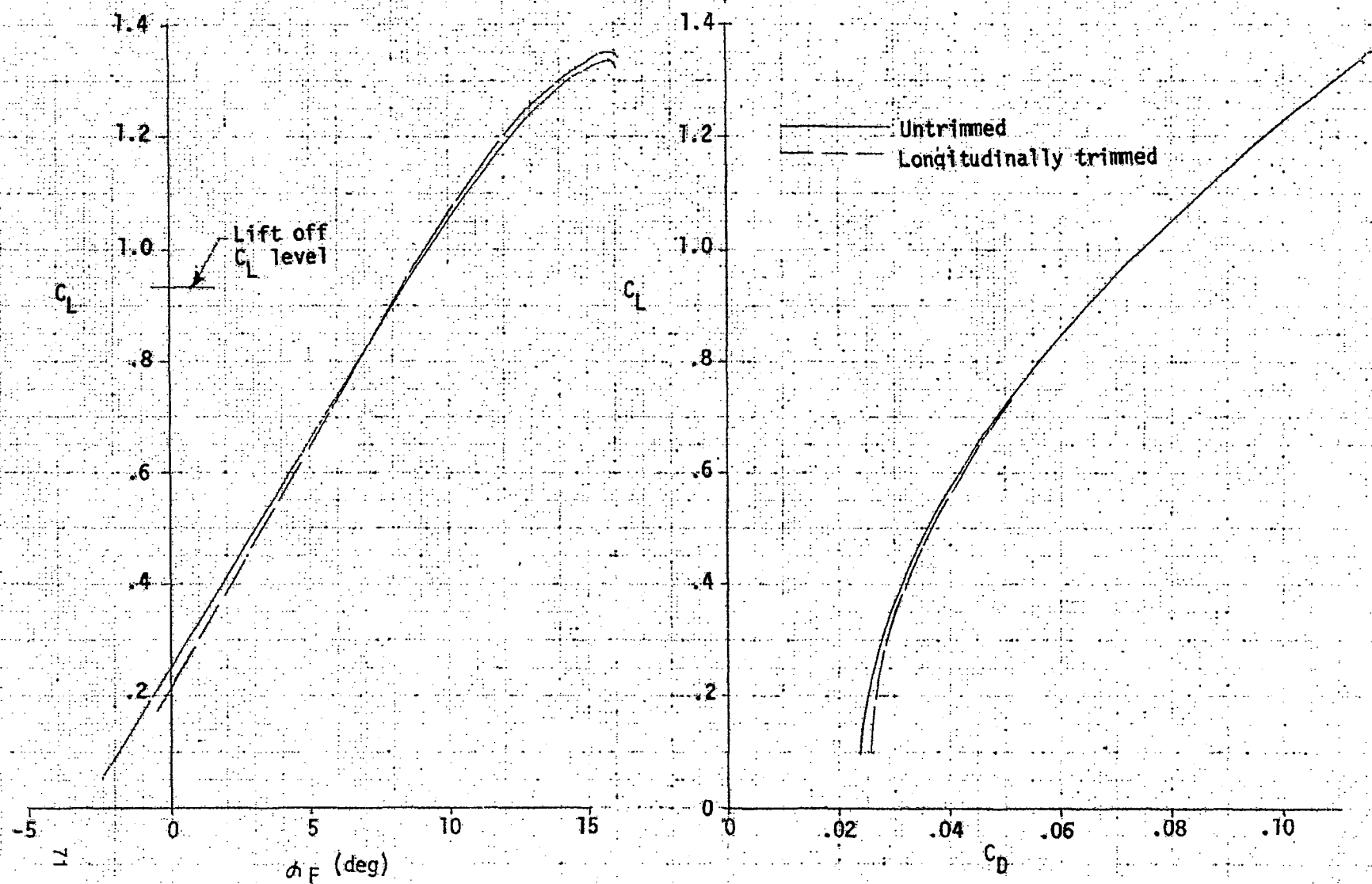


TABLE 4-4
POINT DESIGN PERFORMANCE SUMMARY

	SPANLOADER	
Operating Weight Empty - lb (kg)	396,525	(179,864)
Gross Payload Weight - lb (kg)	618,000	(280,325)
Tare - lb (kg)	80,640	(36,578)
Fuel - lb (kg)	335,235	(150,063)
Takeoff Weight - lb (kg)	1,350,000	(612,360)
Reserve Fuel Weight - lb (kg) *	63,048	(28,599)
Net Thrust per Engine - lb/eng (N/eng)	58,500	(260,208)
Specific Fuel Consumption - lb/hr/lb (kb/hr·N)	0.582	(0.059)
Wing Loading - lb/ft ² (kg/m ²)	73.7	(360)
Thrust to Weight Ratio - lb/lb (N/kg)	.259	(2.54)
Ratio Operating Weight Empty to Takeoff Weight	.894	
Ratio Gross Payload to Operating Weight Empty	1.559	
Ratio Gross Payload to Fuel Weight	1.843	
Cruise Mach Number	.655	
Cruise Lift Coefficient	0.444	0.444
Initial Cruise Altitude - ft (m)	31,500	(9,601)
Maximum Lift to Drag Ratio	18.75	(18.75)
Takeoff Field Length ft (m)	10,737	(3,273)
Landing Field Length- ft (m)	9,960	(3,036)
Approach Velocity - kn (m/s)	169	(87)
Second Segment Climb Gradient	.0736	

* Total Reserve Fuel = 44,288 lbs (20,089 kg) for FAR Landing Reserve plus
18,760 lbs (8,510 kg) for 200 n mi additional
reserve range.

characteristics viewed within the framework of the projected domestic and international airport system. Analysis of the spanloader as an element of the world's air cargo system is required to place this factor and other pertinent operational considerations in proper perspective.

Economic analysis.- This section contains the economic data developed for the Point Design spanloader. They are derived and exhibited in accordance with the requirements shown in the NASA Study Statement of Work and are intended for use as evaluation and comparison criteria. Also, costs for this candidate system are to be considered as rough order of magnitude costs for budgetary and planning purposes. The primary cost measures derived deal with airplane pricing and direct operating costs without considering the financial viability of the operating entities (e.g. discounted cash flow, ROI).

Airplane price: Airplane price is derived by using a combination of estimating relationships and direct estimates from other studies and actual historical experience in both metallic construction and advanced composite construction. Their origin or basis are industrial engineering estimates of similar construction and designs, and for individual components of the airframe (e.g. wing, fuselage, tail, etc.). In this approach non-recurring and recurring costs are derived separately for the fabrication of metallics and advanced composites while subassembly and assembly estimates are developed as an integrated package. The development program and sustaining costs are estimated in the same manner. All of the estimates derived with this approach are first built-up in terms of physical units e.g. manhours of labor, pounds of material, etc. - and then converted into constant 1975 dollars. Additional analyses of the design resulted in modifying certain cost elements to incorporate specific intentional structural efficiency facets of the design. Fabrication particularly benefits from the large degree of commonality that exists in the wing and horizontal tail. The cascading beneficial effects are more readily understood for the metallic portion; but, there is a greater uncertainty associated with the advanced composites, the same commonality benefits attainable with metallic design and construction will be achieved with composites for the time period of this program. Therefore, the credit for commonality has been assumed in estimating the composites. A summary of the price levels are shown in

Table 4-5 segmented into the major cost elements. Two price quantities are shown in order to comply with the NASA SOW (pricing quantity of 350) and also to reflect the derived fleet size required (525) to achieve the assumed available market of 100 billion revenue-ton-nautical miles per year. Figure 4-12 exhibits a price/quantity relationship for further information.

The cumulative average price for the requested quantity of 350 airplanes is \$65.1 M and is \$58.5 M for the 525 quantity required to handle the projected market. These prices contain the assumed credit for composite parts commonality. While specific market estimates are given, a conservative pricing point of 20 percent profit and 8 percent interest over the 350 airplanes was used. It was thought that the upper limit of the market would be in the order of this 350 airplane quantity. Such a market size would require high profit incentives to attract an airplane manufacturer.

Direct operating costs (DOC): The methodology used to compute DOC is essentially the same as that outlined earlier in Section 3.0 except for two significant input values. The factors shown in Table 3-1 remain constant for parametric and Point Design aircraft. The primary difference between these two sets of aircraft are the input values for the first airplane price and the price per engine. Airplane price, airframe price and engine price affect six of the eight cost elements that make up the DOC calculations. During the parametric studies these prices were input as constant dollar per pound values. The DOC associated with the fleet size required is 3.36 cents per ton-mile. A breakdown of the individual elements are shown in Table 4-6.

Stability and control. - Numerous studies have indicated that improved aerodynamic efficiency can be achieved by the use of active controls. Applying this technique for Relaxed Static Stability (RSS) would allow a reduction in tail size and would permit flight at a more aft c.g. range for reduced trim drag. Although not considered herein, other active control functions such as gust and maneuver load alleviation may be of great potential benefit to the spanloader concept. This advanced technology should be sufficiently well developed by the 1990 time period to warrant its inclusion in the basic design of the spanloader.

TABLE 4-5
AIRPLANE PRICING
(Constant 1975 Dollars - Millions)

COST ITEM	AIRPLANE QUANTITY				
	50	100	150	200	350
<u>LABOR</u>					
Manufacturing	2586.2	3837.5	5078.3	6133.3	8935.3
Engineering	1727.5	2004.1	2213.2	2356.1	2699.9
Laboratory & Flight Test	180.2	183.0	185.9	188.8	191.7
Product Support	<u>33.7</u>	<u>33.7</u>	<u>33.7</u>	<u>33.7</u>	<u>33.7</u>
Sub Total	4527.6	6058.3	7511.1	8711.9	11860.6
<u>MATERIAL</u>					
Raw Materials	457.2	887.3	1316.7	1745.6	3031.6
Purchased Parts & Equipment	668.3	1259.0	1624.8	2076.7	3384.3
Flight Test	11.4	11.4	11.4	11.4	11.4
Product Support	<u>38.7</u>	<u>38.7</u>	<u>38.7</u>	<u>38.7</u>	<u>38.7</u>
Sub Total	1175.6	2196.4	2991.6	3872.4	6466.0
Engines	<u>634.9</u>	<u>1269.8</u>	<u>1904.7</u>	<u>2539.0</u>	<u>4444.0</u>
GRAND TOTAL (Labor + Material)	6338.1	9524.5	12407.4	15123.3	22770.6
CUM AVERAGE PRICE	126.8	95.2	82.7	75.6	65.1

FIGURE 4-12
AIRFRAME COST PRICE VERSUS QUANTITY
POINT DESIGN SPANLOADER

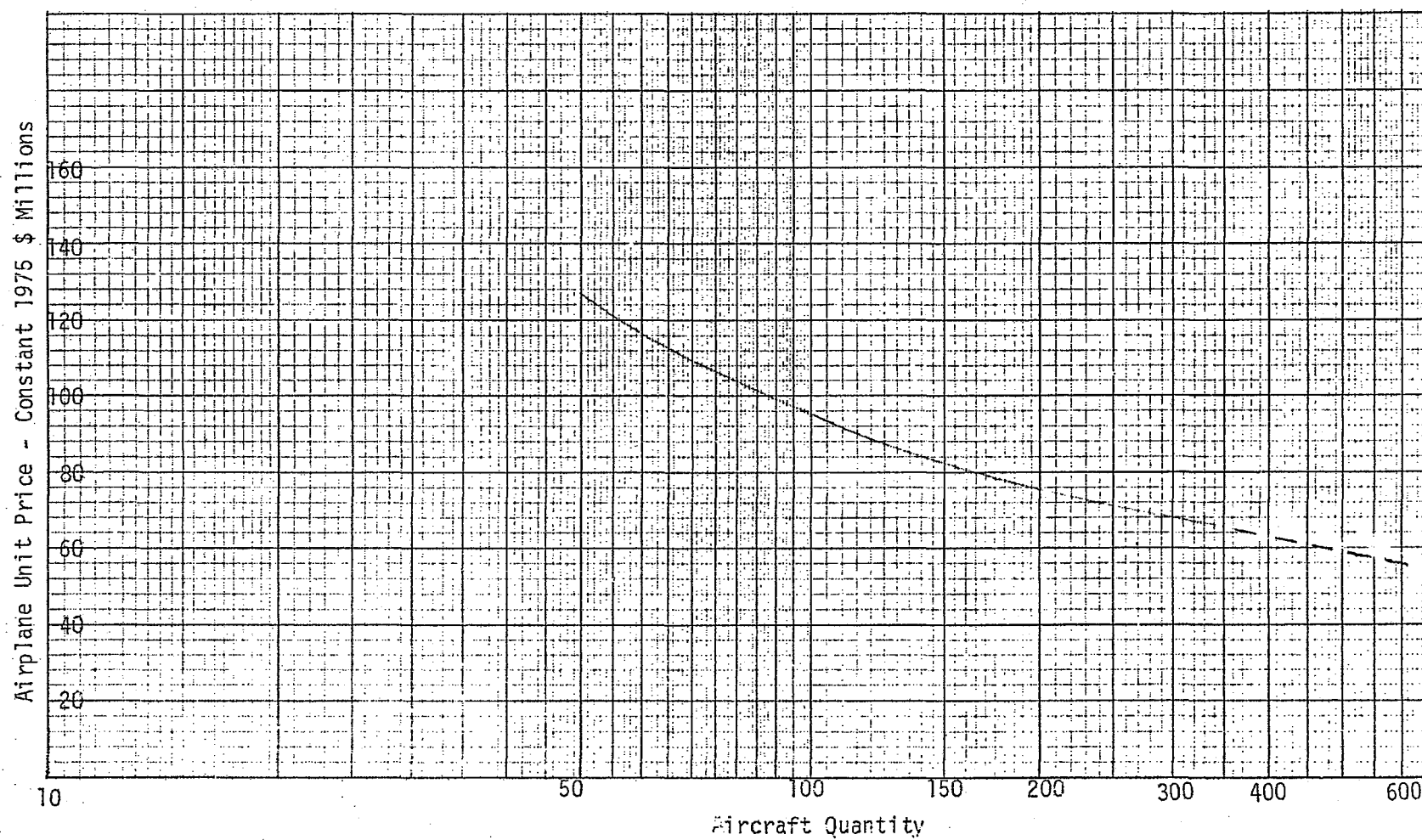


TABLE 4-6
DIRECT OPERATING COST BREAKDOWN

<u>Cost Element</u>	<u>Dollars/Flight</u>
Crew	2666.2041
Insurance	2416.0500
Depreciation	10570.2188
Airframe Maintenance	
Labor	1347.2858
Material	900.2613
Engine Maintenance	
Labor	1108.9460
Material	1940.0432
Fuel	10201.4925
<hr/>	
Total Dollars/Flight	31150.5017
Total Dollars/NM	10.3835
Total Cents Per Ton-Mile	3.863

Limited simulator experiments have shown that an airplane can be flown with a slightly negative maneuver stability margin; a margin where the time to diverge to double amplitude is greater than about five seconds. This level of stability which corresponds to a negative static margin of about 10 percent for transport type aircraft represents the limit of relaxation permitted by present day active-control technology. Failure of the stability augmentation system (SAS) on an airplane with this level of inherent stability would drastically degrade the flying characteristics but would still permit the pilot to fly and land the airplane. Redundant augmentation systems can reduce the possibility of complete failure to the point where a greater degree of stability relaxation can be accommodated.

A negative static stability margin of 10 percent MAC_w has been selected as one of the criteria for sizing the horizontal tail of the Point Design spanloader aircraft. More detailed dynamic analyses, beyond the scope of this study, would be required to define the ultimate limit of RSS.

Conventional type aircraft configurations which carry the cargo in the fuselage permit the fuselage to be positioned on the wing such that control and stability become equally critical at the fore and aft c.g. limits. This method of optimizing the relationship of c.g. and aerodynamic stability and control characteristics is not possible with the spanloader concept. The selected aft permissible aerodynamic c.g. (43 percent MAC_w) of the Point Design can be approached with partial cargo loadings where the cargo is positioned in the aft bays.

Figure 4-13 shows a recommended horizontal tail equal to 16 percent of the wing area ($S_H/S_w = 0.16$) which provides the afore mentioned level of static stability at the high speed cruise condition ($M = 0.7$) when loaded to the extreme aft c.g. limit with partial cargo loading. Without stability augmentation a tail area ratio in excess of 0.35 would be required. The longitudinal control available at any conceivable forward c.g. limit will be more than adequate for nose-wheel-lift-off (NWLO) and for trim at $1.3V_s$ during the landing approach. Also shown in figure 4-13 is an indication of the elevator deflection-to-angle of attack gain ($\delta_e/d\alpha$) that would be required to augment static stability to a level corresponding to that for the same aircraft with a positive five percent static margin.

Figure 4-14 is presented to show that the trim capability of the tail is adequate. The figure does, however, show that a relatively large download ($C_{LH} = 0.28$ at a cruise $C_L = 0.444$) is required to trim the vehicle during high-speed cruise. This results primarily from the large, negative CM_0 contributed by the thick, aft-loaded, "supercritical" type airfoil employed for the spanloader wing. Being basically unstable (i.e., the c.g. is located behind the tail-off aerodynamic center) the vehicle requires a decreasing tail-down load to trim with an increase in wing lift.

The vertical tail was sized to provide one-engine-out control at a speed 10 knots (5 m/s) less than the design lift-off speed of 165 knots (85 m/s). A 30 percent chord single-hinged rudder deflected a maximum of 30 degrees was assumed. This rudder mounted on a vertical tail of 674 square feet (63 sq m) area will provide the desired control with only five degrees of sideslip and two degrees of bank.

The directional stability of the spanloader is considered adequate since

FIGURE 4-13
POINT DESIGN HORIZONTAL TAIL SIZING

$$S_W = 1831 + ft^2$$

$$AR_W = 4.45$$

$$\Delta = 0$$

$$\lambda = 1.0$$

$$AR_H = 3.0$$

$$\Delta = 0$$

$$\lambda = 1.0$$

30% C. Elevator

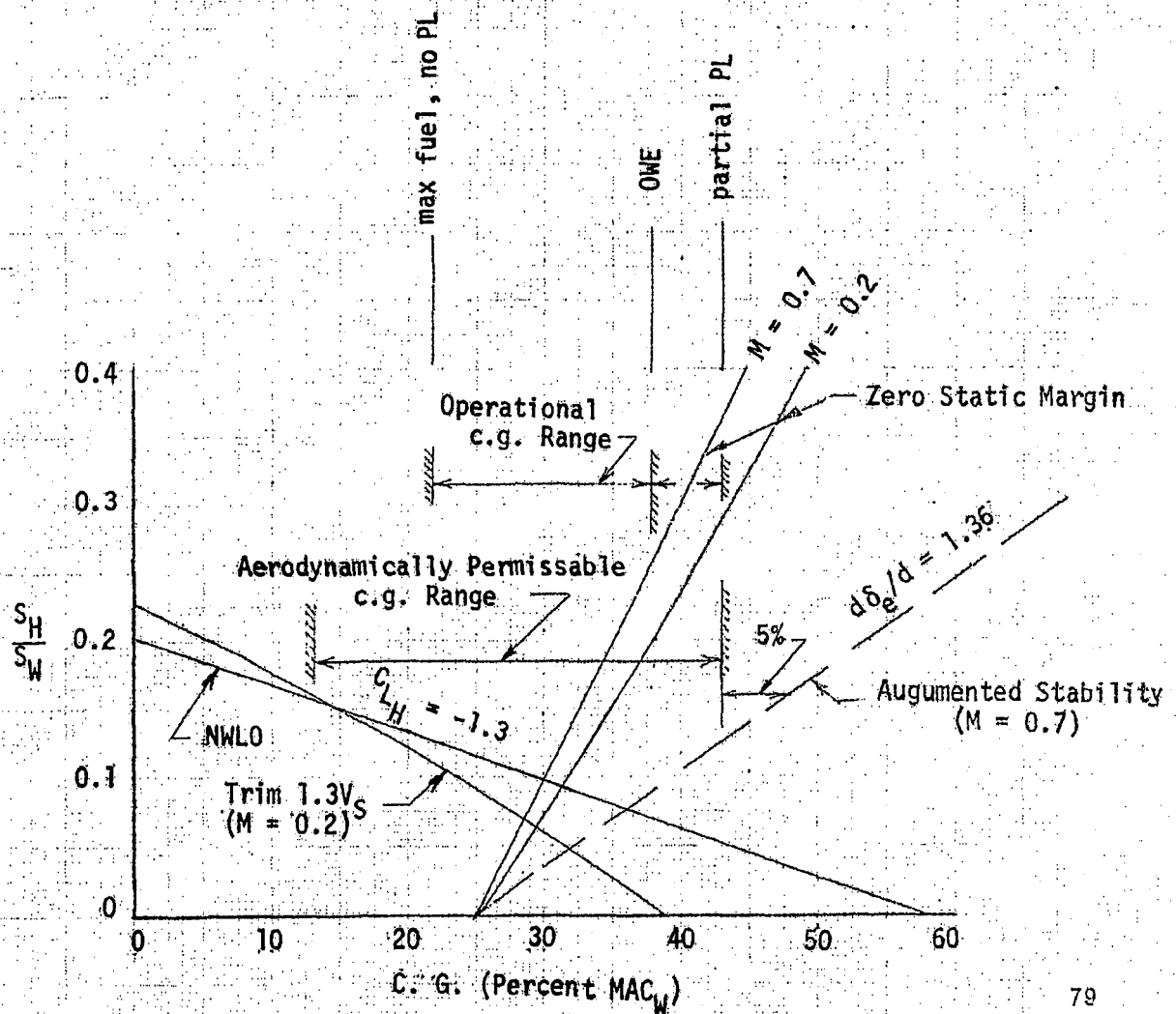
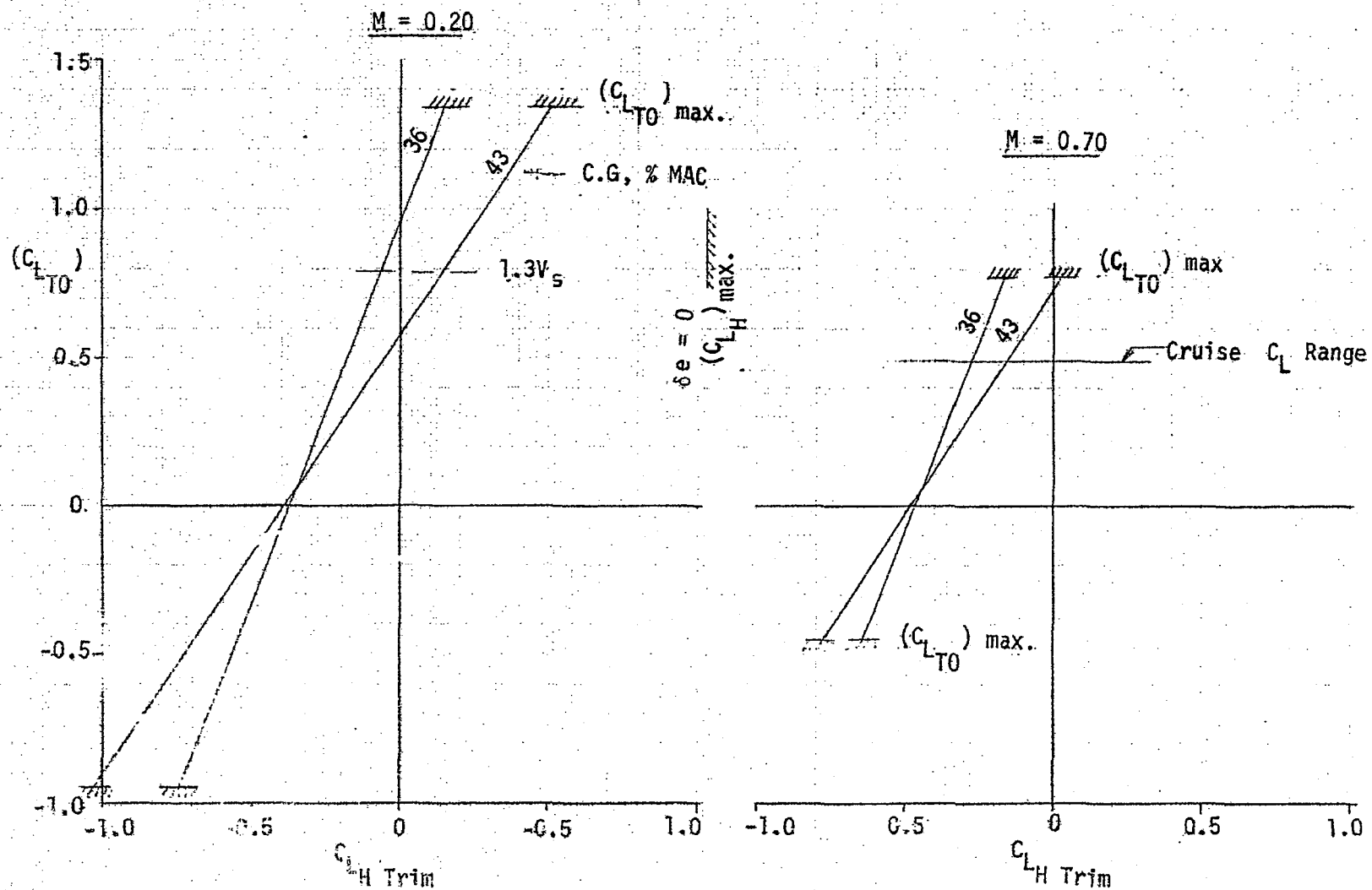


FIGURE 4-14
POINT DESIGN TAIL LIFT COEFFICIENT REQUIRED FOR TRIM



the vertical tail provides a stabilizing contribution that is more than four times greater in magnitude than the destabilizing contribution of the pylons, nacelles, and wing-body combination. The winglets being behind the c.g. are also stabilizing. In contrast the vertical tail of conventional type aircraft is usually sized to provide a stabilizing effect that is only approximately double the magnitude of the tail-off instability.

Structure and loads analysis. - This section contains the results of the external loads and structural design analyses performed on the Point Design spanloader configuration, including significant observations. The primary purpose of the structural design analysis was to provide support for the weight analysis of Section 4.1 in structural areas unique to a spanloader airplane. In addition, the analysis attempted to identify unique structural features, potential problem areas and manufacturing considerations. Priority areas were also identified as subjects for further study.

The wing, with its large size and requirements for accommodating the payload, was the primary subject of the structural analysis since the fuselage is relatively conventional. The portion of the fuselage forward of the wing is pressurized, provides a flight deck and space for required equipment, and supports the nose landing gear. The portion aft of the wing is merely a beam to support the conventional empennage.

In order to make use of existing technology and experience, a conventional aluminum alloy wing structure was established to assist in the weight evaluations, to determine the feasibility of structural arrangements and to determine the distribution of common and unique parts. However, since this airplane is expected to be operational in the 1990 time period the final design will probably make extensive use of composite structural materials. The weight analysis of Section 4.2 therefore applies selected weight reduction factors to the conventional aluminum structure to account for the expected use of these advanced structural materials.

Preliminary sizes of typical major wing structural members were calculated. Shear, bending and torque material along with wing pressurization and cargo vertical support structure were considered. The use of simple methods provided a basic understanding of the effects of the loads and the unusual configuration, established the feasibility of the resulting structure,

and at the same time provided an adequate basis for the weight configurations.

The basic measurements of the member sizes used is the total material in a structural member spread out to give an equivalent thickness, \bar{t} . The total member weight is then determined by multiplying average thickness (\bar{t}) by the material density and the area covered by the member. The sizes derived in this section are optimum and do not include joints or fasteners. The following items not included in this section are included in the weight analysis:

- Side and aft restraint of cargo
- Cargo transport mechanism
- Landing gear and local support structure
- Ailerons and supporting structure
- Wing-fuselage joining structure
- Doors
- Winglet and local support structure
- Fuselage and empennage.

The scope of this study did not permit a detailed structural investigation of these items, most of which are not unique to the spanloader concept. Items such as landing gear support and wing-fuselage juncture could have a significant effect on the configuration and are discussed later as possible subjects for further investigation.

Wing structural arrangement: Figure 4-15 shows the general structural arrangement of the wing and Figure 4-16 shows a typical wing rib between wing stations 240 and 790. The wing has four spars and these spars along with the associated skin panels are continuous through the fuselage. The primary wing bending and torque sections are indicated in Figure 4-16. The cargo is located in three spanwise bays between the spars with specific sections aft of spar 4 being cut out for landing gear wheel wells as illustrated in Figure 4-17. Cargo is loaded in 8 by 8 by 20 foot (2.44 by 2.44 by 6.10 m) containers that are inserted and guided by rails into the wing from either end through hinged cargo doors at the wing tips. The detailed relation of this loading to the wing structural elements is shown in Figures 4-15 and 4-16. The wing spars along with the interdispersed cargo bays are continuous through the fuselage extending in an unbroken

FIGURE 4-15

WING STRUCTURAL ARRANGEMENT

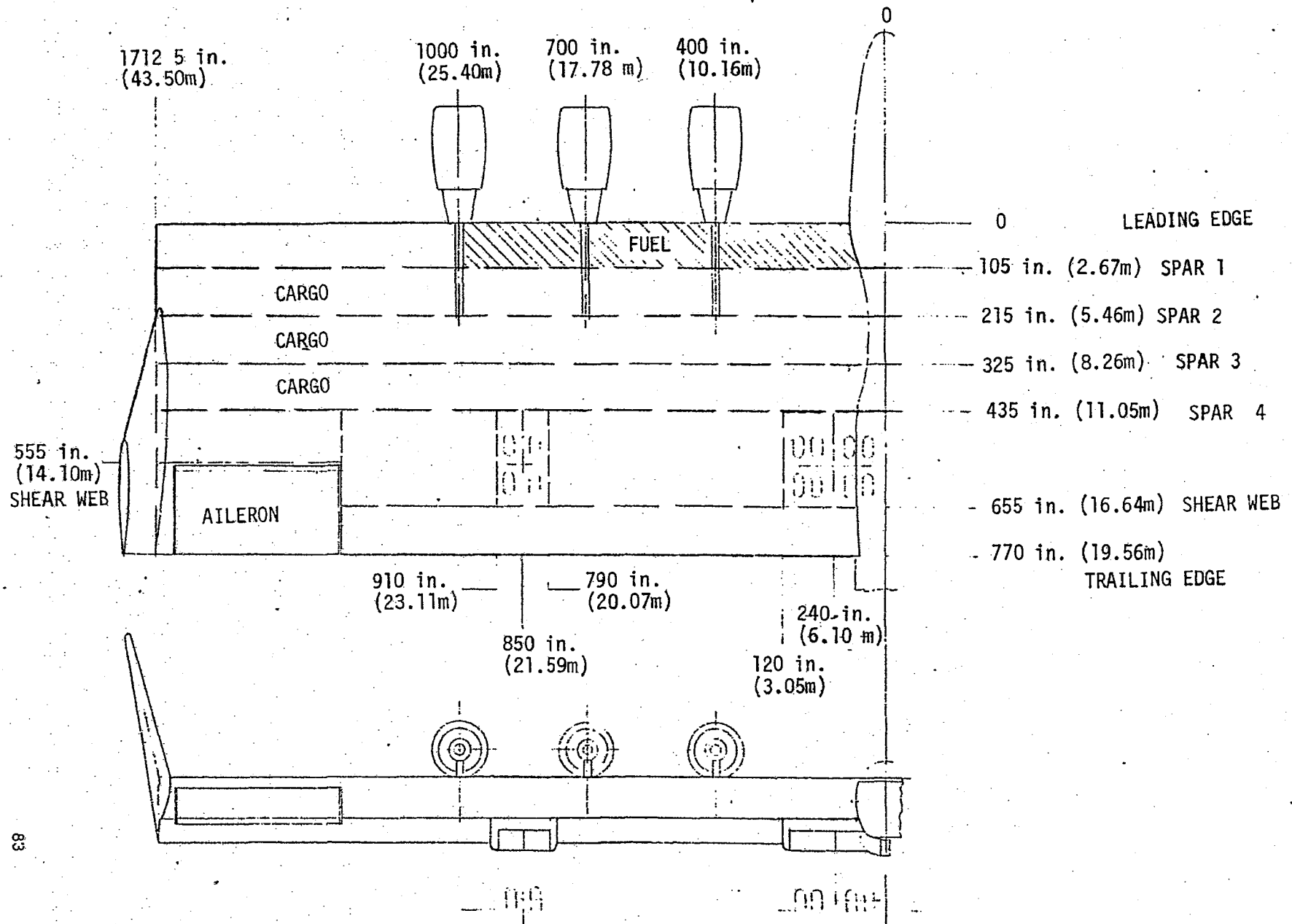


FIGURE 4-16
TYPICAL WING RIB

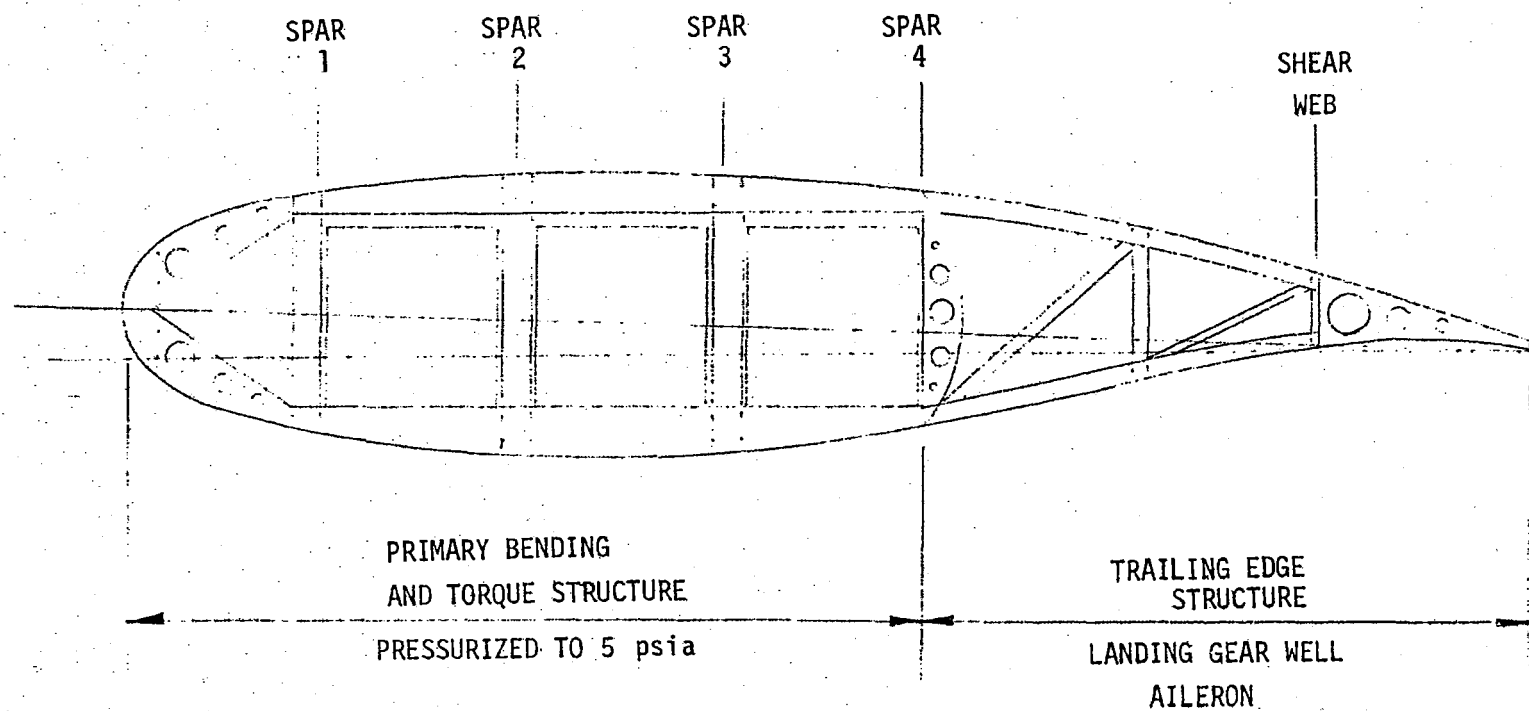
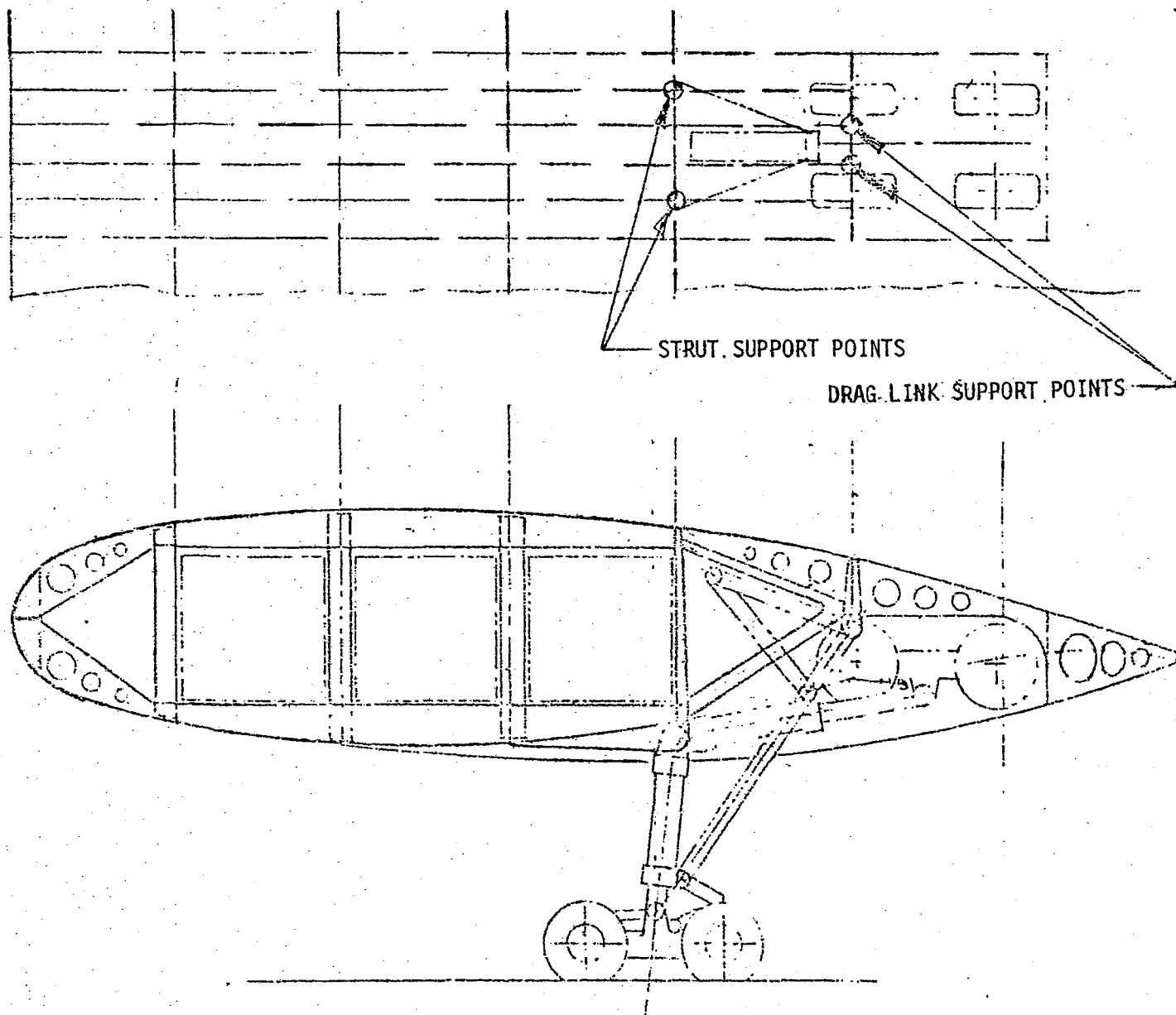


FIGURE 4-17
WING LANDING GEAR STRUCTURE



line from wing tip to wing tip. Detail analysis and design of the wing-fuselage juncture is identified as a subject for future study in Section 6.0. The wing is pressurized to 5psia (34.475 Pa) forward of the rear spar (see Section 3.1) with the rear spar having a curved web to support the necessary pressure differential. Figure 4-17 is a section through the outboard landing gear wheel well between wing stations 790 and 910 which is one of the four spanwise gear locations. A section through the inboard gear is similar. There are two spanwise sections of shear web aft of spar 4, one section acting as a closing web forward of the aileron and the other as the aft closing web of the main gear wheel well.

Wing skin panels consist of skin and spanwise stringers both tapering in thickness as required in the primary bending and torque section. These skin panels are supported by chordwise ribs spaced at 24 inches (.61 m) as shown in Figure 4-16. The twenty-four inch (.61 m) spacing between ribs was chosen primarily because: (a) the ribs have large square cutouts and the close spacing gives reasonable size rib members; (b) the spacing will give adequate support to the roller channels and not overload cargo rollers and containers at the ribs; and (c) close rib spacing offers a more efficient pressurized structure. The rib elements are tension field beams with machined caps for efficient use of material and with webs stiffened by extruded angles. Since these ribs are considered as continuous beams across the spars, their caps are spliced through the spar plane.

The cargo containers are supported by 1.75 inch (.045 m) diameter rollers spaced at eight inches (.20 m) and mounted in spanwise channels that are spaced at 20 inches (.51 m). These roller channels aid the wing lower skin panels in supporting wing bending loads. There is no primary floor, but there are walking provisions in the cargo compartment along with walkways forward of spar 1 and aft of spar 4 for ground maintenance access. The structural shear panels are spaced at every ten rib bays and transfer wing bending shear loads to the roller channels.

Critical design load conditions: A representative spectrum of flight and ground conditions was investigated in order to establish critical loads for wing design purposes. The selection of load conditions processed are identified in Table 4-7. All flight conditions were investigated at the following gross weights;

TABLE 4-7A
DESIGN LOAD CONDITIONS (LIMIT)
English Units

TYPE	COND. NO.	DESCRIPTION
Balanced maneuver, $n = 2.5$ at V_D	1	$W = 1,350,000$ lb., $M = .75$ at 11,300 ft.
	2	$W = 713,000$ lb., $M = .75$ at 11,300 ft.
	3	$W = 410,000$ lb., $M = .75$ at 11,300 ft.
	4	$W = 1,037,000$ lb., $M = .75$ at 11,300 ft.
Gust conditions 50 fps up gust at V_C	5	$W = 1,350,000$ lb., $M = .7$ at 14,700 ft., $n = 2.514$
	6	$W = 713,000$ lb., $M = .7$ at 14,700 ft., $n = 3.106$
	7	$W = 410,000$ lb., $M = .7$ at 20,000 ft., $n = 3.611$
	8	$W = 1,047,000$ lb., $M = .7$ at 14,700 ft., $n = 2.748$
Landing conditions at design landing wt. (1,077,300 lb)	9	Tail-down landing, $n_z = 2.0$, $n_x = 0.25$
	10	'One-wheel' landing, $n_z = 1.5$, $n_x = 0.125$, left wing
	11	'One-wheel' landing, right wing
	12	Lateral drift landing, $n_z = 1.5$, $n_y = 0.35$, left wing
Ground handling at design takeoff wt. (1,350,000 lb)	13	Lateral drift landing, right wing
	14	Taxi, $n_z = 2.0$
	15	Braked roll, $n_z = 1.0$, $n_x = 0.8$
	16	Turning, $n_z = 1.0$, $n_y = 0.5$, left wing
	17	Turning, right wing

TABLE 4-7B
DESIGN LOAD CONDITIONS (LIMIT)
Metric Units

TYPE	COND. NO.	DESCRIPTION
Balanced maneuver, $n = 2.5$ at V_D	1	$W = 612,360$ kg, $M = .75$ at 3,444 m
	2	$W = 323,417$ kg, $M = .75$ at 3,444 m
	3	$W = 185,976$ kg, $M = .75$ at 3,444 m
	4	$W = 474,919$ kg, $M = .75$ at 3,444 m
Gust conditions 15 mps up gust at V_C	5	$W = 612,360$ kg, $M = .7$ at 4,481 m, $n = 2.514$
	6	$W = 323,417$ kg, $M = .7$ at 4,481 m, $n = 3.106$
	7	$W = 185,976$ kg, $M = .7$ at 6,096 m, $n = 3.611$
	8	$W = 474,919$ kg, $M = .7$ at 4,481 m, $n = 2.748$
Landing conditions at design landing wt. (488,663 kg)	9	Tail-down landing, $n_z = 2.0$, $n_x = 0.25$
	10	'One-wheel' landing, $n_z = 1.5$, $n_x = 0.125$, left wing
	11	'One-wheel' landing, right wing
	12	Lateral drift landing, $n_z = 1.5$, $n_y = 0.35$, left wing
Ground handling at design takeoff wt. (612,360 kg)	13	Lateral drift landing, right wing
	14	Taxi, $n_z = 2.0$
	15	Braked roll, $n_z = 1.0$, $n_x = 0.8$
	16	Turning, $n_z = 1.0$, $n_y = 0.5$, left wing
	17	Turning, right wing

Maximum takeoff weight - 1,350,000 lb (612,360 kg)
Maximum zero payload weight - 713,000 lb (323,417 kg)
Operational weight empty - 410,000 lb (185,976 kg)
Maximum zero fuel weight - 1,047,000 lb (474,919 kg)

This range of gross weights provides a conservative envelope for all other payload-fuel combinations and overall loading considerations.

Wing shear force, bending moment, and torque distributions were computed for all design load conditions and the envelope of critical values extracted for each distribution. The ultimate values for the critical shear force, bending moment and torque are plotted in Figures 4-18, 4-19 and 4-20, respectively, and were used to size major structural elements. Two conditions dominate over the complete span;

Balanced maneuver, $n = 2.5$ at maximum takeoff weight for
up-bending

Taxi, $n = 2.0$ at maximum takeoff weight for down-bending

Complete data for these conditions are therefore included in the referenced figures.

Following is a summary of the critical design load conditions for the structural design of the spanloader wing:

Structural Element	Critical Condition
Wing skin panels	2.5 g balanced maneuver at maximum gross weight and, + 5 psia (34,474 Pa) pressurization for the lower panels.
Wing typical ribs	2.5 g balanced maneuver at maximum gross weight.
Wing spar webs	In general the balanced maneuver condition designs the spar with the exception that certain areas at the inboard end are designed by 2 g taxi condition. A portion of spar 1 is designed by fuel tank pressure in the balanced maneuver condition. Spar 4 is designed by wing pressurization in combination with the maneuver condition.

FIGURE 4-18
CRITICAL WING ULTIMATE SHEAR FORCE

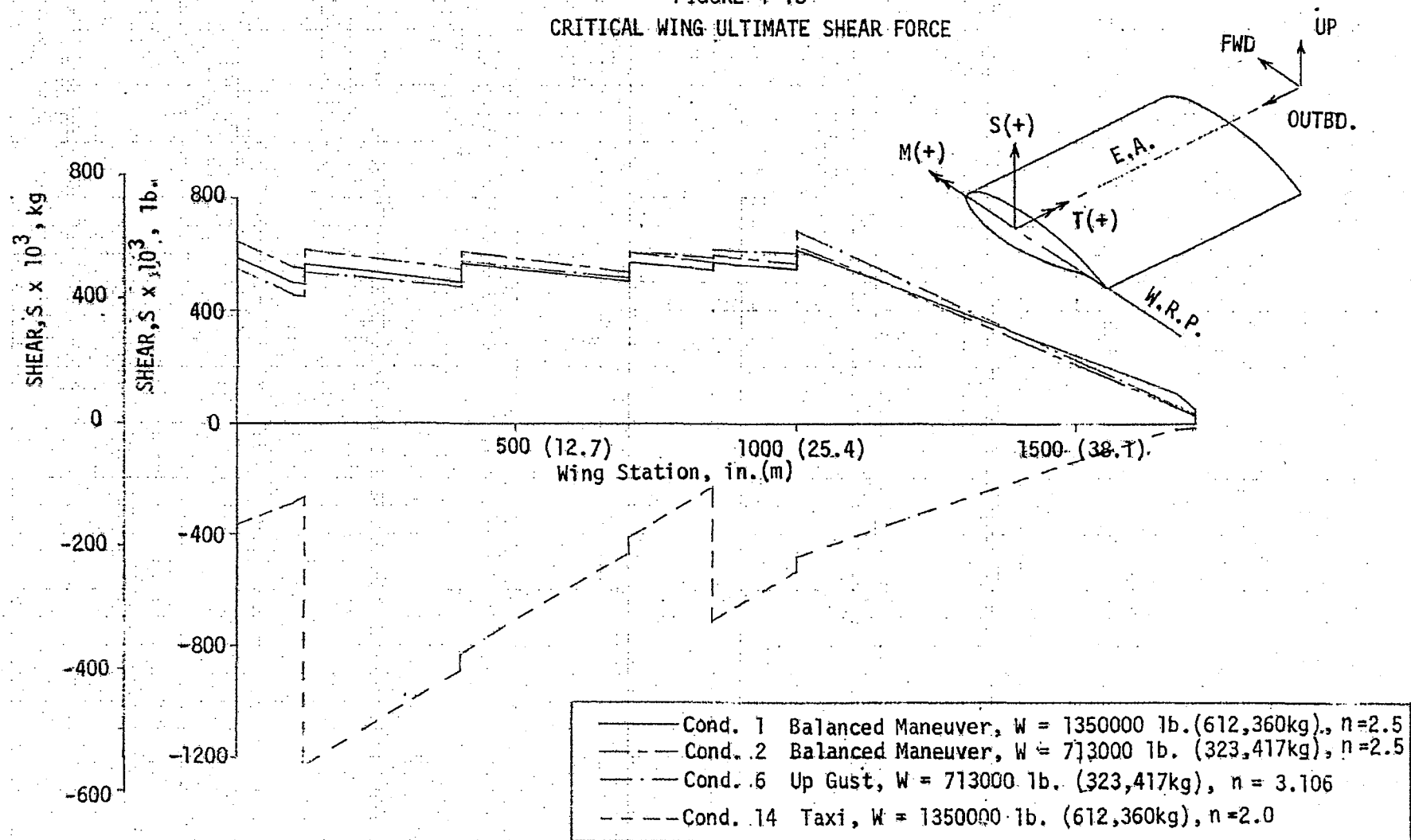


FIGURE 4-19
CRITICAL WING ULTIMATE BENDING MOMENT

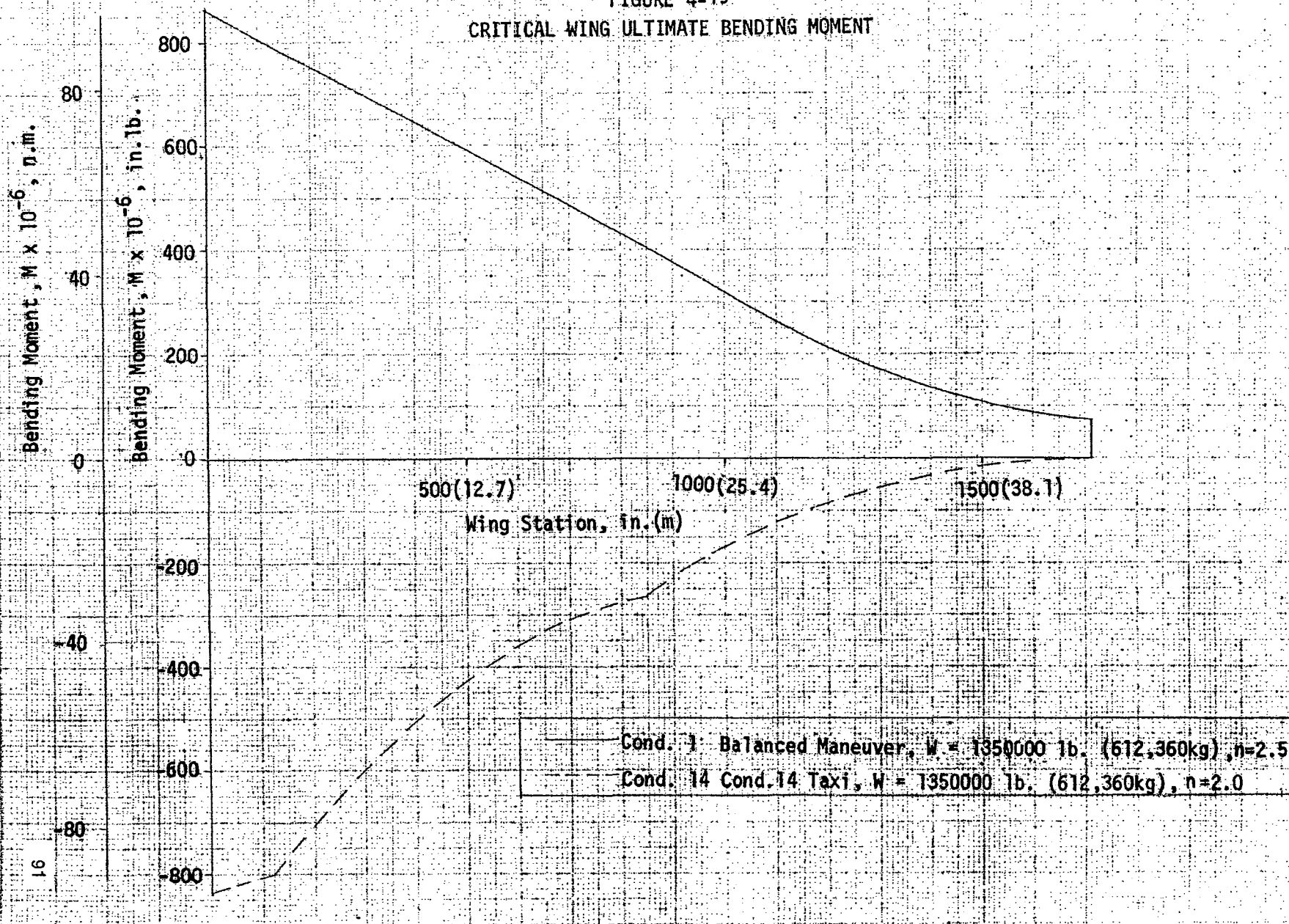
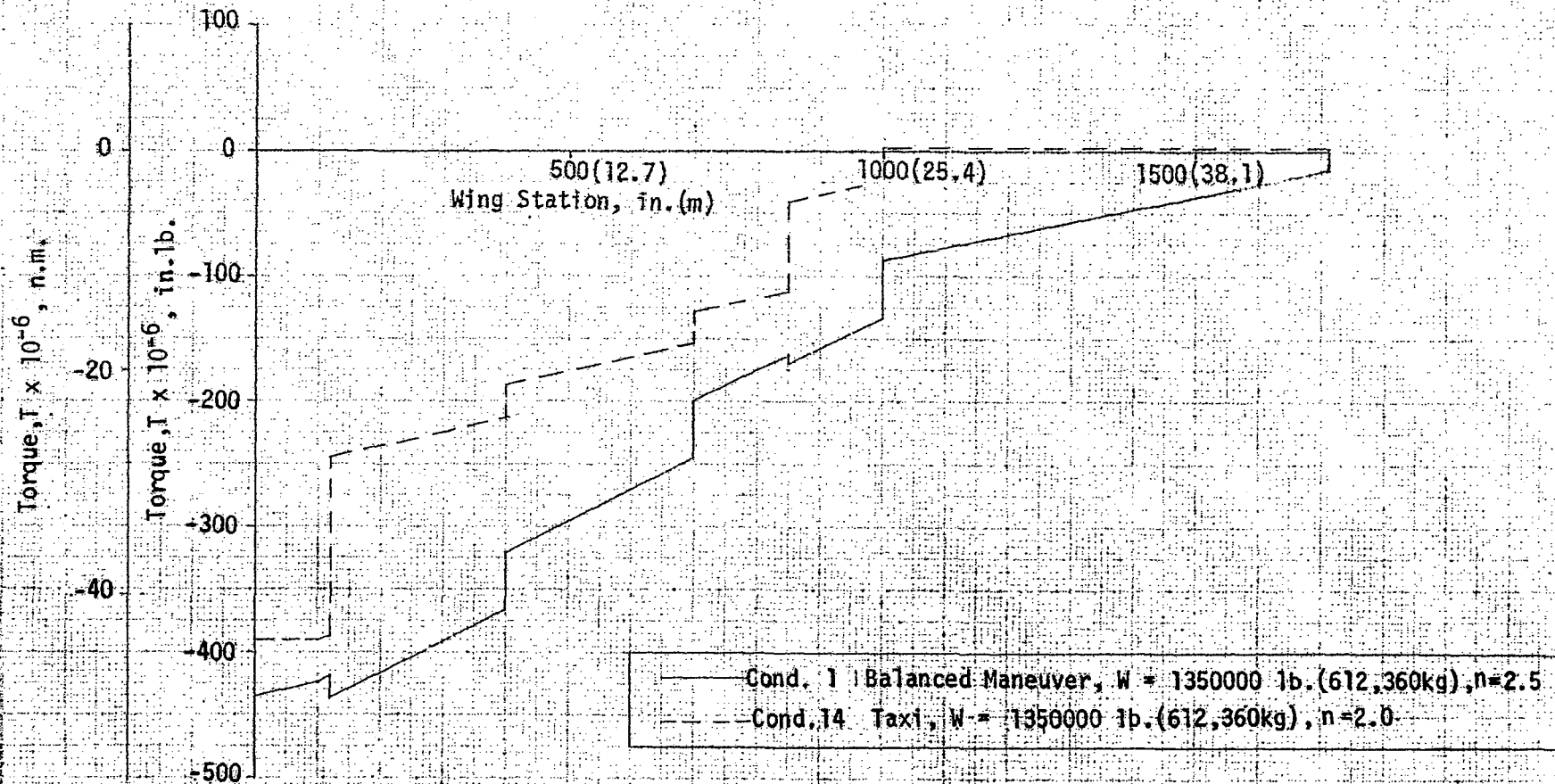


FIGURE 4-20
CRITICAL WING ULTIMATE TORQUE



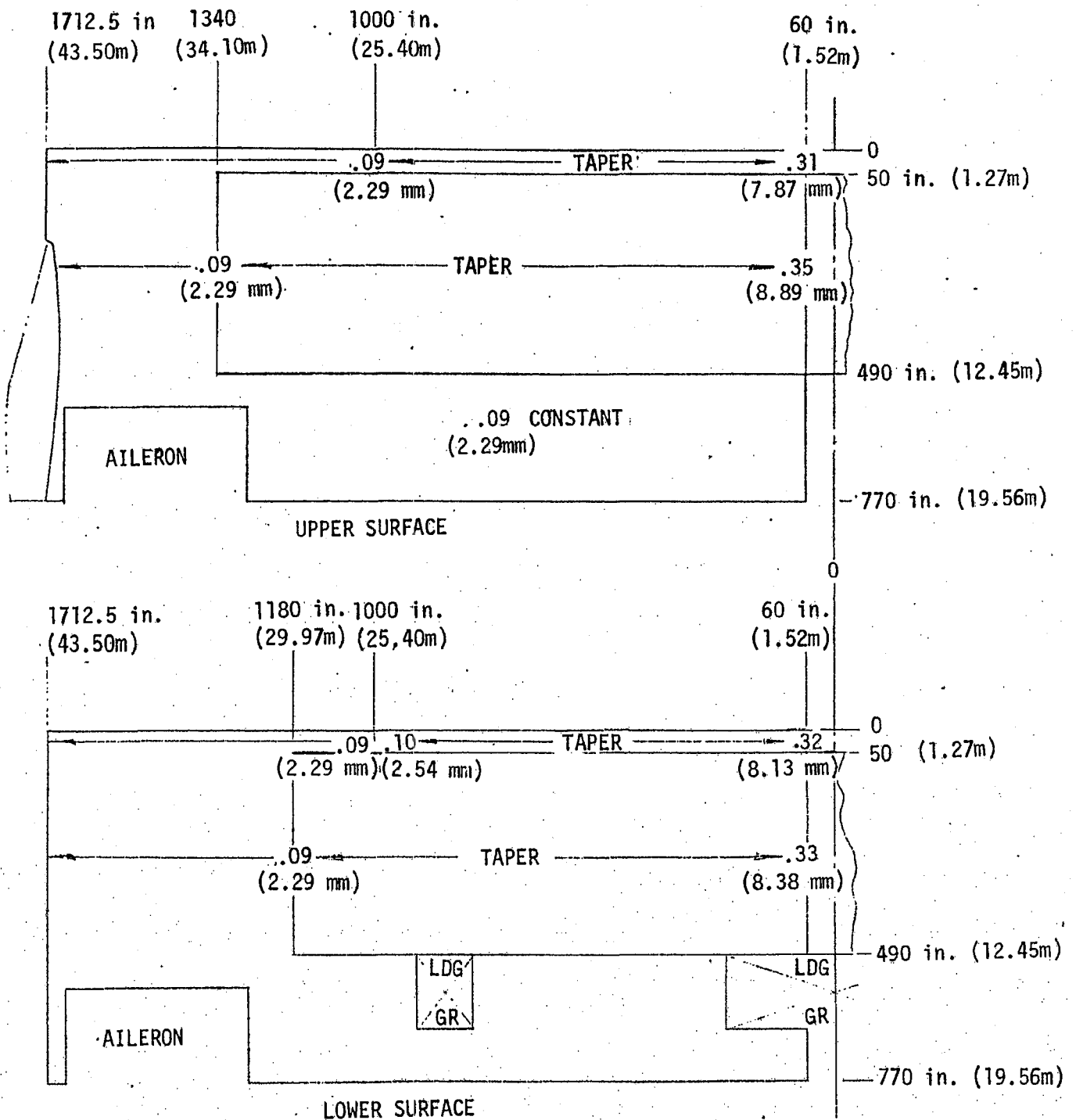
Cargo support	The cargo rails provide vertical support and are designed by the maximum vertical load factor of the 2.5 balanced maneuver at minimum fuel and maximum payload. Forward and aft support of the cargo can be provided by the 24 inch (.61 m) spaced rib beams which are in close proximity to the containers.
Fuel tank	2.5 g balanced maneuver with full fuel and no payload.
Landing gear and support	2 g taxi condition

Structural design analysis results: Figure 4-21 shows the required skin panel thickness with the tapered portion occurring in the primary bending and torque section of the wing as defined in Figure 4-16. Minimum gauges are reached at station 1340 on the upper surface and at station 1180 on the lower. These areas of minimum gauge do not represent the most effective application of the spanloader concept of distributed payload balanced by a distributed lift. Although skin panel thicknesses are relatively thin in this spanloader configuration compared to existing large commercial transports they could be reduced further by optimizing the distribution of masses within and attached to the wing. As an example, since fuel is a major mass item a more uniform spanwise distribution of this item within the wing would reduce the associated bending moments. Furthermore, due to the combined effects of the chordwise locations of the fuel and engines and the aft center of pressure of the super-critical airfoil, the wing has a comparatively high torque at the inboard end. This results in a torque material requirement of the same order of magnitude as the bending material. For this reason additional spanloader studies should include mass distribution optimization as a top priority.

Although a constant thickness skin panel would realize some cost saving it is doubtful that this approach could reduce the number of parts since wing panels should be designed to be a maximum length compatible with manufacturing and handling facilities. However, a straight-wing spanloader configuration tends to allow the use of constant panel thickness across the

FIGURE 4-21

WING SKIN PANEL THICKNESS, \bar{t}



chord without the attendant load concentration at the root of the rear spar encountered with swept wings. This absence of chordwise taper is favorable to achieving parts commonality.

A typical wing rib is defined as one which supports only the distributed loads of the wing; namely, the aerodynamic pressure (lift), cargo loads, wing pressurization, crushing loads due to wing bending, and the chordwise shear transfer of applied loads to the elastic axis. Figure 4-22 illustrates this type of rib loading with the resulting net chordwise rib shear and bending moment presented in Figures 4-23 and 4-24, respectively. The Point Design spanloader configuration, with the constant airfoil section, no sweep and winglets at the tip, has a relatively constant spanwise load distribution with all ribs having the same loading except for the crushing load. Since crushing provided a relatively small part of the total rib load a practical design would make all of the typical ribs identical. Pressurization is balanced by upper and lower surface loading through direct load paths in the vertical members of the rib. Although the loading diagram of Figure 4-22 indicates that pressurization is the dominant load on the rib, the lift with its chordwise shear transfer is more significant. The resulting rib member sizes are shown in Figure 4-25.

All web gauges are minimum thickness, indicating that trusses may be more efficient or that the rib height could possibly be reduced. Further study is indicated for this area, although the effort must be performed in conjunction with an overall wing analysis that includes the ribs which support concentrated loads. As an example, one such concentrated load area is the landing gear support structure (Figure 4-17). Six ribs are available in the span of the wheel well to distribute gear loads into the wing structural box. A three-dimensional wing analysis is required to determine the actual extent of the landing gear loads on the wing ribs. Similar considerations apply to other concentrated load areas at the engine supports, wing fuselage juncture, inboard landing gear attachment, aileron support, and at the winglet support. Figure 4-26 is a diagram showing an estimate of wing rib commonality for the Point Design spanloader airplane.

Wing spar material thickness is shown in Figure 4-27. Spar 4 has the highest load requirement due to the fact that both torque and vertical shear add to the pressurization loads. The next higher load occurs in spar 1

FIGURE 4-22

TYPICAL WING RIB LOADING

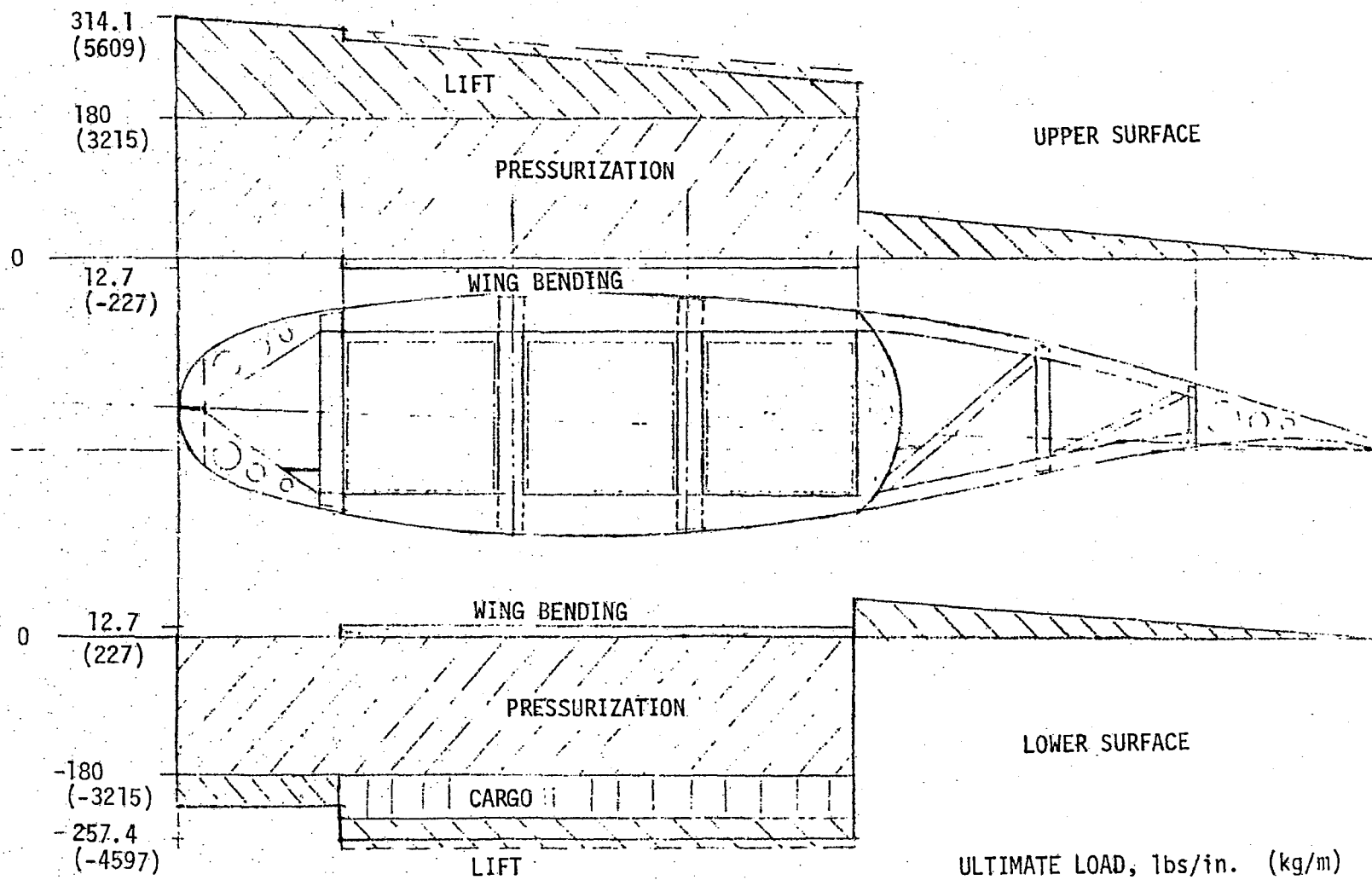


FIGURE 4-23
TYPICAL RIB SHEAR
BALANCED MANEUVER CONDITION

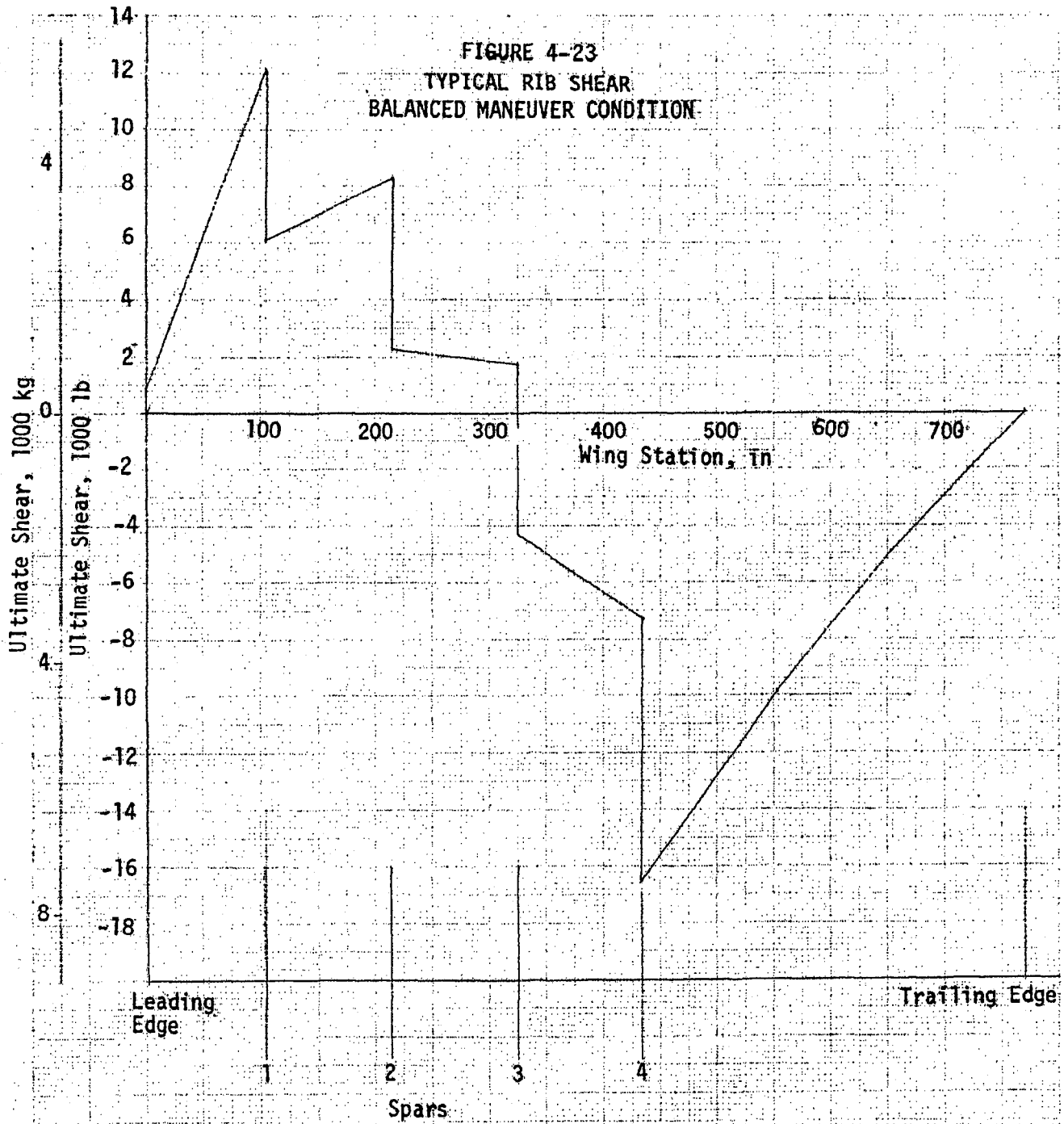


FIGURE 4- 24
TYPICAL RIB BENDING MOMENT
BALANCED MANEUVER CONDITION

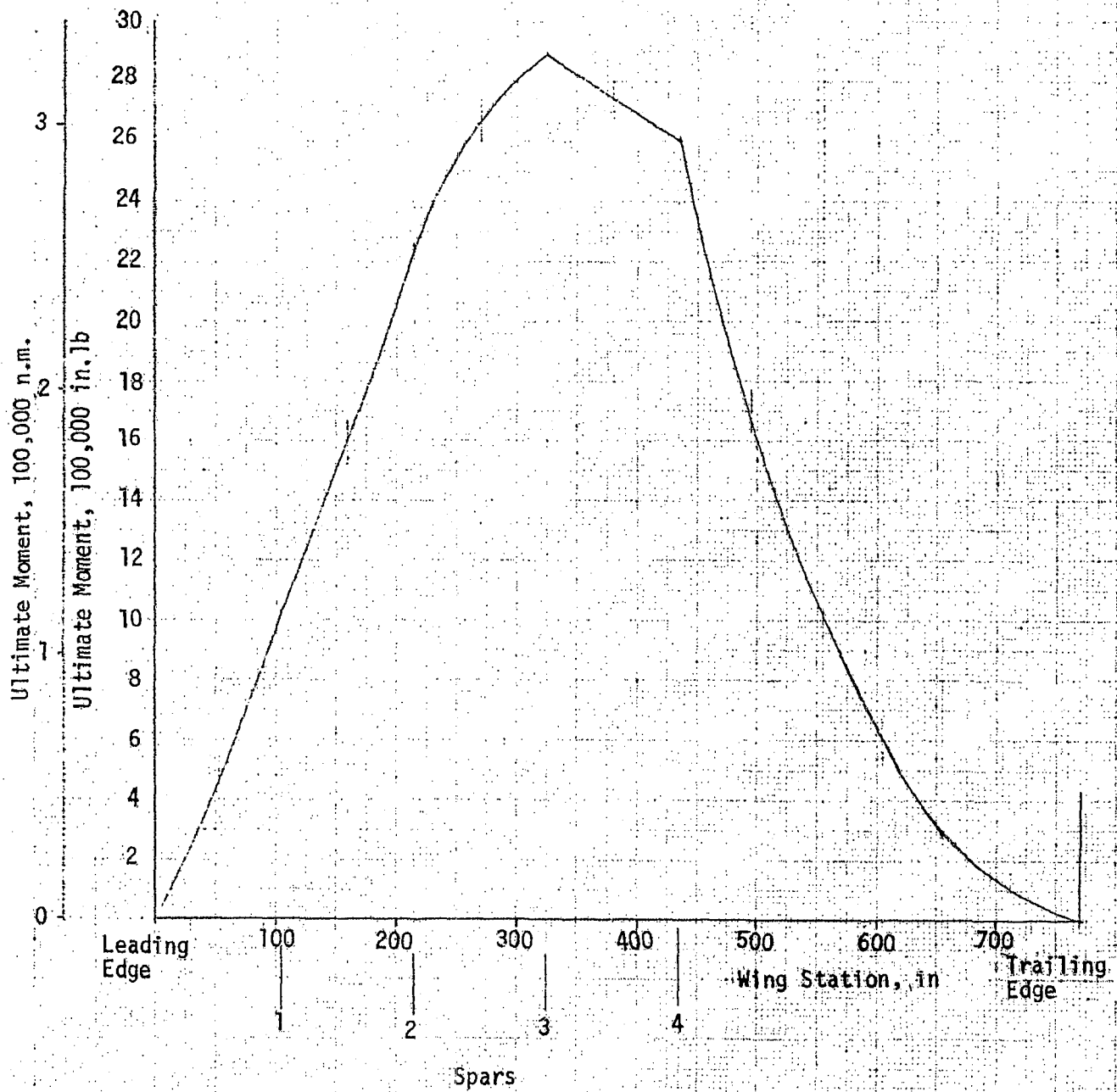


FIGURE 4-25

TYPICAL WING RIB THICKNESS, \bar{t}

\bar{t} INCLUDES CAP, WEB & STIFFENERS, in.

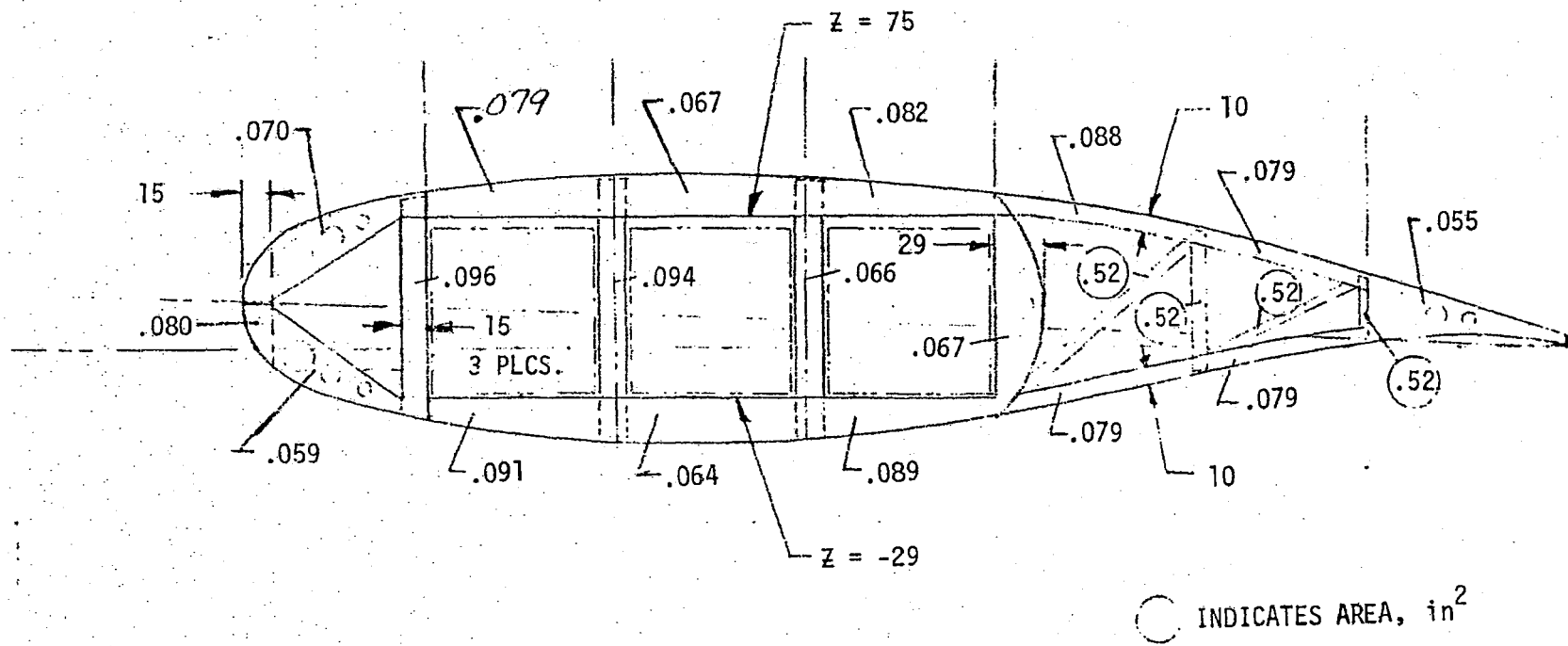
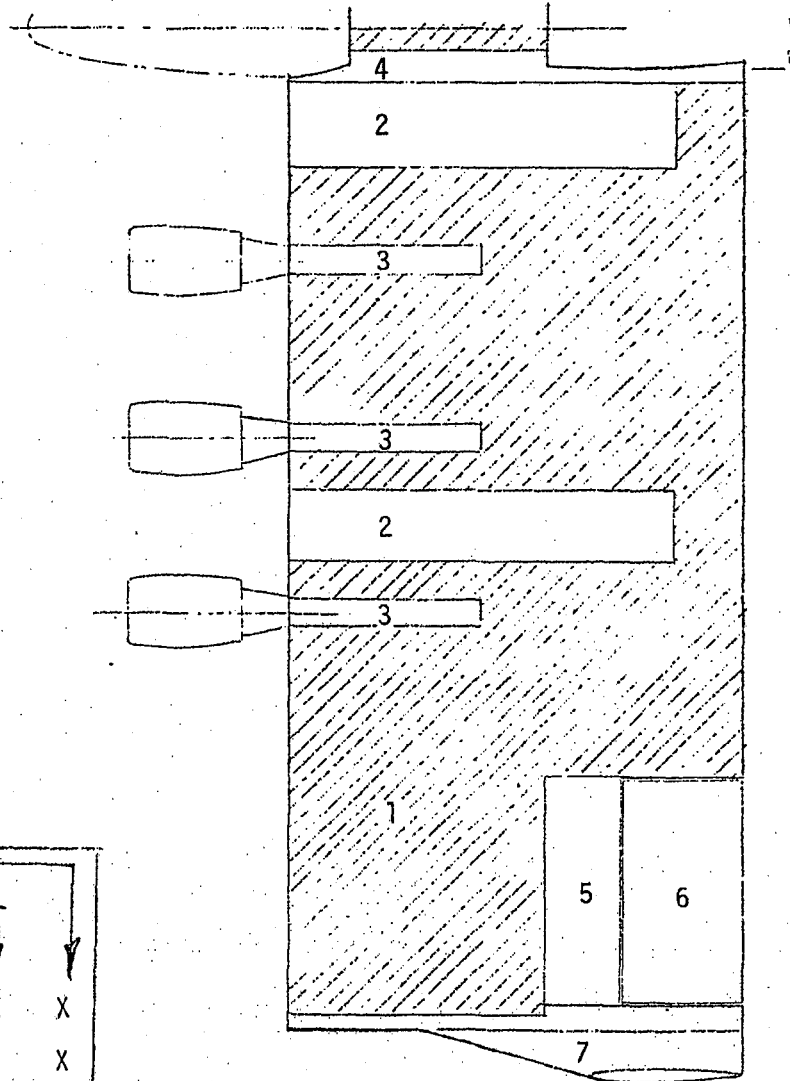


FIGURE 4-26

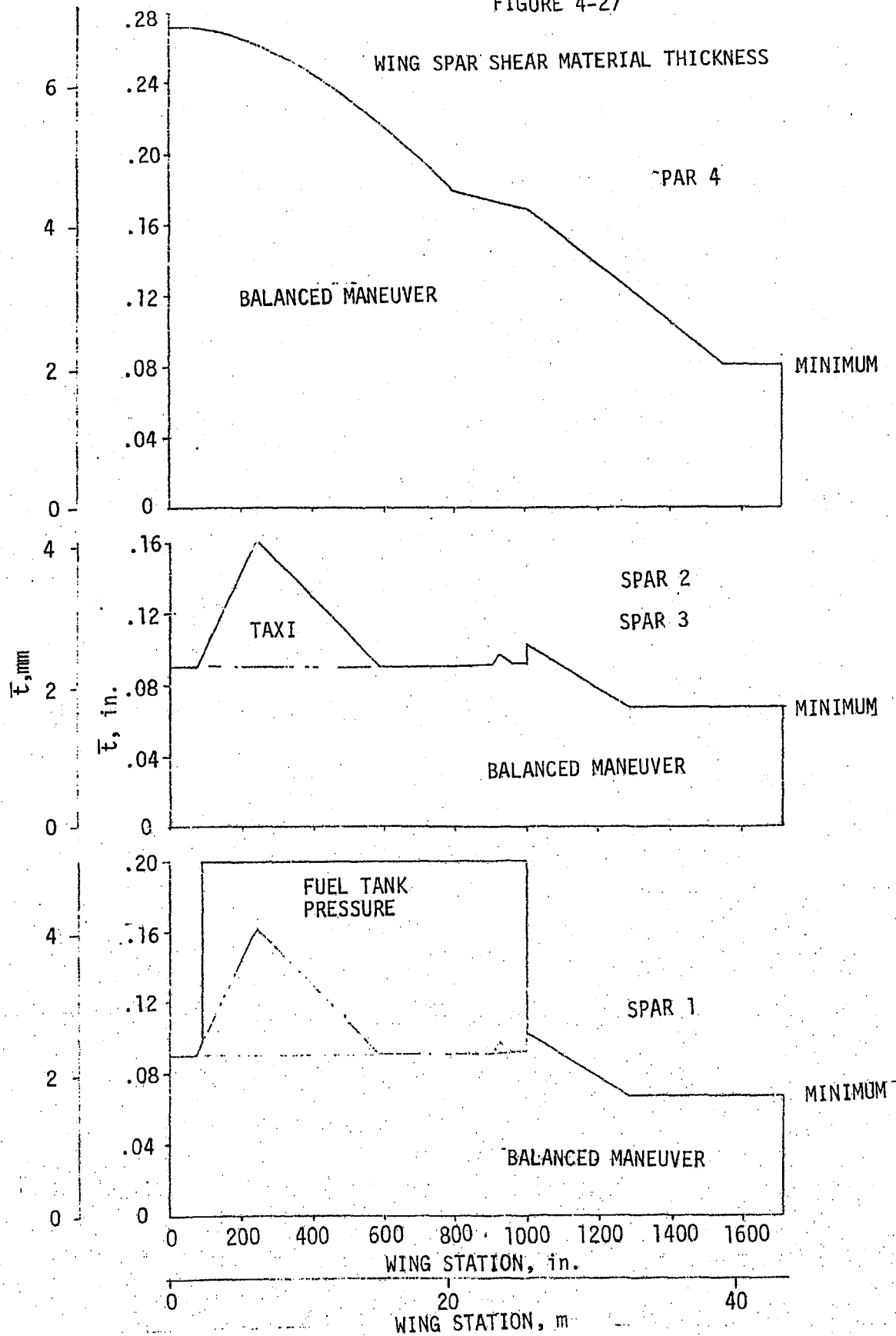
WING RIB COMMONALITY



COMMONALITY		
LEFT TO RIGHT		
STATION TO STATION		
ITEM	↓	↓
1 TYP RIBS	X	X
2 LANDING GR	X	X
3 ENG. SUPPT.	X	X
4 WING-FUS	X	X
5 AILERON SUP.	*	X
6 AILERON	*	X
7 WINGLET		X

* PARTIAL

FIGURE 4-27



which supports the fuel tank pressures inboard of station 1000. As discussed previously these spar thickness requirements could be reduced by optimization of mass distribution in the wing. As an example, moving engines and fuel aft would reduce the torque shear requirements in the rear spar.

4.2 Conventional Aircraft Description

This section presents a summary of the conventional all-freighter aircraft configuration used as a comparator for the Point Design spanloader. The aircraft has been optimized to the same ground rules and performance constraints as the spanloader and in general used the same level of technology where applicable.

This configuration is not documented in detail in this report since it is of conventional design and existing methodologies for estimating vehicle characteristics are adequate and accepted within the industry. The vehicle presented is based upon a considerable background of company experience and recent studies of large conventional all-cargo aircraft.

Configuration arrangement. - The referenced conventional aircraft was derived using the PASAP computer program to optimize (minimum DOC_p) the geometry of the configuration to the same performance requirements as the Point Design spanloader. The resulting configuration is shown in Figure 4-28 and its primary design data and geometry tabulated in Table 4-8. For the base fuel cost value of 25 cents per gallon, the wing aspect ratio optimized at a value of 9.2 with a wing thickness ratio (supercritical airfoil) of .14 and a quarter chord sweep of 28 degrees.

The wing area and engine thrust level were sized by the 12,000 foot (3,658 m) takeoff field length. The landing field length was not critical and a single slotted Fowler motion flap and leading edge slat were found to be appropriate.

The fuselage is of circular cross section to minimize structural weight penalties due to pressurization (5 psia (34.5 k Pa)). Four rows of containers are loaded on two cargo decks - ten 8 x 8 x 20 foot (2.44 x 2.44 x 6.10 m) containers in each row. This gave a gross design payload of 590,000 pounds (267,620 kg) for a net cargo density of 10 pounds per cubic foot (160 kg/m^3) and a container density of 1.5 pounds per cubic foot (24 kg/m^3). The nose door swings upward to open the full cross section of the aircraft

FIGURE 4-28
CONVENTIONAL AIRCRAFT

CHARACTERISTICS DATA			
	WING	H. TAIL	V. TAIL
AREA	8000 ft ² (743 m ²)	1472 ft ² (137 m ²)	1100 ft ² (102 m ²)
AR	9.2	4.0	1.6
T.R.	.30	.35	.35
Λ , c/4	28°	30°	35°
t/c	14°	11°	12°
Vol. Ratio		.797	.067

Gross Payload = 590,000 lbs (267,620 kg)

40 Containers $\rho_{PLN} = 10 \text{ lb/ft}^3$
(160 kg/m³)

$\rho_{TARE} = 1.5 \text{ lb/ft}^3$
(7.38 kg/m³)

TOGW = 1,260,167 lbs (571,613 kg)

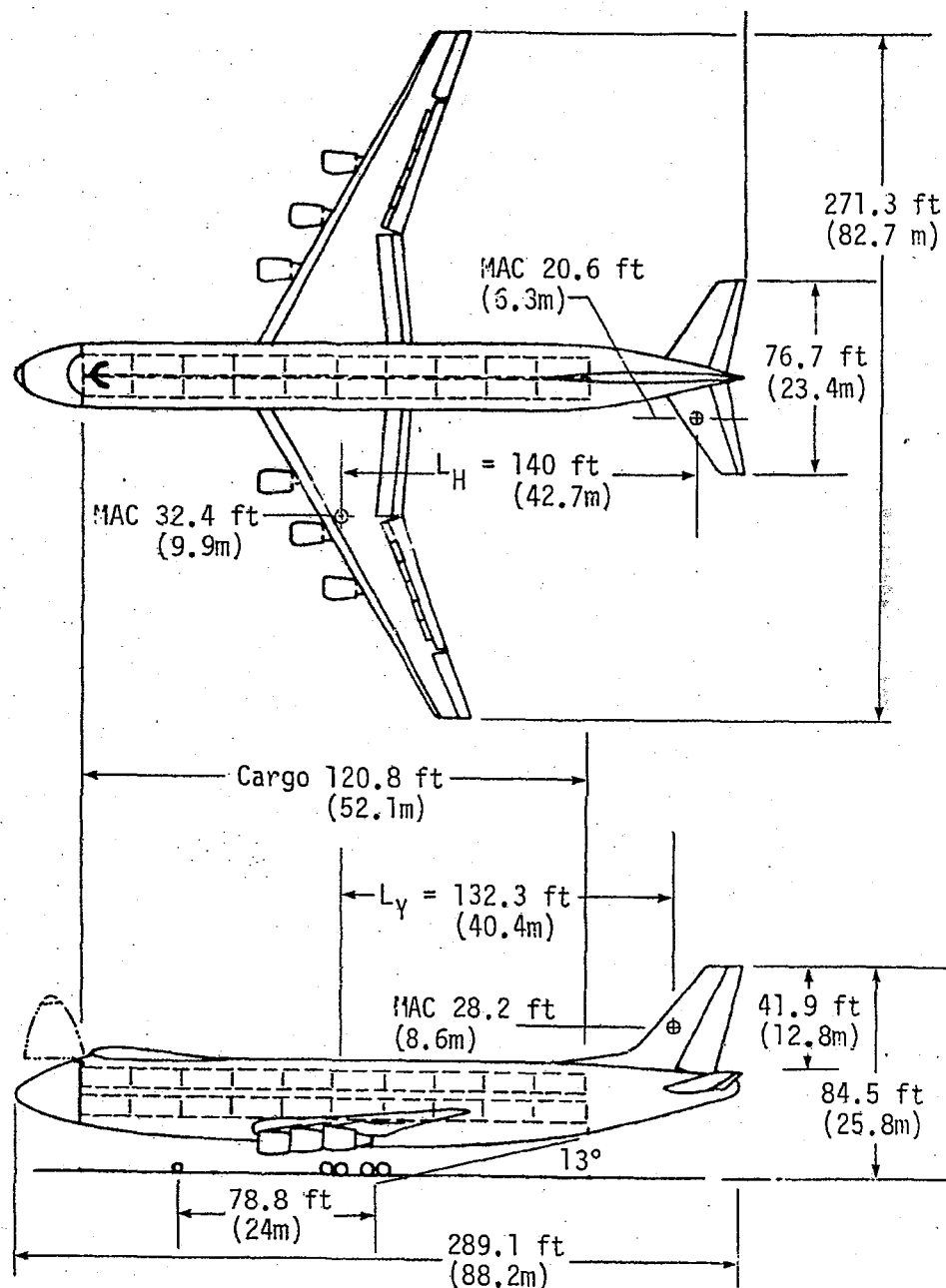
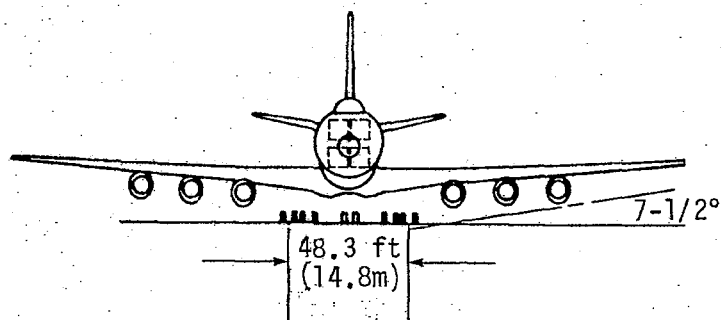


TABLE 4-8
CONVENTIONAL AIRCRAFT
DESIGN DATA AND GEOMETRY

	English Units	Metric Units
Design Weights - lb (kg)		
Takeoff	1,260,167	571,602
Landing	1,030,781	467,554
Zero Fuel	990,509	449,287
Gross Payload	590,000	267,620
Criteria		
Design Pressure Differential - Crew/Fuselage psia (k Pa)	7.46/5	51.4/34.5
Design Limit Load Factor (Airplane @ TOGW)	2.5	2.5
Design Cruise Speed - KTAS (m/sec)	459	236
Design Cruise Mach Number	.78	.78
Design Cruise Lift Coefficient	.50	
Engines		
Number Required	6	6
SLS Thrust/Engine - lb (N)	44,029	195,929
Specific Fuel Consumption-lb/hr/lb (kg/hr·N)	.569	.058
Wing Geometry		
Area - ft ² (m ²)	8,000	743.2
Aspect Ratio	9.2	9.2
Taper Ratio	.3	.3
Sweep @ c/4 - degrees	28	28
Mean Thickness Ratio	.14	.14
Aileron area - ft ² (m ²)	232.3	21.6
Tail Geometry		
Horizontal Tail Area - Theoretical - ft ² (m ²)	1,472	136.8
Horizontal Tail Length - in (m)	1,680	42.67
Horizontal Tail Volume	.797	.797
Vertical Tail Area - Exposed - ft ² (m ²)	1,100	102.2
Vertical Tail Length - in (m)	1,590	40.39
Vertical Tail Volume	.067	.067
Elevator Area - ft ² (m ²)	358	33.3
Rudder Area - ft ² (m ²)	455	42.3
Fuselage Geometry		
Length - in (m)	3,470	88.14
Maximum Height - in (m)	400	10.16
		(excl CAB)
Maximum Width - in (m)	318	8.08
Maximum Perimeter - in (m)	966	24.5
Wetted Area - Gross - ft ² (m ²)	20,380	18.93
Floor Area - ft ² (m ²)	6,716	623.9

for straight-in loading of both decks.

The empennage of the conventional aircraft has been designed to provide stability and control characteristics comparable to those of the spanloader. The horizontal tail was sized to provide, with stability augmentation, satisfactory flight characteristics over a c.g. range of 20 percent MAC. Without augmentation, a negative static stability margin of 10 percent MAC is provided at the critical high speed cruise condition. Aerodynamic and aeroelastic characteristics, based primarily on DC-10 data, were used to size the tail. The vertical tail was designed to provide one-engine-out control in the air, at a speed 10 knots less than the design lift-off speed. This directional control requirement can be met using a 40 percent chord single-hinge rudder similar to that of the DC-8.

The engine used for the conventional aircraft is the same as that used for the spanloader except for size. These were bypass ratio 9 fan jets with an SFC improvement of five percent compared to the present TF-39 engine.

Structures and mass properties. - The structural components of the conventional aircraft were assumed to be of composite material - both primary and secondary. As with the spanloader, the basic structure and weights evaluations were first accomplished for conventional aluminum structure. Specific components of structure were then converted to a composite material base. The resulting weight summary is shown in Table 4-9.

Performance summary. - The performance evaluated for the conventional aircraft is shown in Table 4-10. The design mission, carrying a gross payload of 590,000 pounds (267,620 kg) 3,000 nautical miles (5,550 km), is accomplished at a gross weight of 1,260,167 pounds (571,602 kg). All performance is normal for an aircraft of this type. The cruise Mach number is 0.78.

Economic analysis. - The basic conditions and approach outlined in Section 4.1 that are used to derive the spanloader price and the DOC apply to the conventional design. The conventional aircraft also is designed with a high percentage of composites and the structural distribution is about the same as for the spanloader. However, the conventional design of the wing and horizontal tail precludes any assumption of a high degree of commonality in these airframe components. The costs for both the metallics

TABLE 4-9
CONVENTIONAL AIRCRAFT
WEIGHT SUMMARY

	<u>lb</u>	<u>kg</u>
Wing	158,045	71,688
Tail	11,338	5,143
Fuselage	80,760	36,632
Landing Gear	54,459	24,702
Nacelles	16,815	7,627
Propulsion	44,416	20,147
Fuel System	3,218	1,460
Flight Controls	7,339	3,329
Hydraulics	4,216	1,912
Instruments	1,199	544
Air Conditioning	3,334	1,512
Pneumatics	937	425
Electrical	2,925	1,327
Avionics	2,698	1,224
Furnishings	6,024	2,732
Ice Protection	324	147
Handling Gear	102	46
Manufacturer's Empty Weight	398,149	180,547
Operator's Items	<u>2,360</u>	<u>1,070</u>
Operator's Empty Weight	400,509	181,668
Manufacturer's Empty Weight	348,149	180,597
Less: Engines	42,796	19,412
Rolling Assembly	<u>18,168</u>	<u>8,241</u>
Basic Cost Weight	337,185	152,945
Basic Cost Weight	337,185	152,945
Less: Starters	150	68
Instrument Units	593	269
Electrical Units	511	232
Avionics Units	1,568	711
Air Conditioning Units	<u>757</u>	<u>343</u>
DCPR Weight	333,686	151,357

TABLE 4-10

CONVENTIONAL AIRCRAFT PERFORMANCE SUMMARY

Operating Weight Empty - lb (kg)	400,509	(181,671)
Gross Payload Weight - lb (kg)	590,000	(267,620)
Tare Weight - lb (kg)	78,000	(35,381)
Fuel Weight - lb (kg)	269,660	(122,318)
Takeoff Weight - lb (kg)	1,260,169	(571,613)
Reserve Fuel Weight - lb (kg) *	40,281	(18,272)
Net Thrust per Engine - lb/eng (N/eng)	44,029	(195,841)
Specific Fuel Consumption - lb/hr/lb (kg/hr· N)	.569	.058
Wing Loading - lb/ft ² (kg/m ²)	157.5	(769)
Thrust to Weight Ratio	.210	(2.06)
Ratio Operating Weight Empty to Takeoff Weight	.318	
Ratio Gross Payload to Operating Weight Empty	1.473	
Ratio Gross Payload to Fuel Weight	2.188	
Cruise Mach Number	.784	
Cruise Lift Coefficient	.500	
Initial Cruise Altitude - ft (m)	28,800	(8,778)
Maximum Lift to Drag Ratio	21.50	
Takeoff Field Length - ft (m)	12,000	(3,658)
Landing Field Length - ft (m)	5,210	(1,588)
Approach Velocity - kn (m/s)	134	(69)
Second Segment Climb Gradient	.0360	

* 40,281 lbs (18, 272 kg) for FAR Landing Reserve

portion and the composites reflect a traditional type of estimate. The cumulative average price for the stipulated 350 airplane buy is \$77.4 m, and \$72.0 M for the calculated quantity of 463 airplanes that are required to handle the assumed market of 100 billion ton-miles per year. The cost elements that comprise the \$72.0 M price are shown in Table 4-11 and the price/quantity relationship is exhibited in Figure 4-29.

The DOC calculation is based on price and performance characteristics peculiar to the conventional design and the resultant DOC associated with the required fleet size is 3.240 cents per ton-mile. The individual elements that make up this value are shown in Table 4-12.

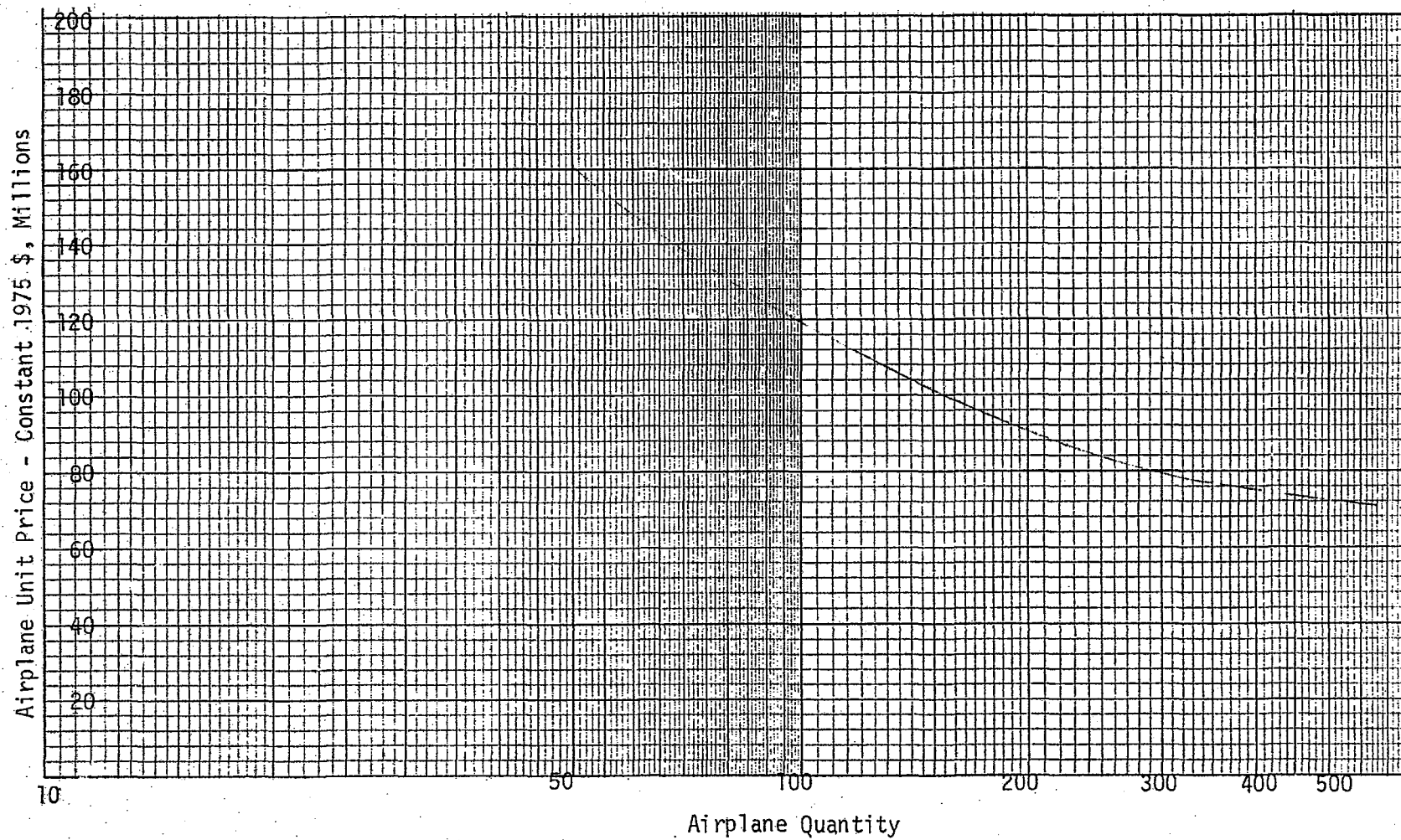
TABLE 4-12
DIRECT OPERATING COST BREAKDOWN

<u>Cost Element</u>	<u>Dollars/Flight</u>
Crew	2187.28
Insurance	2494.80
Depreciation	10914.75
Airframe Maintenance	
Labor	1245.81
Material	1032.36
Engine Maintenance	
Labor	821.66
Material	1385.57
Fuel	8595.67
<hr/>	
Total Dollars/Flight	28677.93
Total Dollars/NM	9.55
Total Cents Per Ton-Mile	3.73

TABLE 4-11
AIRPLANE PRICING (CONVENTIONAL DESIGN)
(Constant 1975 Dollars - Millions)

COST ITEM	AIRPLANE QUANTITY				
	50	100	150	200	350
<u>LABOR</u>					
Manufacturing	4214.1	6202.5	7910.1	9459.9	13568.9
Engineering	1889.6	2192.2	2420.9	2577.1	2953.2
Laboratory & Flight Test	183.0	185.9	188.7	191.7	194.6
Product Support	<u>33.8</u>	<u>33.8</u>	<u>33.8</u>	<u>33.8</u>	<u>33.8</u>
Sub Total	6320.5	8614.4	10553.5	12262.5	16750.5
<u>MATERIAL</u>					
Raw Materials	499.1	954.9	1409.4	1863.3	3223.6
Purchased Parts & Equipment	642.0	1212.2	1574.9	2017.1	3299.1
Flight Test	11.6	11.6	11.6	11.6	11.6
Product Support	<u>38.7</u>	<u>38.7</u>	<u>38.7</u>	<u>38.7</u>	<u>38.7</u>
Sub Total	1191.4	2217.4	3034.6	3930.7	6573.0
Engines	<u>538.9</u>	<u>1077.7</u>	<u>1616.6</u>	<u>2155.4</u>	<u>3772.0</u>
GRAND TOTAL (Labor + Material)	8050.8	11909.5	15204.7	18348.6	27095.5
CUM AVERAGE PRICE	161.0	119.1	101.4	91.7	77.4

FIGURE 4-29
AIRPLANE PRICE VERSUS QUANTITY
CONVENTIONAL AIRCRAFT



5.0 Vehicle Competitive Analysis

The basic analysis and characteristics of the previous section for the Point Design spanloader and conventional aircraft are compared in this section on a side-by-side basis in order to draw a convenient and concise perspective of their relative characteristics. In review, each aircraft was designed to the same level of technology (circa 1990), the primary elements of which consisted of all-composite structures, up to -10 percent negative stability margin, supercritical airfoils and winglets if appropriate. The payoff due to the use of winglets for the conventional aircraft was marginal because of the high aspect ratio and high taper of this configuration and winglets were not used. Engine optimization was not within the scope of the study and a fixed engine cycle was chosen for both configurations. Engine thrust level, however, was a part of the optimization function. Each configuration was designed to carry 8 x 8 x 20 foot (2.44 x 2.44 x 6.10 m) cargo containers. Because of the differences of cargo carriage, however, the spanloader was sized for three rows of 14 containers each (42 total) and the conventional aircraft for four rows of 10 containers each (40 total). This difference in cargo capacity was accounted for in deriving the economic evaluations by standardizing fleet productivity with appropriate fleet sizes. Both aircraft were designed for a 5 psia (34.5 k Pa) pressure differential in their respective cargo bays. The following specific comparative evaluations are pertinent.

5.1 Dimensional Data Comparison

Significant dimensional data is shown in Table 5-1. The spanloader has slightly more span than the conventional aircraft but is significantly shorter and of less height. The product of the three major dimensions is 4.259×10^6 cubic feet ($.121 \times 10^6 \text{ m}^3$) for the spanloader and 6.623×10^6 cubic feet for the conventional aircraft. The use of actual terminal area space, however, is the subject of a separate specific study.

The primary feature of the spanloader aircraft is its wing geometry resulting from the impact of the wing cargo stowage requirement. The impact on its large wing area is evident. The spanloader wing is so large, in fact, that high lift devices are not necessary to achieve acceptable field length performance. The wing area of the conventional aircraft, on the

TABLE 5-1
DIMENSION DATA
SPANLOADER VS CONVENTIONAL AIRCRAFT

COMPONENT	SPANLOADER	CONVENTIONAL AIRCRAFT
Span - ft (m)	285.4 (87.0)	271.0 (82.6)
Length - ft (m)	202.5 (61.7)	289.2 (88.1)
Height - ft (m)	73.7 (22.5)	84.5 (25.8)
Wing		
Area - ft ² (m ²)	18,314 (1,701)	8,000 (743)
Aspect Ratio	4.45	9.2
Sweep - deg	0	28
Thickness Ratio	.20	.14
Taper	1.0	.30 (excluding Yehudi)
Horizontal Tail		
Area - ft ² (m ²)	2,938 (273)	1,472 (137)
Volume Ratio	.30	.797
Vertical Tail		
Area - ft ² (m ²)	674 (63)	1,100 (102)
Volume Ratio	.016	.067
Fuselage		
Surface Area - ft ² (m ²)	10,600 (985)	20,380 (1,893)
Landing Gear		
Number of Main Bogies	4	5
Number of Wheels	24	20
Tread - ft (m)	141.7 (43.2)	48.3 (14.7)

other hand is determined by field length requirements even using very effective high lift devices.

The thicker wing of the spanloader results from the space requirements associated with cargo containment. Study results actually showed that a thickness ratio down to .17 would provide some additional marginal payoff due to the lesser profile drag and higher cruise Mach number of the thinner airfoil sections. However, additional detailed analysis would be required to determine the real nature and magnitude of these potential benefits.

The horizontal tail volume ratio of the spanloader is approximately 62 percent less than that of the conventional aircraft primarily because of the significantly smaller destabilizing fuselage of the spanloader. The tail area, however, is still over twice that of the conventional aircraft because of the large size of the spanloader wing and a significantly smaller horizontal tail arm.

The spanloader vertical tail volume ratio also benefits from the small destabilizing fuselage and the significant stabilizing effects of the two winglets. The resulting tail area is 61 percent of the conventional aircraft.

The smallness of the spanloader fuselage is indicated by comparing the fuselage wetted areas; 48 percent less than that of the conventional aircraft.

The wheel and bogie arrangement of the main landing gears is the result of designer's choice as affected by the ground taxi loads that were found to be critical to wing structure with full-up payload. The tread dimension, however, is fundamental since in conjunction with aircraft weight it limits the permissible airfields for aircraft operations. The impact of this dimension on spanloader operations must await a system evaluation of the concept.

5.2 Structures And Weight Comparison

A summary comparison of the weights characteristics of the two configurations is shown in Table 5-2. The primary impact of the spanloader concept on vehicle weight is appreciated by considering the structural weight ratio, OWE/TOGW. This value is .29 for the spanloader which compares to .32 for the advanced conventional aircraft of comparable technology. This

TABLE 5-2
WEIGHT DATA

COMPONENT	SPANLOADER		CONVENTIONAL AIRCRAFT		Change From Point Design Spanloader	
	lb	(kg)	lb	(kg)	lb	(kg)
Wing	170,929	(77,533)	158,045	(71,689)	-12,884	(-5,844)
Winglets	7,392	(3,353)	-			
Empennage	14,667	(6,653)	11,338	(5,143)	- 3329	(-1510)
Fuselage	28,236	(12,808)	80,760	(36,633)	52,524	(23,825)
Landing Gear (including rolling assembly)	58,987	(26,757)	54,459	(24,702)	-4,528	(-2055)
Propulsion System (including nacelles and engines)	83,700	(37,966)	61,231	(27,774)	-22,469	(-10,192)
Other (Flt controls, Hyd. Instru., Air Cond., Elect., Handling Gear, Etc.	32,614	(14,794)	34,676	(15,729)	2,062	(935)
Operator's Empty Weight	396,525	(179,864)	400,509	(181,671)	3,984	(1,807)

structural performance has been achieved despite the fact that the spanloader wing is approximately twice the size of the conventional aircraft. The unit weight of the spanloader wing (9.3 lbs. per sq. ft. (45.6 kg/m^2)) compares to 19.8 lbs. per sq. ft. (96.5 kg/m^2) for the conventional aircraft. This attests to the high structural efficiency of the spanloader wing resulting from the distributed load effect, thick airfoil, low aspect ratio, and the lack of any lift augmentation devices.

The percent of weight in the spanloader fuselage is 7.1 compared to 20.2 for the conventional aircraft showing the effect of minimizing the fuselage structure. On the other hand, the empennage percentage has been increased (3.7 from 2.8 percent) due primarily to the large spanloader wing.

The structural efficiency of the spanloader is further illustrated by comparing the ratio of weight empty to total wetted area. This ratio is 6.36 pounds per square foot (31.05 kg/m^2) compared to 8.22 pounds per square foot (40.13 kg/m^2) for the conventional aircraft.

There is a notable difference (22,469 lbs) in the weights of the propulsion subsystems for the two configurations. A portion of the differences is due to the fact that the spanloader propulsion subsystem encompasses a non-optimum engine cycle. Additional work to achieve this optimization would undoubtedly reduce the noted weight differential.

5.3 Structural Arrangement Comparisons

The spanloader structural arrangement yields payoffs in aircraft structural weight efficiency as just discussed. Perhaps of equal importance is the impact of the structural arrangement on potential vehicle manufacturing costs. The structures discussion of Section 4.1 shows that a high degree of commonality and interchangeability of parts is possible. This commonality will result in reduced engineering, tooling and manufacturing costs. The net effect of commonality on vehicle weight is not quite so evident. cursory examination indicates that a weight penalty may accompany the design for commonality. Questions such as this will only be answered through detailed strength analysis and structural designs.

The primary feature that allows parts commonality is the constant section straight wing and the uniform spanwise lift distribution. Optimization of the mass distribution in the wing with a resulting shear and torque reduction will be a prime factor in allowing commonality in spar webs. In

addition to the potential parts commonality indicated in the areas of skin panels and ribs the following assemblies may be interchangeable, station to station and left side to right side;

- Engine nacelles and pylons
- Ailerons
- Winglets
- Leading edge segments
- Trailing edge segments
- Cargo roller channels and shear webs

The largest structural weight payoffs, however, occur through the use of composite materials, the final viability of which depends upon their tooling and manufacturing costs. The conventional aircraft experiences weight reductions from the use of composites in two ways; direct material substitution and aircraft resizing possible because of the reduced weight. That is, with a weight reduction in the aircraft for whatever reason, the design wing area can be reduced to maintain constant design field length. Empennage areas which are related to the wing area can also, therefore, be reduced in size. Studies have shown that the total weight empty reduction for conventional aircraft through the application of composites can be of the order of 30 percent.

The spanloader wing area, on the other hand, is constrained by cargo considerations. Composite application to this type of configuration, therefore, will be limited to the first type of payoff only; direct material substitution. The payoff to the study spanloader configuration was approximately 15 percent. The weight saving is achieved through a 22 percent reduction in the wing and winglets, 23 percent in the empennage, 19 percent in the fuselage, 10 percent in the landing gear, and 12.5 to 15 percent in the nacelles. The significance of this observation is that design features and innovations which reduce vehicle weight will benefit the conventional aircraft about twice as much as the spanloader aircraft, bringing the two configurations into closer alignment.

By the 1990s, large numbers of composite secondary structural components should be in production for fighter aircraft and a few large primary structural components should be in commercial flight service. These programs will

provide additional verification of the high reliability and reduced cost potential of composite material systems. This comprehensive use of composite materials is judged to be feasible for an advance spanloader aircraft in the 1990 time period. A major obstacle to the widespread use of composites is the enormous size of the proposed aircraft. Composite components currently obtain their high reliability and low cost through a reduction in number of parts and splices. The large composite primary structural components presently under consideration are dwarfed by the comparable components on the spanloader.

5.4 Aerodynamic Characteristics Comparison

The aerodynamic cruise characteristics of the spanloader aircraft are surprisingly good relative to conventional aircraft, particularly when considering the large difference in aspect ratio of the two configurations. This result springs from two primary features of the spanloader; its large size wing and the effectiveness of the winglets.

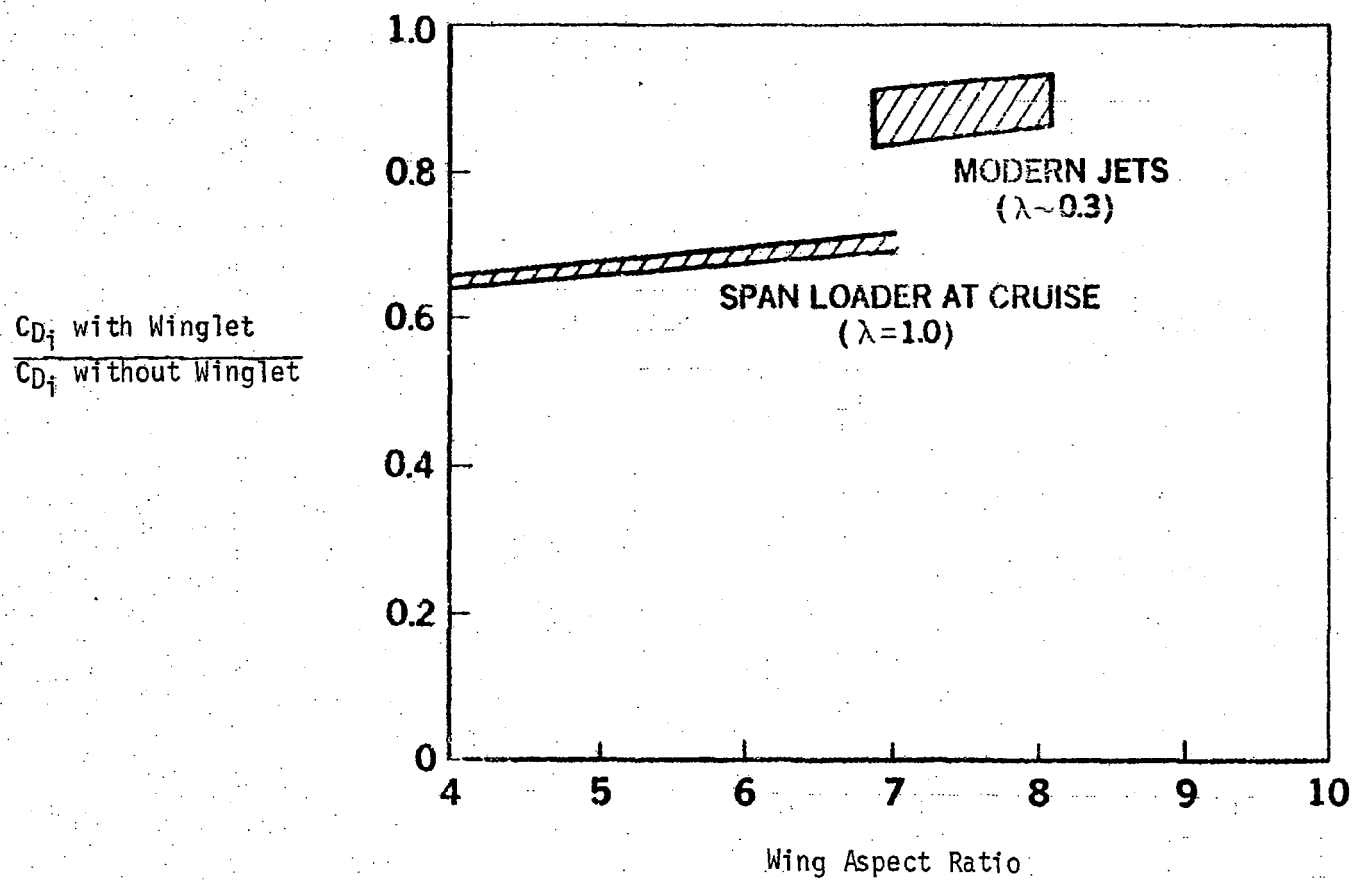
The large spanloader wing is associated with a much larger Reynolds number than the conventional aircraft (Table 5-3). The skin friction drag coefficient for the spanloader is therefore significantly less than that for the conventional aircraft. This in conjunction with the large spanloader wing area gives a zero-lift drag coefficient significantly less than that of the conventional aircraft.

TABLE 5-3
AERODYNAMIC PARAMETERS COMPARISON

PARAMETER	SPANLOADER	CONVENTIONAL AIRCRAFT
Cruise Reynolds Number based on wing MAC	108×10^6	65×10^6
C_{D_0}	.01123	.01476
L/D_{\max}	18.75	21.50

Winglet effectiveness is a function of the aspect ratio and taper of the wing to which it is applied. The low aspect ratio, non-tapered spanloader wing is ideal for winglet application. Figure 5-1 shows the effectiveness of winglets for reducing induced drag as derived from the spanloader configurations

FIGURE 5-1
WINGLET AERODYNAMIC PAYOFF



of the parametric studies (Section 3.0). The induced drag can be reduced 30 to 35 percent for spanloader type wings as compared to a much smaller percentage for the high aspect ratio tapered wings.

The impact of these considerations on overall cruise efficiency is evidenced by the fact that the spanloader configurations can achieve values of L/D_{max} that are comparable to those of today's jets. Due to size and the use of the aspect ratio 9.2 wing, the conventional aircraft considered herein has a L/D_{max} value (21.50) that is greater than today's jets.

The lack of a need for the use of a high lift system on the spanloader configuration has been mentioned previously and is unique in current aircraft design. The need for high lift devices, however, could reappear if a system oriented operational study would show a payoff for a design field length less than that of the aircraft analyzed.

5.5 PERFORMANCE COMPARISON

The performance of the Point Design spanloader is compared to the conventional aircraft in Table 5-4. These aircraft are essentially comparable except that the payload of the spanloader exceeds that of the conventional aircraft by two containers as previously discussed. A more valid comparison can be made, however, by considering the weight fractions. Relative to the conventional aircraft the spanloader is 5.8 percent more efficient on the basis of payload carried per pound of invested aircraft weight (GPL/OWE) but is 15.7 percent less efficient from the standpoint of energy usage (GPL/fuel). Energy usage is effected by the additional reserve fuel, 18,760 pounds (8,510 kg) above the FAR requirement, contained in the spanloader as discussed in Section 4.1. With this added fuel removed the payload/fuel ratio is 1.95 and the energy deficiency is reduced to 10.7 percent. In addition, this energy deficiency of the spanloader can be at least partially corrected by the use of optimum engine cycles.

The wing loading of the spanloader is approximately half that of the conventional aircraft. Because of the lack of a high lift system on the spanloader, however, its approach speed is higher than that for the conventional aircraft (169 kts (87 mps) vs 134 kts (69 mps)).

The takeoff field length of the spanloader is less than that of the

TABLE 5-4
PERFORMANCE COMPARISON

	SPANLOADER		CONVENTIONAL AIRCRAFT		WING SWEEP = 40°	
Operating Weight Empty - lb (kg)	396,525	(179,864)	400,509	(181,671)	296,978	(134,709)
Gross Payload - lb (kg)	618,000	(280,325)	590,000	(267,620)	600,000	(272,155)
Number of Containers	42		40		42	
Tare - lb (kg)	80,640	(36,578)	78,000	(35,381)	80,640	(36,578)
Fuel - lb (kg)	335,235	(150,063)	269,660	(122,318)	218,768	(100,585)
Takeoff Weight - lb (kg)	1,350,000	(612,360)	1,260,169	(571,613)	1,115,746	(506,102)
Reserve Fuel Weight - lb (kg) *	63,048	(28,599)	40,281	(18,272)	30,839	(13,988)
Net Thrust per Engine - lb/eng (N/eng)	58,500	(260,208)	44,029	(195,841)	40,000	(177,920)
Specific Fuel Consumption - lb/hr/lb (hg/hr·N)	.582	(.059)	.569	(.058)		
Wing Loading - lb/ft ² (kg/m ²)	73.7	(360)	157.5	(769)	74.9	(367)
Thrust to Weight Ratio - lb/lb (N/kg)	.259	(2.54)	.210	(2.06)	.2151	(2.109)
Ratio Operating Weight Empty to Takeoff Weight	.294		.318		.266	
Ratio Gross Payload Weight to Operating Weight	1.559		1.473		2.020	
Ratio Gross Payload Weight to Fuel Weight	1.843		2.188		2.743	
Cruise Zero Left Drag Coefficient	.01123		.01476		.0106	
Cruise Mach Number	.655		.784		.701	
Cruise Left Coefficient	.444		.500		.381	
Initial Cruise Altitude - ft (m)	31,500	(9,601)	28,800	(8,778)	31,090	(9,476)
Maximum Left to Drag Ratio	18.75		21.5			
Takeoff Field Length - ft (m)	10,737	(3,273)	12,000	(3,658)	12.025	(3.655)
Landing Field Length - ft (m)	9,960	(3,036)	5,210	(1,588)		
Approach Velocity - kn (m/s)	169	(87)	134	(69)		
Second Segment Climb Gradient	.0736		.0360			

* Spanloader Reserve Fuel = 44,288 lbs (20,089 kg) for FAR Landing Reserve plus 18,760 (8,510 kg) for 200 n mi additional reserve range.

Conventional Reserve Fuel = 40,281 lbs (18,272 kg) for FAR Landing reserve

conventional aircraft resulting from its lower wing loading and higher thrust-to-weight ratio. The landing field length of each aircraft is non-critical.

Again because of the spanloader wing loading and thrust-to-weight ratio, the cruise altitudes are higher. The cruise Mach number of the conventional aircraft is significantly greater than that of the spanloader as would be expected. This higher optimized speed and lower altitude of the conventional aircraft results in this aircraft cruising at a L/D value (19.36) significantly below L/D_{\max} (21.50). The spanloader cruises at its L/D_{\max} value of 18.75.

The primary performance advantage of the spanloader concept is its inherently shorter field length and the attendant increase in operational flexibility. The primary performance disadvantage is its lower cruise speed and its adverse impact on operating costs.

The swept wing spanloader performance as derived in the parametric studies of Section 3 are also included in Table 5-4 for reference purposes.

5.6 ECONOMIC COMPARISON

A comparison of the pivotal system characteristics that are used as the basis to derive the cost data and the resulting cost measures are delineated in Table 5-5. A summary of key findings and observations are as follows:

- o The direct operating cost of the Point Design spanloader and conventional aircraft compared in this section are competitive, with the spanloader cost 3.3 percent above that of the conventional aircraft. The inclusion of further optimization results for the spanloader concept, as discussed in other portions of the report, will reduce the spanloader operating costs below that of the conventional aircraft. For instance, using the indicated results for the effects of reducing the wing thickness to 17 percent, utilizing the swept wing version derived in Section 3 and assuming an arbitrary 5 percent reduction in structural weight due to further structural optimization, the results of Table 5-6 are indicated. The indications are that the spanloader concept has a potential DOC reductions of approximately 15 percent compared to a comparable conventional aircraft.

TABLE 5-5
ECONOMIC DATA COMPARISON

PARAMETER	POINT DESIGN SPANLOADER	CONVENTIONAL DESIGN	Change From Point Design Spanloader	Percent Change
Cost Weight - lb (kg)	317,385 (143,966)	337,185 (152,947)	19,800 (8,981)	+ 6.2
Composite Weight - lb (kg)	206,094 (93,484)	216,543 (98,224)	10,449 (4,740)	+ 4.8
Metallic Weight - lb (kg)	97,103 (44,046)	104,874 (47,571)	7,771 (3,525)	+ 8.0
Systems Weight - lb (kg)	90,970 (41,264)	76,732 (34,806)	-14,238 (-6,458)	-15.7
Gross Payload - lb (kg)	618,000 (280,325)	590,000 (267,620)	-28,000 (-12,705)	- 4.5
Block Fuel - lb (kg)	273,400 (124,014)	230,364 (104,493)	-43,036 (-19,521)	-15.7
Reserve Fuel - lb (kg)	63,048 (28,599) *	40,281 (18,272)**	-22,767 (-10,327)	-36.1
Unit Price @ Fleet Size - \$,M	58.5	72.0	13.5	+23.1
Engine Price - \$, M (6 ea)	9.798	8.316	- 1.482	-15.1
Airframe Price - \$, M	48.702	63.684	14.982	+30.8
Unit Price @ 350 Qty - \$, M	65.1	77.4	12.3	+18.9
DOC - ¢/Ton - n.mi. (¢/kg km)	3.363 (2.01×10^{-3})	3.240 (1.94×10^{-3})	- .123 (-6.00×10^{-5})	- 3.6
Fleet Size - Qty	525	463	62	-11.8
Block Time - hr	8.26	6.93	- 1.33	-16.1
Trips Per Year	363.2	432.9	69.7	+19.2
Cruise Mach No.	.655	.784	.129	+19.7
Thrust per Engine - lb (N)	58,500 (260,208)	44,000 (195,712)	14,500 (64,496)	-24.8

* Includes FAR Reserve of 44,288 (20,089 kg) plus an additional 18,760 lbs (8,510 kg) for an added 200n.mi. safety reserve range.

** 40,281 lbs (18,272 kg) for FAR landing reserve.

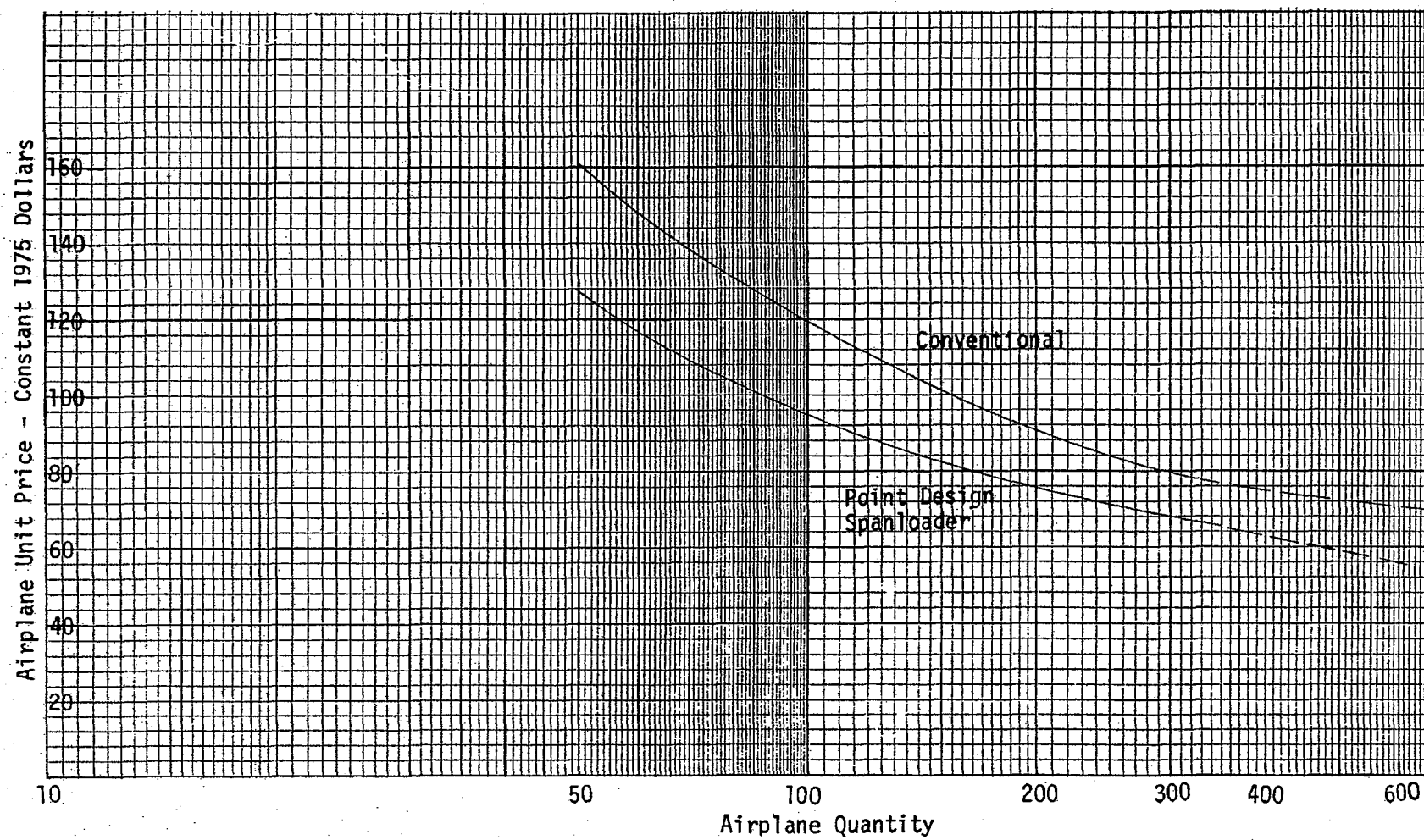
TABLE 5-6
SPANLOADER ECONOMIC POTENTIAL

	SPANLOADER	CONVENTIONAL AIRCRAFT
Point Design Aircraft	3.363	3.240
Reduce thickness of Spanloader wing to 17 percent	3.32	
Use swept wing Spanloader concept	2.79	
5 percent reduction in structural weight	2.78	

- o The price differential between the airplanes is primarily a result of differences in individual design attributes of the configurations and secondarily a result of differences in fleet size.
- o The spanloader design provides greater parts commonality and more simplified construction in the wing and tail components leading to considerably lower manufacturing and tooling costs. The large differential in fuselage weight is another significant factor that impacts on the cost.
- o The significant benefits derived from the design and construction of the spanloader more than offset the increased requirements and costs associated with the propulsion, fuel and winglet subsystems.
- o While airplane performance characteristics tend to induce slightly lower DOC values for the conventional design, the initial investment for fleet airplanes is only \$2.623 M lower for the spanloader (8.5 percent). The differential in unit price between the respective aircraft configurations is illustrated in Figure 5-2.

FIGURE 5-2

AIRPLANE PRICE VERSUS QUANTITY



6.0 CONCLUSIONS

The current study has made significant comparisons between three generic types of future large aircraft systems; the spanloader with cargo containers carried in the wing, a hybrid seaplane with the cargo in the hull, and a conventional aircraft with the cargo in the fuselage. Two variants of the spanloader were analyzed, a straight wing concept and a swept wing concept. Major conclusions emanating from this study are summarized as follows:

1. The swept wing spanloader has the highest payoff potential in terms of operating costs and energy usage followed by the straight wing spanloader and finally the hybrid seaplane.
2. The study results indicate that the spanloader concept has a potential operating cost advantage over an advanced conventional aircraft, of comparable technology, of approximately 15 percent.
3. The spanloader configuration can have an aerodynamic efficiency (L/D_{\max}) exceeding that of today's jet aircraft due to the effectiveness of winglets on the typically low aspect ratio, nontapered wings.
4. The spanloader configuration has superior structural efficiency ($W_e/TOGW$) due to the use of distributed inertia loads in the wing, nearly two-dimensional aerodynamic wing loading, and minimization of fuselage and empennage structure.
5. The straight wing spanloader concept results in a large percentage of common parts with right-left hand interchangeability resulting in a lower acquisition cost than a comparable conventional aircraft.
6. High payoff technologies for the spanloader concept include:

Winglets

Supercritical wing

Negative stability margins

Composite structures for spanloader aircraft may not pay off because the configuration size cannot be reduced to reflect the weight savings and composite material costs are higher than aluminum.

7. Because the cargo carried in the spanloader constrains the wing shape and size, many optimization payoffs that are normally available to a conventional configuration are limited for the spanloader. For instance, weight reduction items are not as significant to the spanloader as for conventional aircraft because the spanloader wing cannot be reduced in size to fully benefit from the weight reduction.
8. Additional detailed investigations should be conducted in the following areas:
 - o Engine/airframe optimization to determine best engine cycle;
 - o further optimization of the location of attachment of all internal and external aircraft components affecting wing static and dynamic loads;
 - o impact of parts commonality for the straight vs. swept wing spanloader;
 - o impact of use of aluminum vs. composite materials, and
 - o compromises due to consideration of military requirements on civil spanloader.

7.0 RECOMMENDATIONS FOR FUTURE WORK

Based on the analyses performed under this effort, a number of areas have come to light which could further augment the benefits resulting from the spanloader concept. These items are discussed throughout the report but are summarized here for conciseness and convenience.

7.1 Airfoil Design

Supercritical wing design is still a new technology item. Considerable wind tunnel work has been accomplished but as yet it is not state of the art on any major transport with the exception of a preliminary introduction on the AMST prototypes. Little work at all has been done on thick supercritical wings applicable to spanloader type vehicles. The spanloader concept hinges on the development of thick supercritical sections with high Mach divergence, little compressibility drag creep, and little tendency toward extreme viscous chordwise boundary layer growth or separation in the operating range of the airfoil. Expanded wind tunnel testing as well as flight article testing of thick supercritical wings is necessary prior to incorporation into full scale vehicles.

Airfoil selection is critical to the structure, weight, and aerodynamic efficiency of this type of configuration. The development of optimum airfoils must recognize the constraints and goals of;

- o Cargo cross section requirements
- o Maximum t/c with regard to M_{CR}
- o Minimize C_{m_0}
- o Low speed high lift without augmentation devices
- o Minimum adverse ground effects
- o Good buffet characteristics

The initial program should use analytical models (Vortex Lattice Program) to develop the required aerodynamic characteristics with weight allocations based on the current contract work, layouts as required to determine clearances between cargo and structure, and the resultant impact of C_{m_0} effects on the configuration.

7.2 Winglet Design

Current studies show that the aerodynamic winglet payoff on low aspect ratio, low taper wings ($\lambda \approx 1.0$) is large (approximately 30 to 35 percent reduction in induced drag). Winglets, however, are also a new technology item that requires extensive investigation to build the data base required to implement a proper design. High speed shock interaction between the wing and winglet cannot be allowed to cause premature aircraft buffet or any kind of separation causing high drag. Low speed may be even more critical. If the winglet is tailored to high speed drag reduction the typically higher wing lift coefficients encountered at low speed may cause high winglet loadings, especially at the winglet root, that could cause wing-winglet separation. This condition would be unacceptable, especially for second segment climb conditions, and may require variable geometry on the winglet such as auto-slats.

Because of the high payoff of winglets for spanloader configurations, extensive trade studies should be performed to optimize winglet shape not only in terms of aerodynamics but for overall impacts including winglet structural weight. Additional development and verification wind tunnel testing (high and low speed) are needed. Finally, winglet flight test work is necessary to bridge the huge winglet Reynolds number gap between wind tunnel and flight conditions.

The initial study should analytically develop the optimum camber, thickness, twist, and planform of the winglet. High speed requirements in the optimization should not compromise low speed stall characteristics.

7.3 Composite Structures

One of the largest payoffs for advanced aircraft will occur through the use of composite materials. The current studies demonstrate that weight savings up to 15 percent in structural weight are achievable on the spanloader concept. In addition, cost projections have indicated that cost savings are possible. By the 1980's, large numbers of composite secondary structural components should be in production for fighter aircraft and a few large primary structural components should be in commercial flight service. These programs should provide verification of the high reliability and reduced cost potential of composite material systems. This increasing use of composite

materials would assure their application to spanloader aircraft by the 1990 time period. A major concern, however, for the use of composites on the spanloader is its enormous size. Composite components currently obtain their high reliability and low cost through a reduction in number of parts and splices. The composite primary structural components presently under consideration are dwarfed by the comparable components of the spanloader.

The following tasks for future studies are proposed to define the critical technology developments for composite usage;

- (1) For each of the major components, define structural arrangements for the optimum use of composite construction with special attention given to high reliability and low cost.
- (2) Identify developments in manufacturing methods and composite material systems that will be required to fabricate the components. Emphasis should be on developments in laminating and curing that allow high volume rates over large areas.

These tasks would be initiated with an examination of existing manufacturing techniques for laminating and curing composite material systems to determine size limitations and size effects on reliability and cost. Based on strength and stiffness requirements, several composite structural concepts for each major component would then be determined. Integration of the structural concepts, material systems, and manufacturing techniques into a structural arrangement and a manufacturing plan that has the best potential for high reliability and low cost would be accomplished. Finally, the technology requirements to develop the selected structural arrangement and manufacturing plan would be evolved.

7.4 Wing Internal Arrangement Studies

As stated in Section 4.0, the concentration of inertia loads in the wing partially defeats the distributed load concept of the spanloader. Additional optimization studies which address the impact of these inertia loads on the critical wing structure are indicated. Such efforts have the potential for further payoffs in structure weight reductions.

Bending moment was shown to be the prime design loading parameter for the wing and for the Point Design configuration, two loading conditions dominated;

- (1) Balanced maneuver, $n = 2.5$ at maximum takeoff weight for up bending.
- (2) Taxi, $n = 2.0$ at maximum takeoff weight for down bending.

All of the upper skin panels and the majority of the lower are designed by the maneuver condition, the taxi condition designs the inboard section of the lower skins. Minimum scantling design is attainable on the outer third of the wing.

Fuel represents 22 percent of maximum takeoff weight and is entirely contained inboard but should be located in keeping with the span loading concept. This could significantly reduce the loading intensity in almost all flight conditions, particularly the present critical one. Power plant location should also be subject to further investigation on the same premise. Chordwise location of both fuel and power plants have a pronounced effect on wing torque; this effect should be minimized.

Ground conditions would become more critical as a result of the above changes. Relocation further outboard of the inner main gear and possibly the outer main gear would help alleviate wing loads. Changes in gear characteristics should also be investigated. The taxi condition load factor used for the Point Design configuration is a conservative estimate based on previous experience and analysis of multiple gear aircraft. A more rigorous estimate of this load factor is warranted.

The study should use the current spanloader configuration to perform the necessary shear, moment and torque analysis to determine functional acceptable engine, fuel, and landing gear locations that will minimize structural loads. Based upon the resulting revised configuration the new structural weight, resulting changes in performance, and the effects of nonuniform cargo loading should be determined. Dynamic taxi analysis using flexible aircraft and $(1 - \cos)$ runway bump shape should also be conducted.

7.5 Structural Design Refinements

Additional analysis of the spanloader concept to define structural approaches and weight allocations for the following elements should be conducted:

- (1) Optimization of a typical wing rib considering wing thickness and rib spacing.

- (2) Wing/fuselage juncture
- (3) Pylon/wing juncture
- (4) Landing gear/wing attach
- (5) Winglet/wing attach (cargo doors)
- (6) Optimization of fuselage structure

The spanloader concept creates new requirements for wing rib design. The space required for rib structure, combined with payload dimensions and clearances determine the wing thickness and therefore an optimum design is important. Additional rib design effort directed to areas of load concentration, such as the wing/fuselage, pylon/wing, winglet/wing junctures, and the landing gear attachment point, is important to confirm the feasibility of this concept and to further define potential high weight areas of the configuration.

The fuselage of this spanloader is merely a housing for the crew and equipment and a cantilever beam to support the empennage. A structural design investigation to optimize this fuselage concept is important to better understand the wing/fuselage juncture and to maximize structural effectiveness.

The study should utilize the configuration and loads developed in this study. A 3-dimensional internal loads analysis of the wing in sufficient detail to obtain a good estimate of the load distributions at the landing gear, engine and fuselage junctures should be conducted. Investigations should be performed for the critical flight and ground conditions and for varying rib heights and spacings. Layouts and analysis of the engine pylon and landing gear supports and the winglet/cargo door juncture in sufficient detail to assure valid weight estimates should be made. In addition, layouts of the fuselage structure and wing/fuselage juncture should also be made.

7.6 Payload Characteristics

Ability to accept (or limit) potential cargo containers will impact the cost effectiveness of spanloaders. Characteristics of future container populations could affect tradeoffs of container compartment height and wing thickness, discontinuous and/or unequal load distribution with resultant aircraft weight, drag, and fuel consumption penalties, and exclusion of potential air cargo because of container height restrictions. The study would survey industry container demands and project trends of container height and weight distributions.

In addition, the practical limits of the permissible lateral c.g. range are contingent not only upon the aircraft design but are related to the payload weight distributions. Accordingly, studies involving a random draw from container populations and sequence of these containers within the spanloader to achieve allowable weight and balance should be conducted. The frequency spectrum of c.g. location, including instances where c.g. location exceeds allowable limits, should be determined.

7.7 Engine Technology Requirements

The propulsion subsystem is a primary component of any efficient system and represents a relatively long lead-time development. Preliminary studies of the next generation engines are already underway and should be impacted by the spanloader requirements. However, current studies of the aircraft are based upon a selected bypass nine engine and optimum engine requirements have not been determined.

The study should consider a matrix of bypass ratios, overall pressure ratio and thrust level, dictated by efficient engine design to perform a parametric analysis of aircraft performance as a function of the size and number of engines. Engine requirements compatible with minimum cost and energy considerations should then be defined. Because of the lower speed regime of the spanloader and the less stringent internal noise requirements, compared to a passenger aircraft, turboprop designs should also be evaluated.

7.8 Dynamic Stability

An aft c.g. location (in the order of 43 percent MAC_w) appears inherent in the spanloader configuration. The horizontal tail required for stability can be reduced through the application of active control stability augmentation. Appropriate control systems also have the potential to reduce the low wing loading gust response, reduce lateral balance requirements, and assist landing approach control.

An expanded study of the spanloader should be conducted to analyze the longitudinal, lateral and directional dynamic characteristics of the configuration with the aft c.g. locations. Control concepts for stability augmentation considering possible failure modes and required reliability levels should be evaluated.

7.9 Operational Considerations

Present allocation of reserves for mission accomplishment may not be adequate in light of restricted operational sites for spanloader aircraft. Unique operational problems therefore include:

- (1) A determination of realistic fuel reserve requirements in light of the restricted number of potential landing sites.
- (2) Effect of headwinds on reserves.
- (3) Engine shutdown for more efficient cruise.

7.10 Military Logistics Evaluation

The development of a spanloader would require an enormous investment in RDT&E funds such that no single airframe contractor could justify sole implementation of the program. A spanloader program will, therefore, in all probability, be implemented with government support and even be designed to accommodate military missions. The aircraft, therefore, will be compromised from the commercial point of view in order to accommodate the outsized military payloads.

Basic payload, range and configuration requirements for these military missions should be defined. Configurations should be developed and comparisons made between pure military and commercial systems to determine compromises and penalties accrued from joint designs.

APPENDIX A
NOMENCLATURE

Latin

A/C	aircraft
AMST	Advanced Medium STOL Transport
AR	aspect ratio
b	span
C_D	three-dimensional drag coefficient
C_{D_c}	three-dimensional compressibility drag coefficient
C_{D_0}	three-dimensional drag coefficient at zero lift
C_{D_i}	three-dimensional induced drag coefficient
C_{D_π}	three-dimensional drag coefficient based on frontal area
C_f	three-dimensional skin friction coefficient
c_f	two-dimensional skin friction coefficient
c.g., CG	center of gravity
C_L	three-dimensional lift coefficient
c_l	two-dimensional lift coefficient
C_{M_0}	three-dimensional pitching moment coefficient at zero lift
c_y	side force on winglet
DCPR	Defense Contractor Planning Report
DOC	direct operating cost
DOC_p	parametric value of direct operating cost
FAR	Federal Air Regulation
F_n	engine net thrust
f	equivalent flat plate drag
GPL	gross payload weight, containers included
h	altitude, height
KTAS	knots true air speed
K_w	ratio of induced drag with winglet to induced drag without winglet

L/D	aircraft lift to drag ratio
M	Mach number
M	structural bending moment
\$M	millions of dollars
MAC	mean aerodynamic chord
M_{DD}	drag divergence Mach number
NPL	net payload weight, containers not included
NWLD	nose wheel lift off
n	load factor
OWE, W_e	operating weight empty, operating empty weight
QCSEE	Quiet, Clean, Shorthaul Experimental Engine
R	range
R_N	Reynolds number
S	structural shear force
SAS	stability augmentation system
SFC	specific fuel consumption
SLS	sea level static engine thrust
SOW	statement of work
STA	wing station
S_w	wing area
S_{wet}	wetted surface area
T	structural torque
TOFL	takeoff field length
TOGW	takeoff gross weight
T.R.	taper ratio
T/W	ratio of engine thrust to aircraft gross weight
\bar{t}	equivalent thickness of total material in structural member
t/c	thickness ratio
V_c	cruise speed
V_d	dive speed for structural design
V_s	airplane stall speed
W.L.	water line

W.R.P.	wing reference plane
W/S	wing loading, ratio of aircraft gross weight to wing area

Greek

α_F	angle of attack based upon fuselage reference line
Δ	incremental change in value of parameter
δ_e	elevator deflection angle
n	fraction of span
Λ	sweep angle
λ	taper ratio
ρ_{PLG}	density of gross payload, container included
ρ_{PLN}	density of net payload, container not included
ρ_{tare}	density of tare weight, container density

Subscripts

H	horizontal tail
max	maximum value
n_y	measured in horizontal plane
n_z	measured in vertical plane
opt	optimum value
T0	tail off
Trim	trimmed value of coefficient
V	vertical tail
W	wing